DEUBIQUITINATION: DOES THE ANSWER TO CARDIOTOXICITY LIE WITHIN THE UBIQUITIN PROTEASOME PATHWAY?

by

Temitope R. Ogundipe

Thesis presented in fulfillment of the requirements for the degree of

Master of Science (Physiological Sciences) at Stellenbosch University

Supervisor: Dr. Balindiwe JN Sishi

March 2017

DECLARATION

By submitting this thesis electronically, I declare that the entirety of the work contained therein is my own, original work, that I am the sole author thereof (save to the extent explicitly otherwise stated), that reproduction and publication thereof by Stellenbosch University will not infringe any third party rights and that I have not previously in its entirety or in part submitted it for obtaining any qualification.

March 2017

ABSTRACT

Introduction: Cardiotoxicity, a complication that arises from anthracycline use is one that has confounded scientists for decades. Attempts have been made to attenuate the development of this condition through the use of anti-oxidants with little success and this has led to calls for new adjuvant therapies. One area that has been identified as a potential intervention involves the ubiquitin proteasome system (UPS) and its regulation and degradation of proteins that control mitochondrial morphology, apoptosis and cellular anti-oxidants. This process can be reversed through the use of de-ubiquitinating enzymes (DUBs); however their role in this context is relatively unknown. Therefore, this study aimed to investigate the role of specific DUBs relevant in this context and whether the manipulation of their protein expression levels will be beneficial.

Methods: Chronic doxorubicin (DOX)-induced toxicity was induced in H9C2 cardiomyoblasts and male Sprague-Dawley rats for 120 hrs (0.2 μM) and eight weeks (2.5 mg/kg/week) respectively. Baseline protein expression of DUBs as well as their down-stream factors was determined by western blotting on both models. Immunocytochemistry was undertaken only for *in vitro* studies. DUBs were down-regulated using SiRNA, and the subsequent effect on downstream proteins was determined through western blotting. Mitochondrial morphology was evaluated by fluorescence microscopy, while cellular toxicity and ATP production were assessed using a mitochondrial toxicity assay.

Results and Discussion: DOX increased the expression of USP9x (103.7 ± 4.7%, $p<0.01$), which regulates MCL1 (long-fragment), an anti-apoptotic protein which was down-regulated in this scenario. Interestingly, the pro-apoptotic short-fragment of MCL1 was up-regulated, suggesting a mechanism by which DOX uses USP9x to promote apoptosis. DOX treatment also reduced USP30 expression (27.5 ± 3.7%, $p<0.01$), as well as its downstream target, the mitofusin proteins (22.7 ± 5.9%, $p<0.001$) which regulate mitochondrial fusion during mitochondrial dynamics. USP36 showed little variation between the two groups however, DOX reduced SOD2 expression (250.9 ± 6.8%, $p<0.001$). While both models utilised produced similar results, there was minor variation in the results. When DUB (SiRNA) was initiated in

the presence of DOX, mitochondrial morphology appeared to improve. Interestingly, while the known-down of some DUBs (USP30 and USP36) did not modify mitochondrial toxicity except when USP9x was abolished, ATP synthesis was significantly upregulated in all intervention groups when compared to DOX treatment alone. Although more research into this topic is urgently needed, it is clear from the positive results obtained above that de-ubiquitination may be a mechanism that can be exploited as a potential treatment strategy in this context.

OPSOMMING

Inleiding: Kardiotoksisiteit, as gevolg van antrasiklien gebruik, is ‘n komplikasie wat wetenskaplikes vir dekades verwar. Antioksidante is gebruik om die ontwikkelling van die toestand te probeer onderdruk, maar pogings was onsuksesvol en het aanleiding daartoe gegee dat nuwe ondersteuningsterapiëe ontwikkel moes word. Een area wat geteiken is vir potensiële intervensies sluit die ubikwitienproteosoomsisteem (UPS) in, en die regulering en degradering van proteïene wat mitochondriale morfologie, aptoptose en sellulêre antioksidante beheer. Hierdie proses is omkeerbaar deur die gebruik van die de-ubikwitieneringsensiem (DUBs), maar die rol in hierdie konteks is onduidelik. Gevolglik het hierdie studie daarin gepoog om die rol van spesifieke DUBs wat in hierdie konteks verwant is, asook of die manipulering van die proteïenuitdrukkingsvlakke voordelig sal wees te ondersoek.

Metodes: H9C2 kardiomioblaste en manlike Sprague-Dawley rotte is onderskeidelik aan 120 uur (0.2 μM) en agt weke (2.5 mg/kg/week) van chroniese doksorubisien (DOX)-geïnduseerde toksisiteit blootgestel. Basislyn DUBs proteïenuitdrukking, asook hulle afstroomfaktore is deur middel van Westerse blattering op beide modelle, en slegs met behulp van immunositochemie *in vitro* bepaal. DUBs is afgereguleer deur van SiRNA gebruik te maak, waarna die gevolglike effekte van die afstroomproteïene deur middel van Westerse blattering bepaal is. Mitochondriale morfologie is deur middel van fluoresensie mikroskopie ondersoek, terwyl sellulêre toksisiteit en ATP produksie deur middel van ‘n mitochondriale toksisiteittoets bepaal is.

Resultate en Bespreking: DOX het die uitdrukking van USP9x (103.7 ± 4.7%, $p<0.01$) verhoog wat MCL1 (langfragment) reguleer. Laasgenoemde is ‘n anti-apoptotiese proteïen wat afgereguleer is in hierdie scenario. Die pro-apoptotiese kortfragment van MCL1 was merkwaardig opgereguleer, wat moontlik ‘n meganisme kan beskryf waarin DOX, USP9x gebruik om apoptose te stimuleer. DOX behandeling het ook USP30 uitdrukking verlaag (27.5 ± 3.7%, $p<0.01$), asook die afstroomteiken, mitofusienproteïene (22.7 ± 5.9%, $p<0.001$) wat mitochondriale fusie tydens mitochondriale dinamika reguleer. Hoewel USP36 min variasie tussen die

twee groepe getoon het, het DOX SOD2 uitdrukking verlaag (250.9 ± 6.8%, $p<0.001$). Beide modelle het soorgelyke resultate opgelewer, maar daar was min variasie in die resultate. Nadat DUB (SiRNA) in die teenwoordigheid van DOX geïnisieer is, blyk dit dat die mitochondriale morfologie verbeter het. Terwyl die onderdrukking van sommige DUBs (USP30 en USP36) nie die mitochondriale toksisiteit kon modifiseer nie, behalwe as USP9x afgeskakel was, was ATP sintese interresant genoeg betekenisvol opgereguleer in alle intervensie groepe in vergelyking met die DOX alleen groep. Alhoewel daar nog baie navorsing gedoen moet word op hierdie onderwerp, is dit duidelik uit hierdie positiewe resultate dat die de-ubikwitienasie moontlik as megansime ondersoek kan word vir die potensiële behandelingsstrategie in hierdie konteks.

"*Rest is Sweet after work has been done*"

–Dr Radiance Ogundipe

"*What is worth doing, is worth doing well"*

– Mrs Kehinde Ogundipe

"For God hath not given us the spirit of fear; but of power, and of love and of a sound mind"
-2 Timothy 1:7

ACKNOWLEDGEMENTS

First I would like to acknowledge God for guiding my path so far.

To my supervisor, **Dr Balindiwe Sishi** for your ever present support, guidance attention to detail, and for helping me grow so immensely. You have been an inspiration to me and a critical backbone to this study. Thank you for being easy to approach, and forming a strong and friendly bond with all your students.

To **Dr and Mrs Ogundipe**, **Tomi** and **Toyin**, my sources of strength, I appreciate you for your support, financially, psychologically and emotionally. The sacrifices you have made for me, I could barely begin to repay, and I can only hope to make you proud.

To **Toni Goldswain**, thank you for your friendship and support throughout all of this. The hours of work, jokes, ideas, frustrations, and sleepy early mornings are moments I hold very dearly.

To **Itumeleng Chabaesele**, thank you for all your advice and help, you were pivotal in helping me settle into the department.

To **Dr Nell** and **Dr Kruger**, a huge thank you for helping with the translation of my abstract.

To **DSG group**, and physiology department at large, I would like to thank you all for your support, encouragement, advice and help, Yigael for your help with techniques, Bianca for always being there to talk to.

To the **NRF**, I would like to express my appreciation for the funding for the project, and also funding my presentation at the PSSA 2016 conference.

To **Relebohile Mohapi**, my confidant and best friend. I can barely begin to quantify how much you imparted on me. You have been the rock on which I was able to lean, your support in all manner, patience, advice, criticism, encouragement, motivation and comfort did more than help me through all this. You saw it all, the up's, down's, failures, success, confidence, doubt and stress, and you kept nudging me in the right direction. I appreciate your impact in my life and would like to thank you immensely.

ABBREVIATIONS

ADR	Adriamycin
ANOVA	Analysis of variance
CHF	Congestive heart failure
CVD	Cardiovascular disease
DEX	Dexrazoxane
DMEM	Dulbecco's Modified Eagles Medium
DNA	Deoxyribonucleic acid
DNR	Daunorubicin
DRP1	Dynamin related protein 1
DOX	Doxorubicin
DUB	De-ubquitinating enzyme
EPI	Epirubicin
ER	Endoplasmic Reticulum
HF	Heart Failure
IDA	Idarubicin
JAB1	Jun activating binding protein
JAMM	Jab1/MPN domain-associated metalloproteases
LC3	Light chain 3
LVEF	Left ventricular ejection fraction
MARCH5	Mitochondrial ubiquitin ligase (MITOL)
MAM	Mitochondria associated membrane
MCL1	Myeloid cell leukemia 1
MFF	Mitochondrial fission factor
MFN1	Mitofusin 1
MFN2	Mitofusin 2
MFNs	Mitofusins
MJD	Machado-joseph domain
MPN	Mpr1/Pad1 N-terminal
mPTP	Mitochondrial permeability transition pore
MTS	Mitochondrial targeting sequence
MnSOD	Manganese superoxide dismutase

MULE	MCL-1 ubiquitin ligase
NRF	Nuclear respiratory factor
NTF	Nuclear transcription factors
OPA1	Optic atrophic protein 1
OUT	Ovarian-tumour domain
OXPHOS	Oxidative phosphorylation
PBS	Phosphate buffered saline
Penstrep	Penicillin Streptomycin
PGC-1α	Peroxisome proliferator-activated receptor gamma co-activator 1 alpha
PINK1	PTEN-induced putative kinase 1
PTEN	Phosphatase and tensin homolog
PVDF	Polyvinylidene fluoride
RIPA	Radio-immunoprecipitation assay
ROS	Reactive oxygen species
SDS-PAGE	Sodium dodecyl sulphate polyacrylamide gel electrophoresis
SiRNA	Silencing ribonucleic acid
SOD	Superoxide Dismutase
SR	Sarcoplasmic reticulum
SQSTM1	Sequestosome 1
TBST	Tris-buffered saline with Tween
TIM/TIMM	Translocase of inner mitochondrial membrane
TOM/TOMM	Translocase of outer mitochondrial membrane
TS	Transmembrane segment
UCHs	Ubiquitin c-terminal hydrolases
UPS	Ubiquitin proteasome system
USP	Ubiquitin specific protease

UNITS

g	gram
mg	milligram
kg	kilogram
mM	millimolar
µM	micromolar
nM	nanomolar
M	molar
nm	nanometer
L	litre
mL	millilitre
µL	microliter
g/mL	gram per milliliter
mg/mL	milligram per milliliter
ng/mL	nanogram per milliliter
mg/m^2	milligram per metre squared
mg/kg	milligrams per kilogram
µg/kg	microgram per kilogram
^{o} C	degrees celsius
%	percentage
Hrs	hours
Mins	minutes
Secs	seconds

TABLES

FIGURES

CONTENTS

LITERATURE REVIEW

1.1 Introduction

Cardiovascular diseases (CVDs) and cancer as identified, are the two leading causes of death in the industrialised world and the two diseases are closely linked (Siegal *et al*., 2015). On the one hand, CVDs are a clinically complex syndrome with a number of causes. According to the American Heart Association (Mozaffarian *et al*., 2015), CVDs are considered the number one cause of death world-wide, accounting for 17.3 million deaths. This number is predicted to grow to over 23.6 million by the year 2030. On the other hand, cancer is a major global health concern, second to CVDs in terms of prevalence and mortality. Together, these diseases accounted for 46.5% of all global deaths in 2012, where 48.5% were male and 44.4% were female (Heron, 2015). In the African context, the picture is slightly different as CVDs and cancers are not the major contributors of death in the adult population but still pose a major burden particularly in Sub-Saharan Africa. Although this region is riddled with communicable diseases such as tuberculosis (TB), HIV/AIDS and malaria (Murray *et al*., 2014), over 80% of the global mortality rates related to CVDs currently occur in developing countries (Perk *et al.,* 2012). Despite aggressive treatments and advanced diagnostic techniques, these diseases lead to substantial morbidity and mortality and will continue to increase in many parts of the world (**Fig. 1.1**) and therefore their prevention is a very important clinical and public health priority. These diseases are not only costly to manage, they have the ability to be highly disabling and in some cases lethal. Due to this, there is a need for novel adjuvant therapies that function differently to those currently established.

The advances in cancer treatment have brought hope to patients with this disease which was long thought to be incurable. This has led to a significant reduction in mortality rates particularly amongst women who suffer from breast cancer where survival rates are as high as 85-90%; a major accomplishment in today's cancer treatment strategies (Ginsburg, 2013). Chemotherapy is essential in cancer therapy; however an overwhelming body of evidence has established that patients exposed to different types of anti-neoplastic treatments have numerous laboratory and clinical indices of cardiovascular dysfunction that become progressively evident as the patients live longer (Broder *et al.,* 2008). Apart from the growth and ageing of the

population, the increased adoption of cancer-associated lifestyle behaviours such as physical inactivity, westernized diets and smoking, contribute to the severity of this health burden (Mozaffarian *et al., 2015)*. As a result of this phenomenon, cancer patients who have or are at risk of cardiovascular complications are now being treated collaboratively by oncologists, cardiologists, haematologists and radiologists in an initiative that has led to the development of an exciting but novel interdisciplinary field known as Cardio-Oncology (Albini *et al.,* 2010; Patane, 2014).

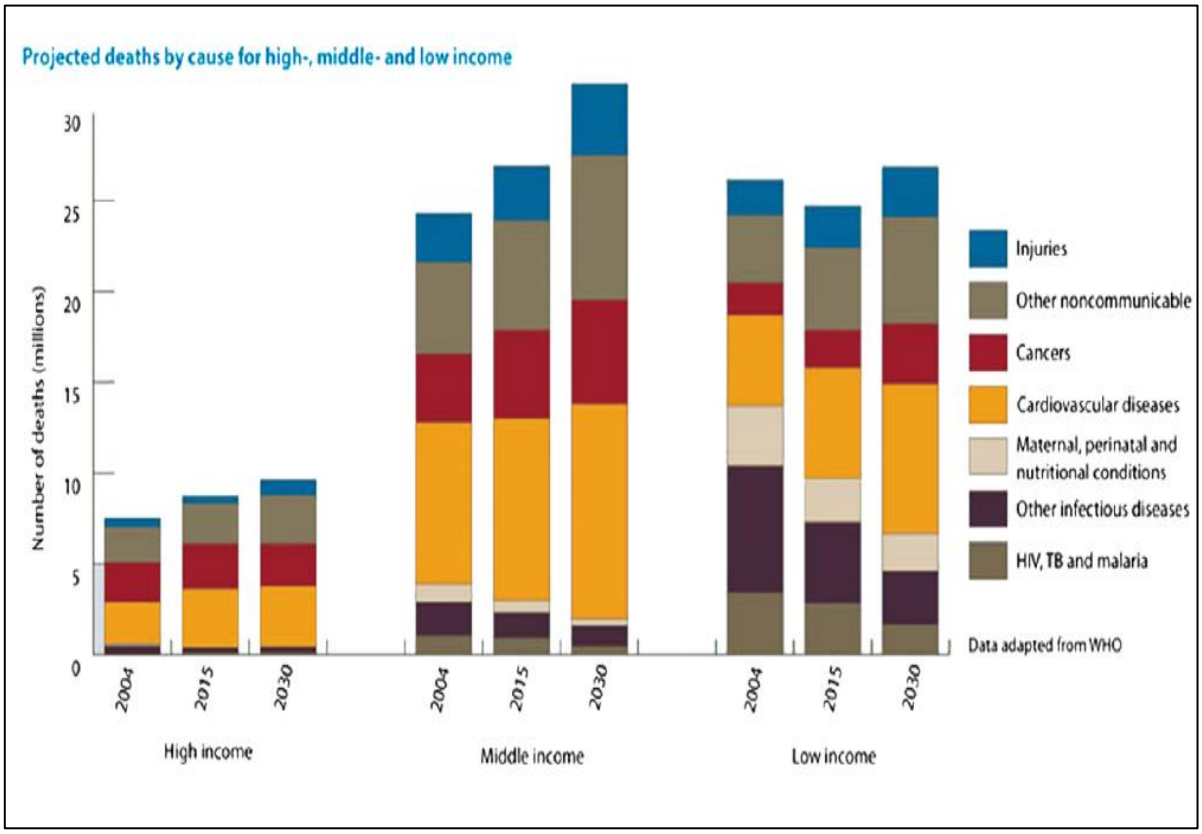

Figure 0.1: CVD and Cancer Mortality per Economic Region. CVD mortality is projected to increase in many parts of the world, with the largest increases projected for middle income and developing regions. Cancer mortality is also on the rise in middle income and low income regions. Abbreviations: **HIV** - Human immune deficiency virus, **TB** – Tuberculosis (Laslett *et al.,* 2012).

1.2 Cardiotoxicity

Cardiotoxicity was initially defined by the National Cancer Institute in very general terms as “toxicity that affects the heart” (NCI dictionary of cancer terms:

www.cancer.gov/publications/dictionaries/cancer-terms?cdrid=44004; April 6, 2016). While this definition is somewhat acceptable, it is considered incomplete and lacks specificity. Some have defined this condition as a multi-factorial process that in the long run induces cardiomyocyte death as the terminal downstream event (Minotti *et al*., 2004), while others describe it as a broad range of adverse effects on heart function induced by therapeutic molecules (Montaigne *et al*., 2012). Although these definitions are to some extent better than the previous, they are still very vague since it is well known that various chemotherapeutic agents are toxic to the heart and its vasculature (Albini *et al*., 2010). Therefore an unambiguous interpretation of exactly what cardiotoxicity is, is still lacking. A more comprehensive and expansive definition was then postulated by the Cardiac Review and Evaluation Committee and they defined cardiotoxicity induced by anti-cancer treatment regimens as including one or more of the following:

(i). Cardiomyopathy with a reduction in left ventricular ejection fraction (LVEF), either globally or more severely in the septum or,

(ii). Symptoms associated with heart failure (HF) such as S3 gallop, tachycardia or both or,

(iii). A reduction in LVEF that is less than or equal to 5% or less than 55% with accompanying signs or symptoms of HF or,

(iv). A reduction in LVEF that is greater or equal to 10% or less than 55%, without accompanying signs or symptoms (Seidman *et al*., 2002).

Whereas this definition describes cardiotoxicity in terms of HF characteristics, it is currently the most appropriate considering that cardiotoxicity induced by anthracycline treatment (discussed below) culminates in congestive heart failure (CHF) (Swain *et al*., 2003). Despite the fact that cardiotoxicity is mainly induced by chemotherapeutic treatments, it can also be induced from complications of anorexia nervosa as well as incorrectly administered drugs (Lask *et al*., 1997). Classic chemotherapy-induced cardiotoxicity is generally classified into two main types: early/acute and late/chronic cardiotoxicity (Minotti *et al*., 2004).

1.2.1 Early/Acute cardiotoxicity

The more infrequent form of early/acute cardiotoxicity occurs anytime from the initiation of chemotherapy up to approximately two weeks after termination of treatment (Simunek *et al*., 2009). Symptoms observed in patients experiencing this type of cardiotoxicity include hypotension, vasodilation, transient cardiac rhythm disturbances, pericarditis, and left ventricular dysfunction (Volkova & Russell, 2011). Although improvements in left ventricular dysfunction have previously been observed, the mechanism that is postulated to be responsible for acute cardiotoxicity may potentially involve an inflammatory response, which is in contrast to the commonly accepted cause of the chronic form of cardiotoxicity (Bristow *et al*., 1978). Acute cardiotoxicity is also described as Type II cardiotoxicity as it is induced by cardiomyocyte dysfunction rather than cell death and is thus considered to be reversible. Typically a rare complication, early/acute cardiotoxicity is generally not considered a clinical cause of concern as it can either be clinically treated, or it can resolve on its own without intervention once chemotherapy has ceased (Simunek *et al*., 2009).

1.2.2 Late/Chronic Cardiotoxicity

Late/chronic cardiotoxicity, also known as Type I cardiotoxicity, is more serious taking into account that it is governed by cell death, either through apoptosis or necrosis. Cardiomyocyte death results in permanent damage to the myocardium and therefore is deemed irreversible. This progressive toxicity traditionally takes place following the completion of treatment and may manifest within a year (early onset) or many years to decades (late onset) after chemotherapy has been completed (Shan *et al*., 1996). Early onset chronic cardiotoxicity is characterized by dilated cardiomyopathy which eventually leads to left ventricular contractile dysfunction and culminates in CHF, while late onset chronic cardiotoxicity is characterized by asymptomatic systolic and/or diastolic left ventricular dysfunction that can lead to severe congestive cardiomyopathy and eventual death of the individual (Simunek *et al*., 2009). This type of cardiotoxicity is particularly relevant in adult survivors of childhood cancers as up to 65% of these patients display echocardiographic

indications of left ventricular contractile abnormalities (Grenier & Lipshultz, 1998; Choi *et al*., 2010). The risk for such toxicity depends on the cumulative dose, the rate of drug administration, mediastinal radiation, age, gender, hypertension and pre-existing heart disease (Volkova & Russell. 2011). While the chemotherapeutic drugs often associated with cardiotoxicity include alkylating agents (e.g. Cisplatin, Cyclophosphamide) and monoclonal antibodies (e.g. Bevacizumab, Cetuximab), the most problematic of these are the anthracyclines (e.g. Doxorubicin, Daunorubicin) (**Table 1**).

Systemic therapy class		Incidence					
Drug Name	Indication(s)*	Arrhythmia	Long QTc	Systolic dysfunction	Hypertension	Myocardial ischemia	Thromboembolism
Anthracycline							
Daunorubicin	Leukemia	++/+++	✓	+	–	–	–
Doxorubicin	Breast, lymphoma	+/++	✓	++/+++	–	–	✓
Doxorubicin (liposomal)	Sarcoma	+	✓	–	–	+/++/+++	–
Epirubicin	Breast, gastric	–	✓	+/++	–	–	✓
Idarubicin	Leukemia	++/+++	✓	++/+++	–	–	✓
Mitoxantrone	Leukemia	++/+++	✓	++/+++	++	++	–
Alkylating agent							
Cisplatin	Bladder, HNC, lung, ovarian	✓	✓	✓	✓	✓	++
Cyclophosphamide	Heme cancer	–	–	✓	–	–	+
Ifosfamide	Cervical, sarcoma	✓	–	+++	–	–	+
Antimicrotubule agent							
Docetaxel	Breast, lung	+/++	✓	++	++	++	✓
Nab-paclitaxel	Breast, pancreas	+/++	✓	–	–	–	+
Paclitaxel	Breast, lung	++	✓	+	–	+	–
Antimetabolite							
Capecitabine	Colorectal, breast	✓	✓	✓	–	++	+/++
5-Fluorouracil	Gastrointestinal	✓	✓	+	–	++/+++	✓
Hormone therapy							
Abiraterone acetate	Prostate	++	–	++	++/+++	++	–
Anastrozole	Breast	–	–	–	++/+++	++	++
Exemestane	Breast	–	–	–	++	++	+
Letrozole	Breast	–	–	–	++	++/+++	++
Tamoxifen	Breast	–	✓	–	++/+++	++	++
Monoclonal antibody-based targeted therapy							
Bevacizumab	Colorectal	++	✓	+/++	++/+++	+/++	++/+++
Brentuximab	Lymphoma	–	–	–	–	+	++
Cetuximab	Colorectal, HNC	++		✓	++	✓	+/++
Ipilimumab	Melanoma	–	–	–	–	–	–
Panitumumab	Colorectal	✓	–	–	++	++	+
Pertuzumab	Breast	–	–	++	–	–	–
Rituximab	Heme cancer	✓	–	–	++	++	++/+++
Trastuzumab	Breast, gastric	++	–	++/+++	++	–	+/++
Small-molecule targeted therapy							
Bortezomib	Multiple myeloma	+	–	+/++	+	+	+
Dasatinib (TKI)	Leukemia	++/+++	+/++	++	++	++	+/++
Erlotinib (TKI)	Lung	✓	–	–	–	++	++
Gefitinib (TKI)	Lung	✓	✓	–	–	+/++	✓
Imatinib (TKI)	CML	–	–	+/++	–	+++	+
Lapatinib (TKI)	Breast	✓	+++	++	–	–	–
Nilotinib (TKI)	CML	++	++	++	++	✓	+
Pazopanib (TKI)	RCC	–	–	+	+++	+/++	++
Sorafenib (TKI)	RCC, HCC	+	✓	+	+++	++	++
Sunitinib (TKI)	GIST, RCC	+	+	++/+++	+++	++	+/++
Vemurafenib (TKI)	Melanoma	++	✓	+	++	++	++
Miscellaneous							
Everolimus	RCC	–	–	++	++	–	+
Lenalidomide	Myeloma	+/++	+	++	++	++	++/+++
Temsirolimus	RCC	–	✓	–	++	+++	++

Table 1: Available anti-neoplastic treatments and their associated side-effects. Most anti-neoplastic drugs have some sort of side-effect, negating the option of just avoiding DOX, seen here are several available anti-neoplastic treatments and the side effects associated with them. **+++:** > 10%, **++:** 1-10%, **+:** 1% or rare, √: observed, but precise incidence not well established, **−:** not well recognized complication with no/minimal data. Abbreviations: **CML** - Chronic myeloid leukaemia, **GIST** - Gastrointestinal stromal tumour, **HCC** - hepatocellular carcinoma, **HNC** - Head and neck cancer, **RCC** - Renal cell carcinoma, **TKI** - Tyrosine kinase inhibitor (Truong *et al*., 2014).

1.3 Anthracyclines

Anthracyclines are a family of drugs initially discovered in the 1950s from the identification and isolation of β-rhodomycin II from the bacterium *Streptomyces peucetius.* This discovery led to the eventual identification of Daunorubicin (DNR) in the 1960s (Lown, 1993; Minotti *et al*., 2004). DNR was established to be quite successful in treating cancers of the immune system (lymphomas) and of the blood (leukaemia) (Tan *et al.,* 1967). Within a decade, derivatives of DNR such as Doxorubicin (DOX), also known as Adriamycin (ADR), Epirubicin (EPI) and Idarubicin (IDA) (**Fig. 1.2**) were developed (Lown, 1993). While DOX is considered the one of the most effective and most potent anti-tumour drugs ever developed, DNR, EPI and IDA are considered effective, but less potent than DOX.

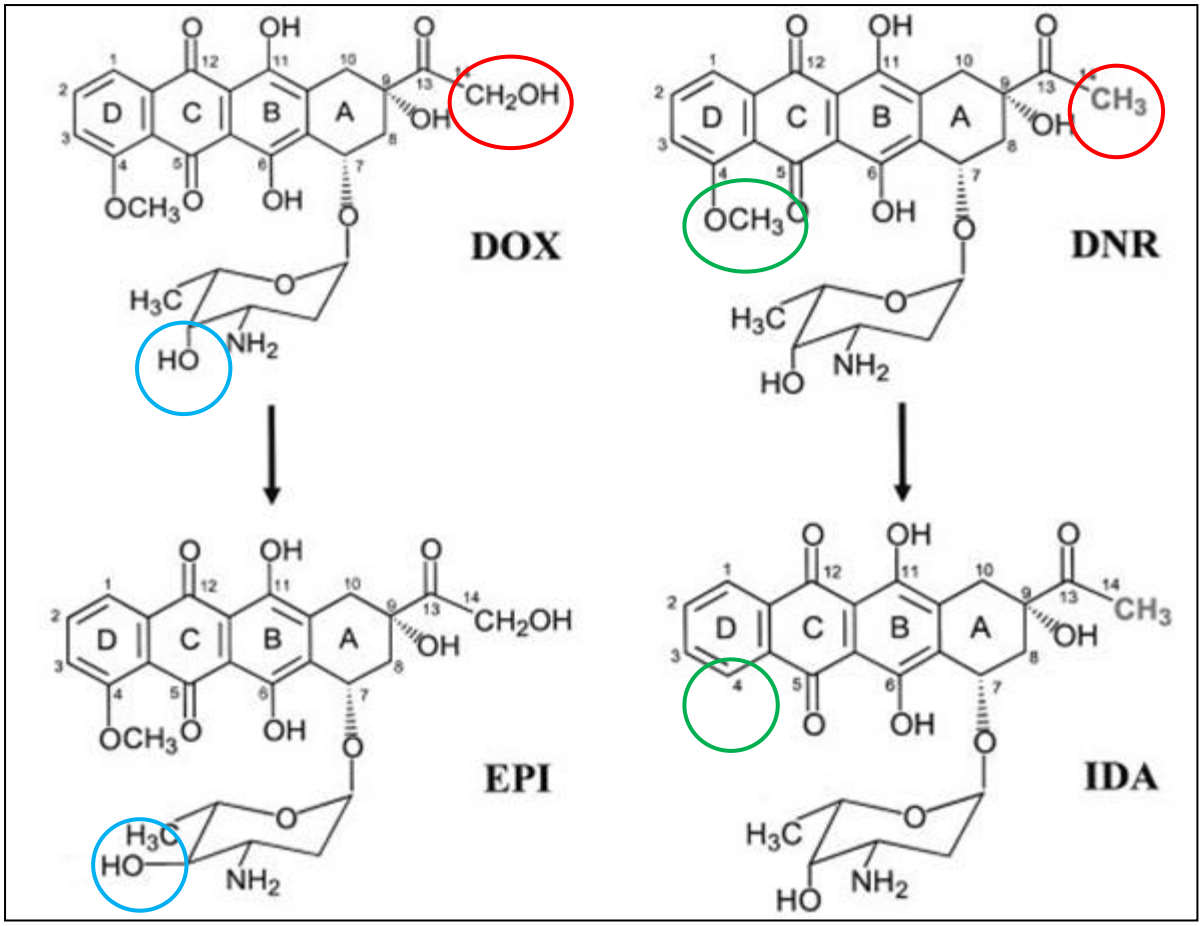

Figure 0.2: The evolution of anthracyclines. Chemical structures of four of the most common anthracyclines and their minor structural differences. Whereas DOX and IDA were developed from DNR, EPI was developed from DOX. Green circles (**O**) indicate differences between DNR and IDA, red circles (**O**) indicate differences between DNR and DOX and, blue circles (**O**) indicate differences between DOX and EPI. Abbreviations: **DNR** - Daunorubicin, **DOX** - Doxorubicin, **EPI** - Epirubicin, **IDA** – Idarubicin (Minotti, *et al*., 2004).

Since the late 1990s, anthracyclines, and in particular DOX have been considered the gold standard of chemotherapy in treating a wide variety of solid tumours and hematologic malignancies (Volkova & Russell, 2011). Soon after their discovery, it was observed that their clinical utility was limited by their cumulative, dose dependent myocardial injury which led to irreversible HF and a reduced quality of life (Lown, 1993). This phenomenon has since been known as anthracycline-induced cardiotoxicity. In a retrospective study conducted by Van Hoff and colleagues (1979) of over 4000 patients receiving DOX treatment, 2.2% of these patients displayed signs and symptoms of CHF. While this percentage may appear to be small, this

number could possibly have been higher had the authors included reductions in left ventricular function without obvious signs and symptoms of CHF. It was further demonstrated that the independent risk factor for the development of CHF was the cumulative dose of DOX, where the incidence of HF increases with each subsequent dose received (**Fig 1.3**). It was only in 2003 when Swain *et al*., demonstrated that cumulative doses that range between 275-399 mg/m^2 resulted in a decrease in LVEF in 4% of the patients treated with DOX. This number increased to 15% and 28% when the cumulative doses were between 400 and 500 mg/m^2, and greater than 500 mg/m^2 respectively. As a result, the recommended lifetime cumulative dose for DOX that should not be exceeded is ± 450 mg/m^2 (versus 900 mg/m^2 for Epirubicin) as cardiotoxicity limits further therapy (Torti *et al*., 1986).

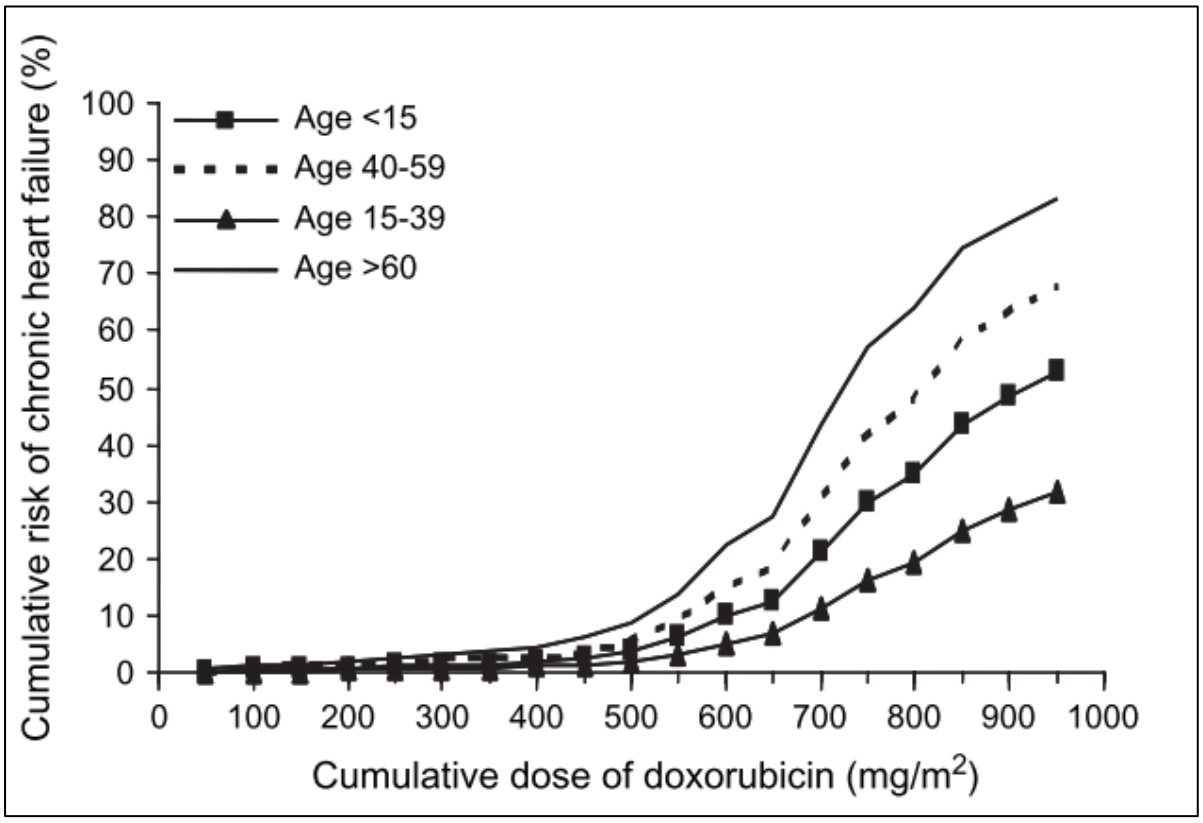

Figure 0.3: Cumulative dose related risk of CHF across different age groups. Percentage risk of developing HF rose with increases in the cumulative dose of DOX as shown above. This increase was also more evident in ageing populations. (Barrette-Lee *et al*., 2009)

Although substantial efforts have been made in the current clinical setting to identify patients that display signs of cardiotoxicity based on the aforementioned risk factors;

the current detection methods are not sensitive enough to distinguish early signs of damage prior to left ventricular dysfunction (Volkova & Russell, 2011). Furthermore, despite the fact that clinical evaluation can identify patients at risk, there is currently no consensus on the optimal strategy to delay or prevent the onset of cancer-associated heart disease. The ideal cardioprotective approach within this context remains controversial and thus represents an unmet clinical requirement. Notwithstanding that over 50 years of intense research in this field has already been spent, the lack of acceptable guidelines for the management of this critical complication predominantly originates from the limited understanding of the molecular mechanisms that govern cardiotoxicity and its transition to HF. An important question that arises from this is whether the mechanisms by which DOX kills actively replicating cancer cells are also the same mechanisms by which it induces cardiac toxicity? From this point onwards, the anthracycline that will be referred to in the rest of this thesis is DOX.

1.3.1 Doxorubicin's mechanism of action

DOX is known to possess a Quinone moiety connected to a glycoside group (**Fig. 1.4**). Its chemical structure is not only responsible for its anti-neoplastic activity but also for its toxicity. More specifically, the inhibition of DNA synthesis through DNA intercalation causing DNA strand breaks and ultimately apoptosis, is the primary mechanism by which DOX exerts its cytostatic effects on neoplastic cells (Gewirtz, 1999); whereas the toxicity exhibited in cardiomyocytes is related to free radical production stimulated by DOX metabolism (Minotti *et al*., 2004). Firstly, NADH dehydrogenases reversibly reduce DOX at complex I of the mitochondrial respiratory chain forming a semi-Quinone radical (an unstable metabolite) that reacts with oxygen to produce superoxide radicals. In a vicious cycle, the continuous redox cycling also produces hydrogen peroxide and hydroxyl radicals, and thus a condition of oxidative stress arises (Bachur *et al.,* 1978). Secondly, iron is a vital cofactor in the formation of toxic reactive oxygen species (ROS). The iron-catalysed conversion of hydrogen peroxide to hydroxyl radicals (Fenton reaction) occurs as a result of the formation of DOX-iron complexes (Minotti *et al*., 1999). Due to their high reliance on oxidative phosphorylation and reasonably inferior anti-oxidant defences, (Olsen *et*

al., 1981; Doroshow *et al.,* 1980), cardiomyocytes are likely to be more sensitive to oxidative stress and thus prone to oxidative damage.

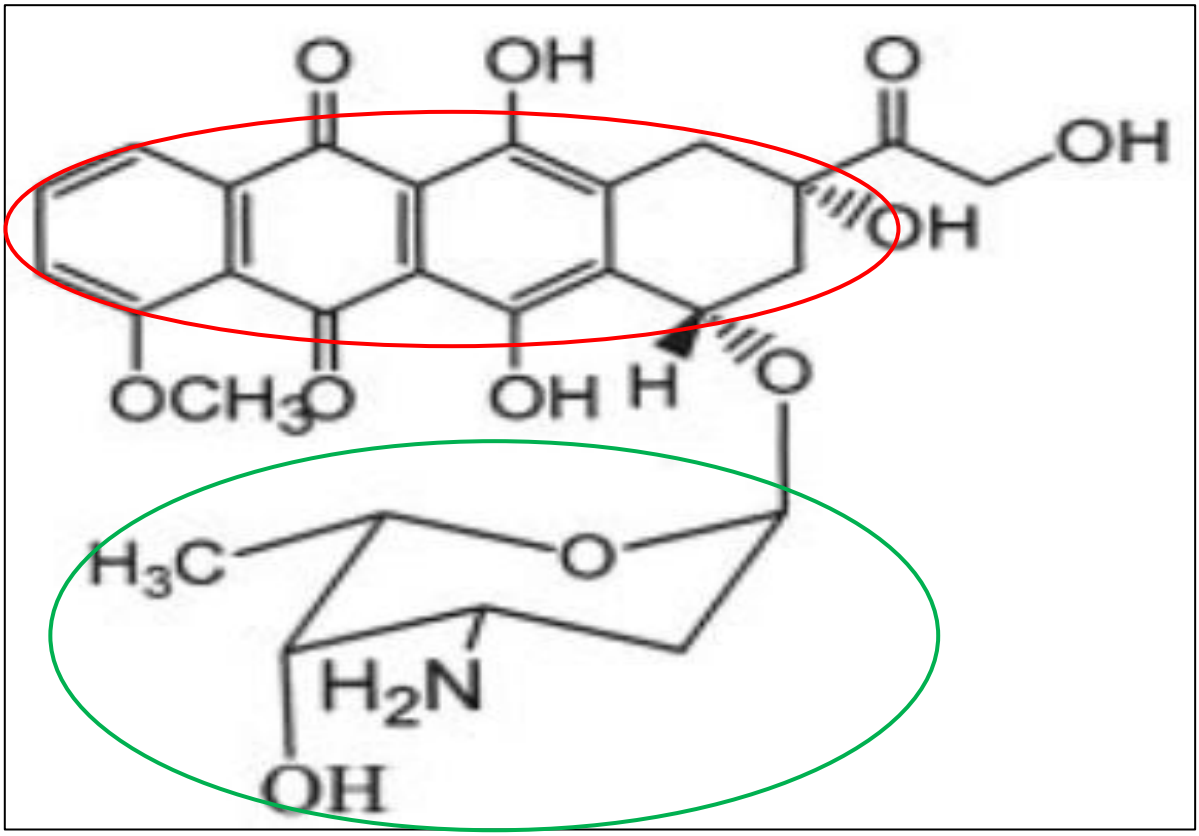

Figure 0.4: Functional structure of DOX. DOX possess four Quinone moieties (circled in red) connected to a glycosidic group (circled in green) (Minotti *et al*., 2004).

The importance of this oxidative stress theory was demonstrated by the observation that reducing ROS and consequently oxidative stress, ameliorates the cardiotoxic effects associated with DOX treatment, including cell death. Elegant studies utilizing transgenic models have demonstrated that the over-expression of anti-oxidants such as MnSOD (Su *et al*., 2014) and catalase (Kang *et al*., 1996) improves left ventricular function and reduces apoptosis in DOX treated animals. Others have shown that a decline in left ventricular function can be prevented by deleting proteins such as nitric oxide synthase that initiate free radical production (Vasquez-Vivar *et al*., 1997). Furthermore, DOX has a high affinity for cardiolipin, a crucial phospholipid located in the inner mitochondrial membrane. This binding disrupts the association that cardiolipin has with other inner mitochondrial membrane proteins and this affects

mitochondrial membrane potential and enhances cytochrome c release in response to oxidative stress (Goormaghtigh *et al.,* 1980).

Life and death signals within cardiomyocytes are a delicate balance between cytoprotective and cytotoxic pathways, and understanding the relationship between these two mechanisms may provide insight into novel treatments that may reduce toxicity without affecting the neoplastic activity of DOX. In this regard, a number of approaches have been taken in an attempt to ameliorate the toxic effects of DOX, one being the use of anti-oxidants to combat oxidative stress and its downstream effects. Van Dalen *et al*., (2005) observed that the use of various anti-oxidants such as vitamins E and C, and N-acetylcysteine (NAC), have all shown promise *in vitro* and *in vivo* in reducing oxidative stress, however these interventions produced disappointing results clinically. In fact, these patients went on to develop HF, with D'Andrea, (2005) going as far as to recommend the avoidance of anti-oxidants during chemotherapy, as their limited beneficial effects are compromised by the fact that they could also protect cancer cells from chemotherapy. Another intervention that has had more success than anti-oxidants is the iron chelating agent Dexrazoxane (DEX). This iron-chelator has been identified as particularly effective in reducing early myocardial injury during chemotherapeutic treatment with DOX (Lipshultz *et al*., 2010). DEX becomes hydrolysed to its metabolites and its potent iron-chelating form ADR-925 by dihydroorotase (**Fig. 1.5**). ADR-925 binds free iron released from ferritin and iron bound to DOX in DOX-iron complexes, and thereby prevents ROS formation through the Fenton and Haber-Weiss reactions.

DEX also offers protection against DOX-induced cardiotoxicity via the inhibition of topoisomerase II expressed in high concentrations, such as in cancer cells. Interestingly, the inhibition of topoisomerase II is the same mechanism by which DOX induces cytotoxicity in cancer cells. However, it has been speculated that DEX may protect cancer cells by reducing the anti-tumour activity of DOX, and thus may play an active role in the development of secondary malignant neoplasms (Choi *et al*., 2010; Lipshultz *et al*., 2010). Furthermore, DEX may also increase the incidence of side-effects such as infection, fever and myelosuppression (Langer, 2007). Since the above interventions have failed to achieve desirable results clinically, the focus of research has shifted from oxidative stress to rather the cellular organelles that produce ROS. These ROS producing organelles known as mitochondria are central

to cardiotoxicity, considering that damaged mitochondria are one of the earliest and most prominent histomorphological features of DOX cardiotoxicity.

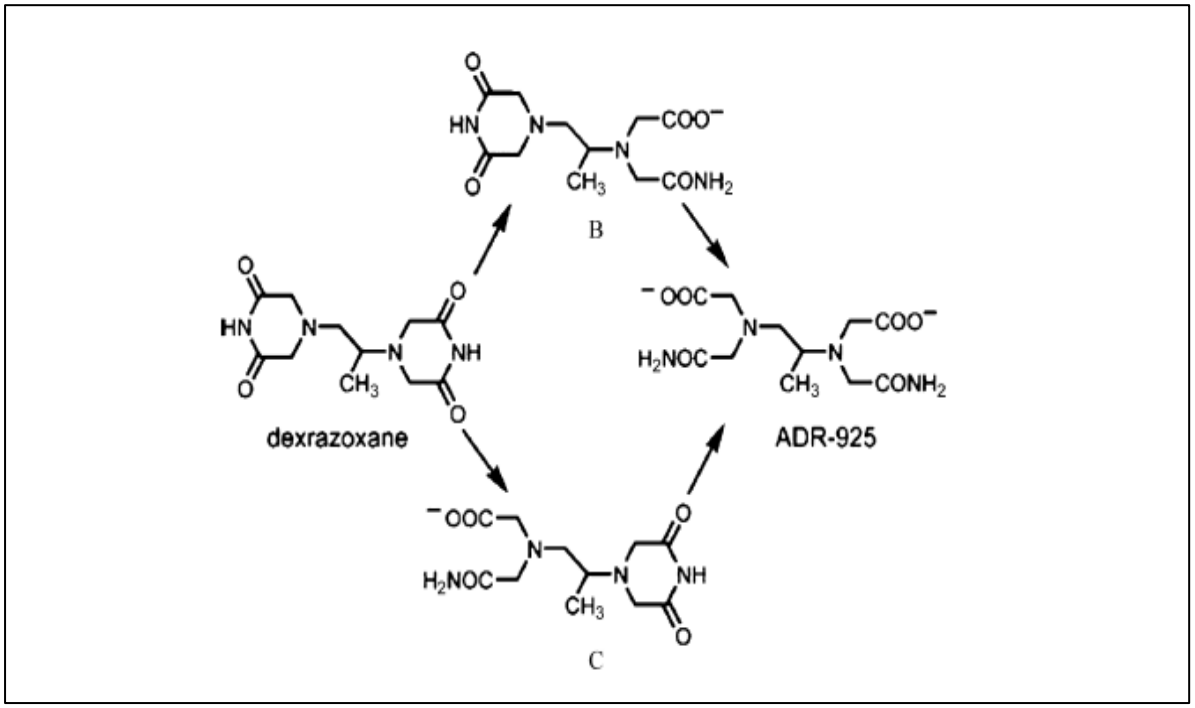

Figure 0.5: Conversion of DEX to ADR-925. In a reaction catalysed by dihydroorotase, Dexrazoxane is converted to the potent iron-chelating agent ADR-925 (Junjing *et al*., 2010).

1.4 Mitochondria

Mitochondria are aptly named after two forms in which they represent their networks; '*mitos'* meaning thread, is indicative of fusion and '*chondros*' meaning grain and indicates fission (Hom & Sheu, 2009). These powerhouses fulfil the high energy demands of the heart due to their ability to produce ATP through oxidative phosphorylation (Martinou & Youle, 2011). As a result, cardiomyocytes have a dense population of mitochondria, accounting for 35% of the myocardial volume (Hom & Sheu, 2009). However, as much as these organelles are crucial for cellular function and ATP production, they are also known for their role as the main producers of ROS (Daosukho *et al*., 2005).

1.4.1 Mitochondrial Dynamics

Mitochondrial integrity is vital in governing cellular homeostasis. It is influenced by mitochondrial morphology which is controlled by two processes known as mitochondrial fusion and fission (**Fig. 1.6**) in an overarching process known as mitochondrial dynamics (Hom & Sheu, 2009). These processes contribute to overall cellular health as mitochondrial fission is essential for cell cycle regulation and cell division through the isolation and removal of polarised or damaged mitochondria. This event is characterised by highly fragmented and disconnected mitochondria that produce excessive ROS, and is often accompanied by mitophagy, a degradative system for damaged mitochondria (Kim *et al.,* 2007). Mitochondrial fusion also contributes to mitochondrial network homeostasis by 'diluting' damaged mitochondrial regions through fusion with healthy mitochondria (Youle *et al*., 2012). Characterized by elongated, tubular and interconnected mitochondrial networks (**Fig. 1.7**), fusion enables mitochondria to squeeze out as much efficiency as possible by keeping the network intact during damaging insults.

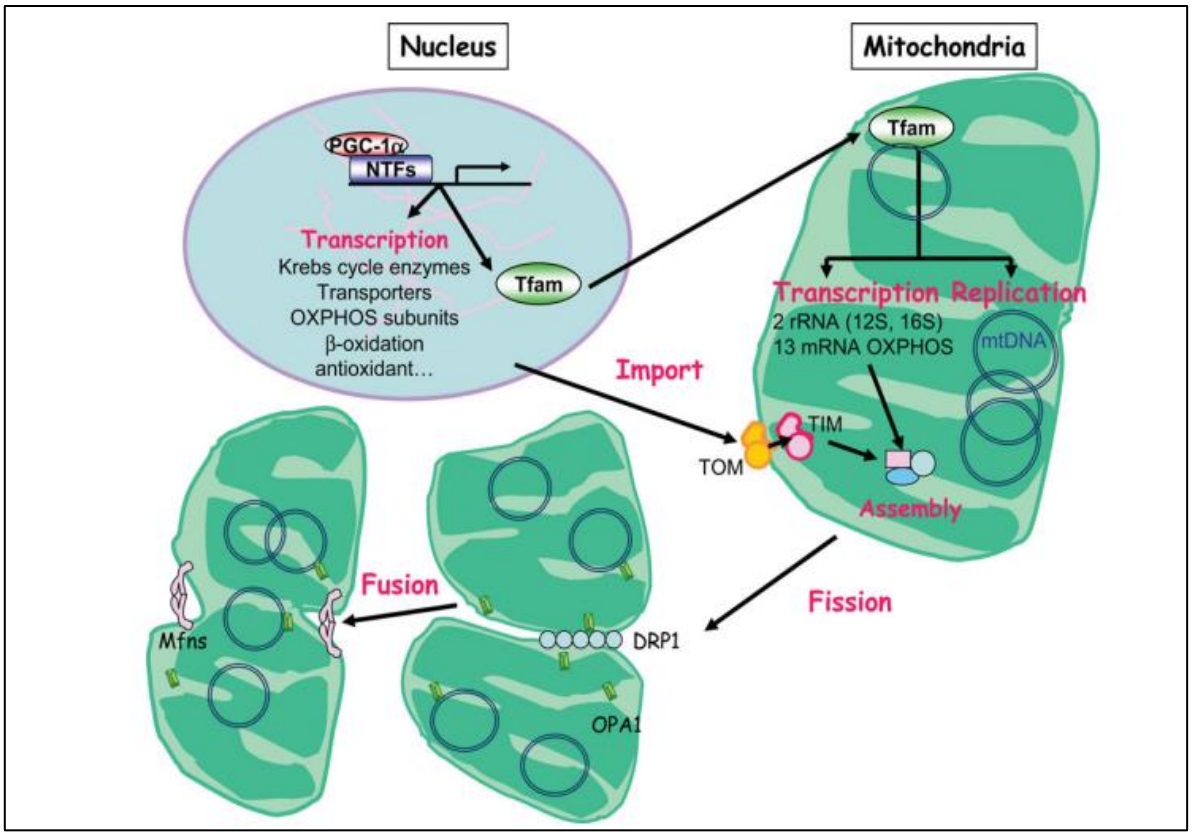

Figure 0.6: Mitochondrial Biogenesis. PGC-1α associates with NTFs, which lead to the transcription of Tfam a protein which induces transcription and replication of the mitochondrial genome. Mitochondrial fusion is enabled by the mitofusins, while mitochondrial fission is enabled by

DRP1. Abbreviations: **DRP1** - Dynamin related protein 1, **MFN**: mitofusin, **NTF-** Nuclear transcription factor, **OPA1**: Optic atrophic protein 1, **OXPHOS**: Oxidative phosphorylation, **PGC-1α** - Peroxisome proliferator-activated receptor gamma co-activator 1α, **Tfam** - mitochondrial transcription factor, **TIM**: Translocase of inner membrane, **TOM**: Translocase of outer membrane, (Ventura-Clapier *et al*., 2008).

Mitochondrial fusion is regulated by dynamin related GTPases mitofusin 1 (MFN1) and mitofusin 2 (MFN2), and the optic atrophic protein (OPA1). The mitofusins facilitate fusion of the outer mitochondrial membrane while OPA1 undergoes splicing into a long and short subunit. The long subunit (L-OPA1) merges and becomes part of the inner mitochondrial membrane, while the short subunit (S-OPA1) remains in the inner mitochondrial membrane space. These proteins are essential for mitochondrial stability and a loss of MFN2 alone has been shown to have a significant impact on mitochondrial fusion levels and mitochondrial translocation (Ni *et al*., 2015). Mitochondrial fission is mediated through the interactions of the Dynamin related protein 1 (DRP1) with mitochondrial fission protein 1 (hFIS1) and mitochondrial fission factor (MFF). DRP1 is initially recruited from the cytosol to the mitochondrial membrane under conditions of stress, and this prompts DRP1 to constrict the mitochondrial membrane which leads to division into daughter organelles.

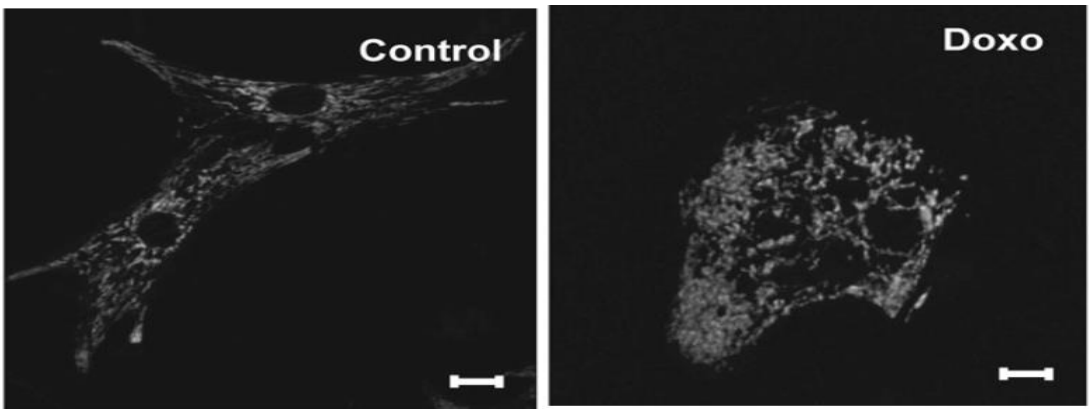

Figure 0.7: Microscopic presentation of mitochondrial morphology. Healthy mitochondria present as well defined interconnected networks indicative of fusion (**Control**), while ailing mitochondria present as fragmented networks indicative of fission (**Doxo**) (Parra *et al*., 2008).

These dynamic processes are regulated by mitochondrial biogenesis; a process which is defined as the growth and division of pre-existing mitochondria. Mitochondrial biogenesis itself is controlled by the peroxisome proliferator-activated receptor gamma co-activator (PGC-1α). As indicated in **Fig. 1.6**, PGC-1α interacts with nuclear transcription factors (NTFs) and stimulates mitochondrial biogenesis through the transcriptional regulation of the mitochondrial genome and mitochondrial proteins (Ventura-Clapier *et al*., 2008).

As mitochondrial fusion and fission complement one another in a delicate balance, controlled by mitochondrial biogenesis, it has previously been observed that this balance is disturbed in many CVDs including cardiotoxicity (Parra *et al*., 2008). In these pathologies, the balance favours mitochondrial fission which induces mitochondrial membrane depolarization, due to hFIS1-linked Bax recruitment to the mitochondrial membrane and subsequent formation of pores within the mitochondrial membrane by Bax (Bae *et al*., 2000, Lee *et al*., 2004). This depolarization induces DRP1-dependent cytochrome c leakage and ultimately apoptosis induction (Zungu *et al*., 2011). Due to the high accumulation of DOX in cardiomyocytes as a result of binding to cardiolipin, the resulting oxidative stress and the uncontrolled fission, damaged mitochondria are the first histomorphological features of DOX-induced cardiotoxicity (Minotti *et al*., 1999). This damage, if unresolved could have catastrophic consequences for the cell and ultimately affect heart function as a whole.

1.5 Mitochondrial associated degradation

With the critical role that mitochondria play in cellular homeostasis, maintaining mitochondrial health is a major cellular priority. The regulation of mitochondrial proteins used to maintain mitochondrial quality and integrity has led scientists to believe that there is a mitochondrial-associated degradation pathway that plays this role. This degradation system is known the Ubiquitin Proteasome System (UPS) and serves as a quality control mechanism not only for this organelle, but also for the cell in its entirety.

The UPS is a known proteolytic pathway that tags proteins with ubiquitin molecules and degrades them via its catalytic centre, the 26S proteasome made up of a 20S core subunit and a 19S regulatory subunit (Ciechanover, 1994). In the presence of ATP, the first step in this process begins when an ubiquitin moiety is transferred to the ubiquitin conjugating enzyme (E2) by the ubiquitin activating enzyme (E1). In the second step, ubiquitin ligases (E3) cause ubiquitin chain ligation onto the targeted protein (**Fig. 1.8**). This process of tagging proteins with ubiquitin molecules is repeated until the proper conformation of ubiquitin molecules is formed and the ubiquitin molecules are attached to the correct lysine residue. In this case for degradation to take place, poly-ubiquitination needs to occur at lysine 48. It is only in the third and final step does the 26S proteasome target the ubiquitinated proteins for degradation while the ubiquitin molecules are recycled (Jiang *et al.,* 2015). Bearing in mind that there are numerous E3 ligases, this review will highlight two such E3 ligases that are considered important in the context of mitochondrial dysfunction during cardiotoxicity.

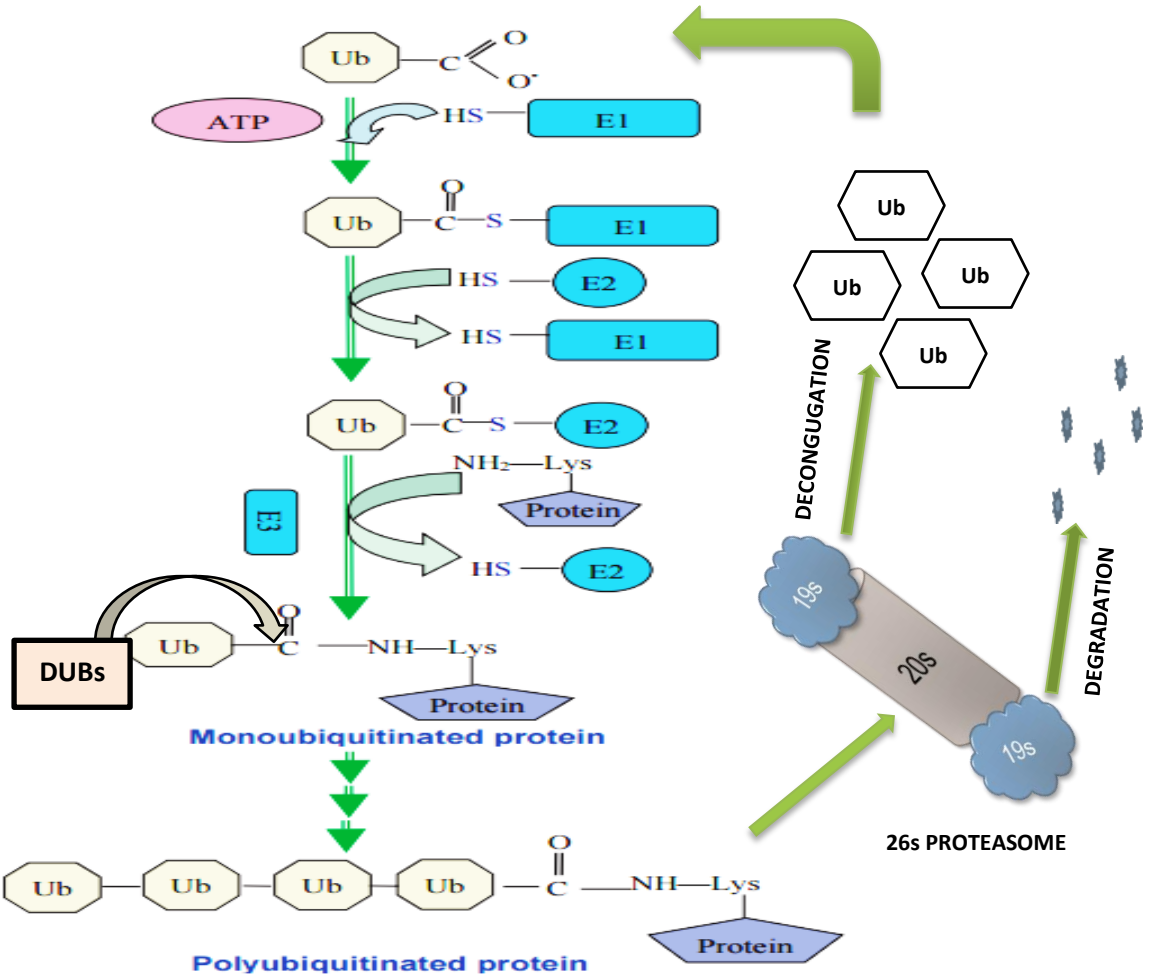

Figure 0.8: The Ubiquitin Proteasome System. Ubiquitin molecules get transferred to the E2 enzyme by the E1 enzyme in an ATP-dependent fashion. This ubiquitin conjugated E2 enzyme then binds an E3 enzyme which is also bound to the substrate protein and then the E3 enzyme facilitates transfer of ubiquitin from the E2 to the substrate. The tagged substrate is recognized by the 26S proteasome and degraded whilst the ubiquitin molecules are recycled. DUBs interfere in this process by removing ubiquitin molecules from tagged substrate proteins. Abbreviations: **DUBs** - Deubiquitinating enzymes, **E1** - ubiquitin activating enzyme, **E2** - ubiquitin conjugating enzyme, **E3** – ubiquitin ligase, **Lys** - lysine, **Ub** – ubiquitin. Adapted from Nandi *et al*., (2006).

1.5.1 PINK1 and Parkin

Severely polarized mitochondria that are marked for degradation through mitophagy accumulate PTEN-induced putative kinase 1 (PINK1); a serine/threonine kinase that contains an N-terminal mitochondrial targeting sequence (MTS) and a transmembrane segment (TM). When PINK1 associates with healthy mitochondria, its MTS translocates across the mitochondrial membrane where it gets cleaved by

the mitochondrial processing peptidase (MPP) leaving the remaining TM cleaved by presenilin-associated rhomboid-like (PARL). This causes the dissociation of PINK1 from the mitochondria and its degradation by the UPS. However, when PINK1 associates with polarized mitochondria, the MTS is unable to translocate through the mitochondrial membrane and thus PARL becomes inactivated. As such, an intact PINK1 associates with translocases of the outer membrane (TOM) via TOMM7 to form a complex which homodimerizes PINK1 to activate its kinase function (Youle *et al*., 2012; Eiyama & Okamoto, 2015). Once the PINK1 complex is stabilized on the outer mitochondrial membrane, it recruits Parkin, an E3 ubiquitin ligase. Parkin subsequently becomes phosphorylated and activated by PINK1, which then ubiquitinates mitochondrial proteins, particularly those responsible for mitochondrial fusion. The degradation of these fusion proteins thus throws the mitochondrial dynamic balance in favour of fission (Eiyama & Okamoto, 2015). Additionally, Parkin also enhances mitophagy by recruiting p62 (sequestosome 1, SQSTM1), which interacts with LC3, a protein that is integral in autophagosome formation during mitophagy (Ni *et al*., 2014).

1.5.2 MARCH5

MARCH5 is a transmembrane protein expressed on the outer mitochondrial membrane. It is a relatively novel protein known to localise with MFN2 and DRP1. Being a RING-finger E3 ubiquitin ligase, it is an integral membrane protein which when over expressed triggers mitochondrial fusion, resulting in elongated mitochondria with an extensive network. However, when MARCH5 is down-regulated or when mutated forms are expressed; increased fragmentation is observed indicating elevated mitochondrial fission (Nakamura *et al*., 2006). They concluded that MARCH5 ubiquitinates DRP1 for proteasomal degradation, which in turn reduces fission in a MFN2-dependent manner. This suggested that MARCH5 could also play a role in the regulation of fusion.

Interestingly, Karbowski, (2011) demonstrated that MARCH5 induced lysine-63 linked regulatory ubiquitination of DRP1, an observation supported by Neutzner *et al*., (2008). In an earlier study by Karbowski *et al*., (2007), RING finger mutations of

MARCH5 led to abnormally elongated mitochondria indicative of fusion. According to this study, MARCH5 regulates the sub-cellular trafficking of DRP1 and while the over-expression of MARCH5 causes no changes in mitochondrial morphology, mitochondrial network elongations are observed when MARCH5 is inhibited. This points to an interdependent association between DRP1 and MARCH5 rather than a direct association because when DRP1 is ectopically expressed, it leads to a reduction or reversal in the abnormalities induced by the expression of MARCH5 mutants (Karbowski *et al*., 2007). The mechanisms by which PINK1/Parkin and MARCH5 lead to the regulation of mitochondrial dynamics and morphology indicate the influence that these E3 ubiquitin ligases have on the functioning these organelles and highlights their importance during UPS activity in the control of mitochondrial homeostasis.

The tagging of proteins ubiquitin molecules can have different outcomes. As mentioned previously, poly-ubiquitination of proteins on lysine-48 leads to proteasomal degradation, whereas mono-ubiquitination on lysine-63 leads to regulation of protein activities through inhibition, activation or transport within the cell. It is believed that the most likely mechanism by which ubiquitin-tagged proteins are transported out of the mitochondrial membrane is via translocation enabled by the ATPases, which are associated with diverse cellular activities. Once in the cytosol, the proteins can then be degraded by the 26S proteasome (Neutzner *et al*., 2008). In the context of DOX-induced cardiotoxicity, research conducted by our group has previously demonstrated that therapeutically relevant doses of DOX can either augment or diminish proteasomal activity, and this is associated with an increase the expression of ubiquitin E3 ligases Parkin and March5 (Opperman, 2015). The elevation of these E3 ligases induces proteasomal degradation of fusions proteins and consequently fission ensues in cardiac mitochondria. The influence of E3 ligases is not only limited to mitochondrial E3 ligases, but also to ligases that target proteins involved in the regulation of ROS, apoptosis and other cellular processes (Ranek & Wang, 2009). Considering that ubiquitination is a reversible process regulated by de-ubiquitinating enzymes (DUBs), it is thus plausible to speculate that the manipulation of these enzymes in preventing mitochondrial specific protein degradation is a viable option to promote healthy functional mitochondria and prevent cell death in an effort to improve survival.

1.6 De-ubiquitinating enzymes

De-ubiquitinating enzymes (DUBs) are a group of enzymes whose main purpose is to remove ubiquitin molecules from ubiquitin tagged proteins (**Fig. 1.8**). There are ± 100 known mammalian de-ubiquitinating enzymes and are classified into five main categories:

i. Ubiquitin specific proteases (USPs) are the largest group of DUBs with ± 60 USPs identified
ii. Ovarian-tumour domain DUBs (OTU)
iii. Machado-joseph domain DUBs (MJD)
iv. Ubiquitin c-terminal hydrolases (UCHs)
v. Zinc-dependent JAB1/MPN domain-associated metalloproteases (JAMM)

The first four categories are thiol proteases, while the fifth has a domain called JAMM (JAB1/MPN/Mov34 metalloenzymes) (Endo *et al*., 2009). These enzymes are numerous and are highly expressed and thus ensure their specificity *in vivo*. A soaring number of disease states have been linked to dysfunctional or unexpressed DUBs. While dysfunctional DUBs have been linked with tumour cell survival in cancer patients, Ataxia, Alzheimer's and other neurological disorder have been linked to defective DUBs (Yue *et al*., 2014). DUBs have a catalytic function and possess active sites specific for ubiquitin molecules and their target proteins. When bound to ubiquitin molecules on substrate proteins, they remove the ubiquitin molecule and the protein can function as normal. DUBs also associate with E3 ligases independent of substrate proteins, for reasons that could include regulation of the E3 enzyme function, or an interdependent regulatory relationship between the E3 ligase and the specific DUB (Nijman *et al*., 2005). In the context of DOX-induced cardiotoxicity, there is little research that has been conducted to assess the role that these enzymes play in the broad context of cardiotoxicity; however, research has shown that a number of DUBs play a vital role in the more generalised mechanisms of mitochondrial homeostasis. With these mechanisms in mind, three DUBs have been identified that could prove crucial in this context: USP30, USP9x and USP36.

1.6.1 USP30

USP30 is a DUB whose role is still being explored. Recently, Bingol *et* al., (2014) demonstrated that USP30 inhibits mitophagy by up to 70% and its over-expression induces the de-ubiquitination of proteins ubiquitinated by Parkin. It was further demonstrated that the knockdown of USP30 stimulates mitophagy, leading to the conclusion that USP30 de-ubiquitinates mitochondrial proteins and as a result increases mitochondrial fusion while opposing fission-associated mitophagy. In support of this notion, Nakamura *et al*., (2008) reported that the knockdown of USP30 generates to elongated mitochondria and the development of extensive networks. However when this knockdown was accompanied by the knockdown of the mitofusin proteins, the increase in mitochondrial fusion that was initially observed was inhibited, implying that USP30 promotes fusion in a mitofusin-dependent manner. Interestingly, a diterpenoid derivative, S3, also elevated mitochondrial fusion and rescued previously lost mitochondrial DNA *in vitro* (Yue *et al.,* 2014). The positive results were attributed to the down-regulation of USP30 by S3 since mitofusin or OPA1 mutant cells demonstrated no increase in mitochondrial fusion. Although the above described study was conducted in the neurological context, extensive research remains to be conducted as USP30 inhibition also induced Lys 63 ubiquitination of the mitofusins.

1.6.2 USP9x

USP9x stabilizes E3 ligases, and de-ubiquitinates proteins that are important for cell polarity and adhesion (Nathan *et al*., 2008). It is considered important in this context as it has been associated with the anti-apoptotic protein MCL-1. MCL-1, a member of the Bcl-2 family of apoptosis-regulating proteins, is ubiquitinated during cellular stress by the E3 ligase MULE (MCL-1 Ubiquitin Ligase). Therefore, USP9x de-ubiquitinates MCL-1 by removing lysine 48 linked ubiquitin molecules tagged by MULE and inhibits its degradation (Karbowski & Youle, 2011). USP9x has also been shown to play a significant role in the increased expression of MARCH7, a protein closely related to MARCH5 but functions as a regulator of T-lymphocytes and

cytokine signalling (Nathan *et al.,* 2008). However, for this study, MARCH7 will not be explored further.

1.6.3 USP36

USP36 has previously been described to play a role in oxidative stress levels of the cell by localizing to the nucleoli. This enzyme has been found to interact with a major mitochondrial anti-oxidant, MnSOD (manganese superoxide dismutase, SOD2) (Kim *et al*., 2011). MnSOD undergoes poly-ubiquitination and eventual degradation during conditions of stress by unknown E3 ligases. USP36 thus de-ubiquitinates MnSOD and prevents its degradation which could prove beneficial in this context. Keeping anti-oxidants at optimum levels is important seeing that MnSOD reduces the levels of the superoxide anions which are major contributors of oxidative stress (Kim *et al.,* 2011). In a different context, USP36 has also been shown to regulate autophagic activity and thereby possibly influences mitophagic activity. Evidence of this was provided by Taillebourg and colleagues (2012) who demonstrated that USP36 inhibition stimulates elevated autophagy which when excessive is detrimental in this context.

1.7 Study Rational

While extensive research has been conducted on various facets of DOX-induced cardiotoxicity, very little attention has been paid to research investigating the potential role that DUBs have in the ability to reduce the cardiomyopathies associated with DOX treatment. Much of the effort has been concentrated on the oxidative stress hypothesis and the concept of anti-oxidants serving as adjuvant therapies to little success (Van Dalen *et al*., 2005); whereas others have focused on anthracycline derivatives and the use of iron-chelating agents. Despite these efforts, all have faced road blocks resulting in very little sustainable clinical success.

As observed above, cardiac mitochondria play a central role in the development of cardiotoxicity (Parra *et al*., 2008), and key to this is mitochondrial dynamics regulated by mitochondrial fusion and fission. This process becomes dysregulated in the presence of DOX via oxidative stress, the association of DOX with cardiolipin, as

well as the degradation of fusion proteins by the UPS, whilst promoting fission. Therefore, by investigating the role of DUBs in this context, this study anticipates that the results obtained will lead to a better understanding of the mechanism/s that induce cardiotoxicity and identify avenues for exploration for therapeutic intervention.

1.8 Hypothesis

In light of the above information, this study hypothesizes that manipulating the expression of de-ubiquitinating enzymes reduces mitochondrial dysfunction by promoting fusion and improving ATP synthesis in the context of chronic DOX-induced toxicity.

1.9 AIMS

- Develop models of chronic DOX-induced cytotoxicity and cardiotoxicity
- Establish the role of specific DUBS in this context

1.10 OBJECTIVES

- To establish chronic model of DOX-induced toxicity
    - *in vitro* (cytotoxicity) and *in vivo* (cardiotoxicity)
- To determine the relative expression of DUBs during chronic DOX-induced toxicity *in vitro* and *in vivo*
- To assess the relative expression of downstream proteins associated with the specific DUBs *in vitro* and *in vivo*
- To determine the relative protein expression of downstream proteins following the down-regulation DUBs (via SiRNA) *in vitro*
- To establish the effect of down-regulation of these DUBs on mitochondrial health by measuring mitochondrial toxicity, ATP synthesis and mitochondrial morphology

MATERIALS and METHODS

2.1 H9C2 CARDIOMYOBLAST CELL CULTURE

H9C2 rat cardiomyoblasts (European Collection of Cell Cultures, Salisbury, UK) were utilized for the duration of this study. These cells are a commonly used cell line in this context as they are robust, easy to maintain and have the advantage of being an *in vitro* alternative. Moreover, these cells have previously been shown to respond in a similar fashion to primary cardiomyocytes to hypertrophic stimuli, thus validating their importance as a model for *in vitro* studies investigating various heart diseases (Watkins *et al*., 2011). The cells were seeded in T25 culture flasks (1,000,000 cells) and 6-well plates (200,000 cells per well). Once seeded, the cells were cultured under sterile conditions in Dulbecco's Modified Eagle's Medium (DMEM) (Gibco, 41965-039) that was supplemented with 10% Fetal Bovine Serum (FBS) (Biocom Biotech, FBS-G1-12A) and 1% Penicillin/Streptomycin (ThermoFisher Scientific, 15140-122). The cells were maintained at 37 ^{o}C in a humidified atmosphere of 95% oxygen (O_2) and 5% carbon dioxide (CO_2). Cellular health was maintained by refreshing culture media every 48 hours (hrs) and cells were sub-cultured and seeded into culture plates or flasks for further experimentation once 70% confluence was attained (for detailed methods, refer to **Appendix B**, pg. 83).

2.1.1 Doxorubicin treatment (*in vitro* model)

The anthracycline antibiotic DOX (Sigma-Alrich, D1515) was used as the chemotherapeutic agent to induce cytotoxicity in this model. This anthracycline antibiotic is often used as the first-line treatment for various types of cancers (Minotti *et al*., 2004). A 3.4 mM stock was prepared in sterile DMEM and stored in the dark (light sensitive) at -20 ^{o}C until required. As this study attempted to simulate chronic cytotoxicity, cells were treated daily with 0.2 µM DOX for 120 hrs (5 days). This was done to take into account the cumulative dose dependent characteristics of the chronic form of cytotoxicity. Therefore, after treatment was complete, the total cumulative dose of DOX would be 1.0 µM (0.2 µM x 5 days = 1.0 µM). This cumulative dose also falls within the clinically relevant DOX concentration

appropriate for *in vitro* models (Minotti *et al*., 2004) (for detailed methods, refer to **Appendix B**, pg. 86).

2.2 Animal Care and Ethical Consideration (*in vivo* model)

2.2.1 Study Approval

This animal study was reviewed and approved by the Stellenbosch University Animal Ethics committee (SU-ACUD 15-00038). The guidelines followed are those from the South African National Standards 10386:2008. (**Appendix D**, pg. 101)

Eight four week old male wild-type Sprague Dawley rats, of average weight 120g were purchased from the Stellenbosch University animal unit. The animals were randomly housed 3-4 per cage (sterile and ventilated) and were acclimatized to the new environment for one week before experimentation commenced. The temperature (21-25 ^{o}C) and 12-hour day/night cycles were controlled and constantly monitored by qualified animal house managers throughout the duration of the study. The animals were nourished with a constant supply of standard rat chow and water *ad libitum*. Environmental enrichment was achieved through the use of red Perspex tubing and shredded paper.

2.2.2 DOX treatment

Animal body weights were recorded three times a week each morning that injections were prepared. The animals were treated from five weeks of age with 2.5 mg/kg DOX over a period of eight weeks, resulting in a cumulative dose of 20 mg/kg. As mentioned previously, this work was conducted to simulate chronic DOX-induced cardiotoxicity and, in this model in particular, paediatric cancer survivors suffering from cardiotoxicity during their adult lives, considering that this is the group that is most affected by chronic cardiotoxicity (Choi *et al*., 2010). All injections were conducted via intraperitoneal (i.p) administration once a week. Since there were only two experimental groups, the control also received saline injections (i.p) as this was the solvent for the DOX. Although body weight measurements were taken three times a week, animals were observed daily by the researchers involved in this study. Considering the toxic nature of DOX, humane endpoints were put in place to as a

"cost to benefit" measure to ensure minimal animal suffering. The following observations were regarded as humane endpoints at which animals would be euthanized to prevent excessive suffering:

- Loss of >15% body weight
- Failure to eat or drink for a period >24 hrs
- Continuous inflammation of the areas where DOX was injected
- Signs of pain or discomfort (normal posture, clean coat and facial grimacing)

2.2.3 Animal sacrifice and organ harvest

One week after the last DOX injections (week 9), the animals were anesthetized (i.p) with a lethal dose of pentobarbitone (60 mg/kg). Once the pedal reflex was no longer evident, the hearts were excised, weighed and perfused. Therefore, all blood was removed during the perfusion process. Once completed, the hearts were frozen in liquid nitrogen and stored at -80 °C for further analysis. Repeated freeze-thaw cycles were avoided to prevent protein degradation and maintain tissue sample quality. Figure 2.1 below indicates the various experiments that were conducted in this study using the different *in vitro* and *in vivo* models and the techniques are briefly described below the figure.

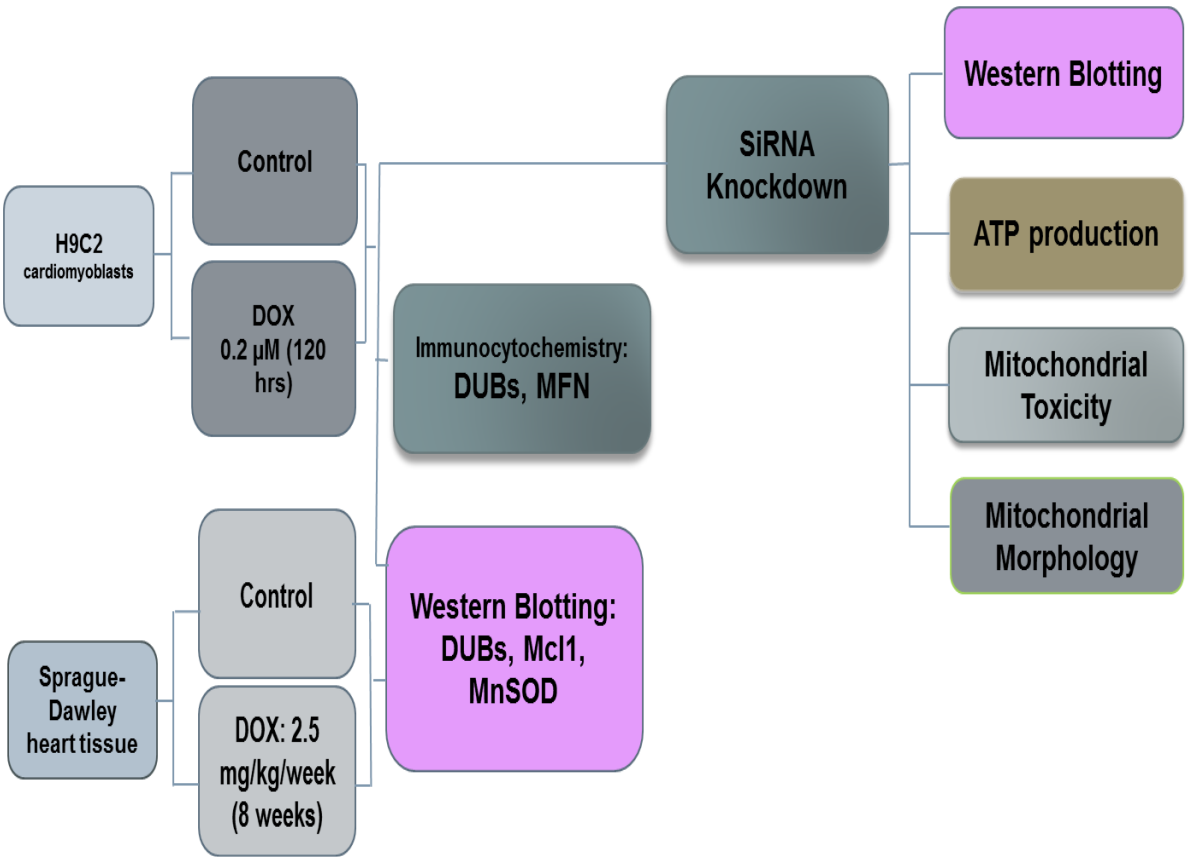

Figure 0.1: Schematic diagram showing the approach used to achieve the research objectives

2.3 Western Blotting

2.3.1 Preparation of cell and tissue lysates

Cell lysates: 24 hours after treatment, growth medium was removed and the monolayer of cells was washed with sterile ice-cold phosphate buffered saline (PBS). The cells were scraped off the surface of the flask or plates, after 50 µL radio-immunoprecipitation assay (RIPA) buffer was added. This process was then followed by the transfer of cell/lysis buffer solutions into chilled Eppendorf tubes for sonification using an ultrasonic homogenizer (Misonix, Qsonica, USA). The cells were sonicated for ±10 seconds at amplitude of 10 m, after which the contents were centrifuged at 8000 rpm (5900 g) for 10 minutes. The pellet was discarded, and the supernatant was preserved for protein determination. All of the above was conducted on ice.

Tissue lysates: a similar process to the above was followed for the preparation of the tissue lysates, with minor modifications. Briefly, 250 µL RIPA was added to each thawed tissue sample placed into chilled test tubes. All samples were then homogenized with a polytron benchtop homogenizer (Kinematica, USA) separately for ±30 seconds at 30000 rpm (20124 g). Careful attention was paid during this process to avoid cross contamination between samples. The content of each test tube was transferred into chilled Eppendorf tubes for centrifugation (Labnet) (12000 rpm/ 13300 g, 4^{o}C, for 20 minutes). The pellet was discarded and the supernatant was preserved (for detailed methods, refer to **Appendix B**, pg. 87).

2.3.2 Protein determination of cell and tissue lysates.

Determination of protein concentration was performed using the Direct Detect ™ Spectrometer (Merck Millipore DDHW00010-WW Darmstadt, Germany). This system determines protein concentration within the ranges of 0.25 – 5 mg/mL accurately by measuring amide bonds in protein chains. As such, it accurately quantifies this intrinsic property of every protein without relying on amino acid composition, dye binding properties, or redox potential, eliminating the pitfalls of colorimetric assays such as the Bradford technique often used to determine protein concentrations. 2 µL of RIPA buffer (blank) was used to calibrate the system, where after 2 µL of each sample was also placed into an Assay-free card. The card was then inserted into the Direct Detect ™ machine, and protein concentration (mg/ml) was determined per sample. This process was conducted in triplicates (for detailed methods, refer to **Appendix B**, pg. 87).

2.3.3 Sample preparation and gel electrophoresis

50 µg protein from cells and 100 µg protein from tissue samples were subjected to polyacrylamide gel electrophoresis using 12% graded gels (Bio-Rad, 456-8084). The proteins were transferred onto polyvinylidinefluoride (PVDF) membranes (Bio-Rad, 170-4156) and blocked in 5% milk for two hrs. PVDF membranes were incubated with specific primary antibodies overnight at 4 ºC in Tris-buffered saline tween (TBST). Following a few wash steps, the membranes were incubated in appropriate secondary antibodies (**Table 2**) for one hr at room temperature, where after the membranes were then processed for chemiluminescent detection using the clarity ECL substrate (Bio-Rad, 170-5061) in the Chemi-Doc™ XRS system (Bio-Rad,

USA). Band intensity quantification was conducted using ImageLab software version 5.0 (for detailed methods, refer to **Appendix B**, pg. 88).

Table 2: A list of various antibodies used throughout the study.

	Primary antibodies		
Name	**Size (kD)**	**Company**	**Catalogue Number**
USP9x	270	Cell Signalling	5751
USP30	59	Santa Cruz	Sc-109455
USP36	123	Santa Cruz	Sc-82104
MCL1	40 and 32	Santa Cruz	Sc-819
MFN1	84	Abcam	ab129154
MFN2	86	Abcam	ab124773
SOD2 (MnSOD)	24	Cell Signalling	1314S
TOMM20	16	Cell Signalling	42406
β-actin	45	Cell Signalling	5125
	Secondary antibodies		
Anti-rabbit		Cell Signalling	7074

Donkey anti-goat	Abcam	ab97110
	Fluorescent antibodies	
FITC	Lifetech	A-31577
TxsRED	Lifetech	A-21432

Also indicated are the companies where these were purchased from, as well as the catalogue numbers. Abbreviations: **FITC**: Fluorescein Isothiocyanate, **MCL1**: Myeloid Cell Leukaemia 1, **MFN**: Mitofusin, **SOD**: Superoxide Dismutase **TOMM**: Translocase of Outer Mitochondrial Membrane, **TxsRED**: Texas Red, **USP**: Ubiquitin Specific protease.

2.4 Immunocytochemistry

Cells were cultured, monitored and treated as previously described on micro cover slips in 6-well plates (200,000 cells per well). After treatment media was removed and the monolayer of the cells was washed twice with warm PBS. The coverslips were removed and placed onto glass slides where after they were washed twice in cold PBS, and then fixed for ten minutes at 37^{o}C with 4% paraformaldehyde (Sigma, 158127). The cells were permeated using 0.1% triton solution (Sigma, X-100) and then blocked with 5% donkey serum (Cell Tech, UK) for 30 minutes at room temperature. Cells were washed three times with cold PBS and then incubated with primary antibodies against USP36, USP30, MCL1, MFN1 and MFN2 overnight in a wet chamber at 4 ^{o}C. Following this incubation period, the cells were washed with cold PBS and incubated in secondary antibody (Donkey anti-goat, and rabbit anti-mouse) for an hour at room temperature in a dark wet chamber and then stained with Hoechst (Thermofisher Scientific H1399) for ten minutes and then washed again with PBS. After this step, the coverslips were mounted onto glass slides using DAKO fluorescent mounting media (Diagnostech, s3022380), sealed with nail polish and then stored at -20 degrees in the dark until imaging (for detailed methods, refer to **Appendix B**, pg. 90).

2.4.1 Imaging

Imaging was achieved using a Nikon eclipse E400 fluorescent microscope equipped with a DMX1200 CCD camera 200. Images were acquired through the Nikon plan Flour 10x and 40x objective lenses. Each experimental group consisted of three replicates and three random images were taken per replicate either at 10x or 40x magnification and these served as representative images per group. It must be noted that no quantification was conducted as this experiment served only as a visual supplementation to the data obtained from the western blots.

2.5 Transfection with siRNA

Transfection was performed on H9c2 cells at a transfection density of $2.5x10^5$ cells/mL by electroporation with the Neon® transfection system (Invitrogen MPK5000) and then seeded into 6 and 96-well plates. The cells were maintained in an incubator at 37^o C, in a humidified atmosphere of 95% O_2 and 5% CO_2. 24 hours post siRNA administration, culture medium was replaced with fresh media, and maintained for 72 hours after which the cells were subjected to chronic DOX (0.2µM daily for 120 hrs) treatment and used for a toxicity assay or harvested for western blots. USP30 (SI01668807), USP36 (SI01661331), USP9x (SI101840363) siRNA and negative control (1027280) were purchased from Qiagen. The SiRNAs were used at a working concentration of 20 µM and diluted to 200 nM for transfection via electroporation (for detailed methods, refer to **Appendix B**, pg. 92).

2.6 Mitochondrial Toxicity

Mitochondrial toxicity was measured using the MitochondrialToxGlo ™ Assay (Promega G8000). This assay assesses mitochondrial dysfunction as a result of xenobiotic exposure. It measures membrane integrity first using bis-AAF-R110, a fluorogenic peptide substrate to measure “dead cell protease activity”, which is the activity of a specific protease associated with necrosis. The intact membranes of healthy cells are impermeable to the substrate, and as such non-viable cells produce higher signals. It also measures ATP concentration through an ATP detection reagent which causes cell lysis and the generation of a luminescent signal proportional to the ATP present.

Following transfection, 10000 cells were seeded at a density of 5 x 10^6 cells/mL in a 96-well plate for 48 hrs and treated as previously described. The assay was conducted and measured according to the manufacturers' protocol, where after the fluorescent signal produced was measured with a FLK800 fluorescence microplate reader (Bio-tek, USA) and luminescence measured using the GloMax® 96 Microplate Luminometer (Promega, USA) (for detailed methods, refer to **Appendix B**, pg. 94).

2.7 Mitochondrial Morphology

Mitochondrial shape often regulates life or death signals and this study found it appropriate to assess their morphology under these conditions. Following transfection, cells were seeded (10000 cells per well) and treated as previously described in Nunc Lab-Tek™ 8-well chambers (ThermoFisher Scientific, 154534). Once treatment was complete, cells were washed with sterile PBS and incubated with MitoTracker Green™ (ThermoFisher Scientific, M-7514) and Hoechst for 20 mins. MitoTracker Green™ (0.5 μM) binds to free sulfhydryl proteins present in mitochondria, and produces a green fluorescent signal which can be visualized by fluorescence microscopy. Cells were visualised live at 60x magnification with the OLYMPUS Plan Apo N60x/1.4 oil objective of the Olympus IX81 wide field fluorescent microscope (Zeiss). Z-stack images using appropriate upper and lower focal points were acquired and images were processed and displayed at maximum intensity projection using the Cell^R software (for detailed methods, refer to **Appendix B**, pg. 92).

2.8 Statistical analysis

Data are presented as mean ± standard error of the mean (SEM). A p-value of less than (<) 0.05 was considered statistically significant. All data was normalized to a percentage of the respective control groups. Experiments involving two groups were analysed with the Student's unpaired t-test, followed by the Mann-Whitney test. Experiments with more than two groups were analysed through one-way ANOVA with Bonferroni post-hoc correction using Graph-pad Prism ™ software version 5 for visual representation and statistical significance.

RESULTS

3.1 Protein expression

To determine baseline protein expression of the different DUBs and their downstream proteins, western blotting was performed on both the cell lysates (*in vitro)* and tissue samples (*in vivo*). This was deemed important to establish the effect that DOX induces on these proteins when compared to the controls.

3.1.1 USP9x and MCL-1

USP9x, a 270 kD protein is a ubiquitin specific protease responsible for the de-ubiquitination of MCL-1, an important protein involved in the regulation of apoptosis. Our results demonstrate that chronic DOX treatment significantly increased the expression of USP 9x *in vitro* (337.2 ± 41.6%, $p<0.05$) and *in vivo* (194.6 ± 15.2%, $p<0.05$) when compared to the control (**Fig. 3.1**).

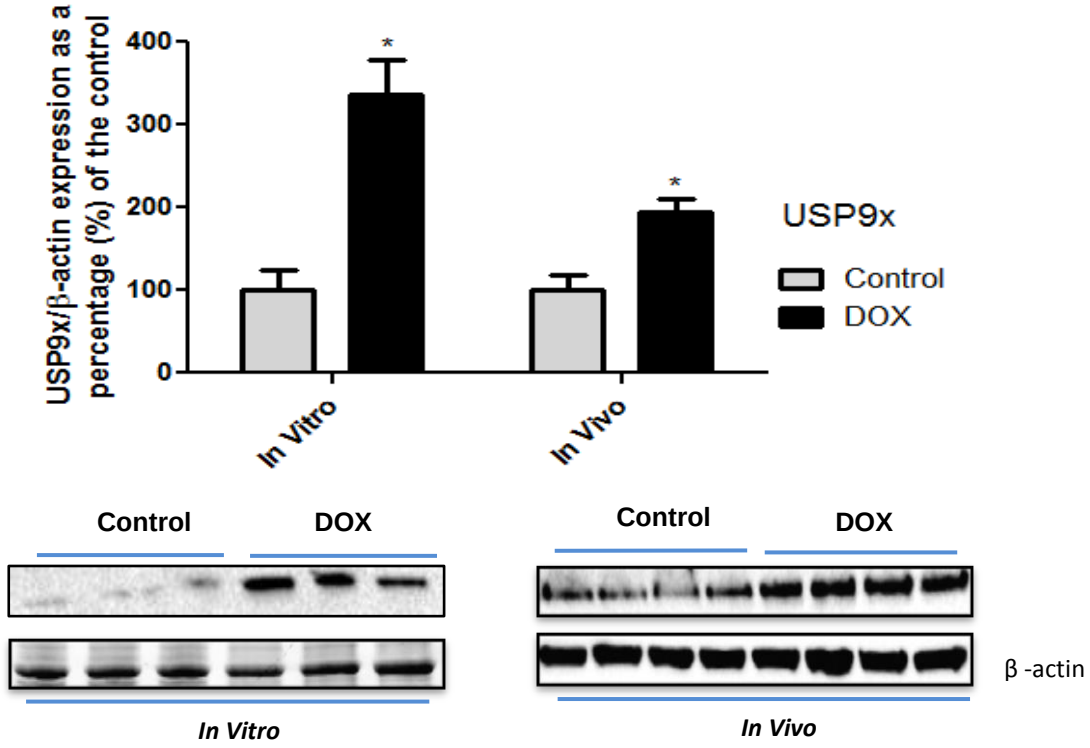

Figure 0.1: Relative protein expression of USP9x following prolonged treatment with DOX *in vitro* and *in vivo*.

H9C2 cells were treated with 0.2 µM DOX daily for 120 hrs, and Sprague-Dawley rats treated i.p. with 2.5 mg/kg DOX for 8 weeks. Results are represented as mean ± SEM (n = 3-5) *p<0.05 vs. control. β-actin was used as a loading control. Abbreviations: **DOX -** Doxorubicin **USP -** Ubiquitin specific protease.

Myeloid Cell Leukemia 1 (MCL-1) is an anti-apoptotic protein that is de-ubiquitinated by USP9x, and therefore, its expression is important for this context. While MCL-1 is ubiquitinated for degradation, it also undergoes post-translational modification, resulting in two fragments that have opposing functions (Bae *et al*., 2000). On the one hand, the anti-apoptotic long fragment of MCL-1 (MCL-1L) was significantly reduced *in vitro* (43.18 ± 16.3%, p< 0.05) in the DOX treated group, whereas only a trend towards a decrease was observed *in vivo* when compared to the control (**Fig. 3.2**).

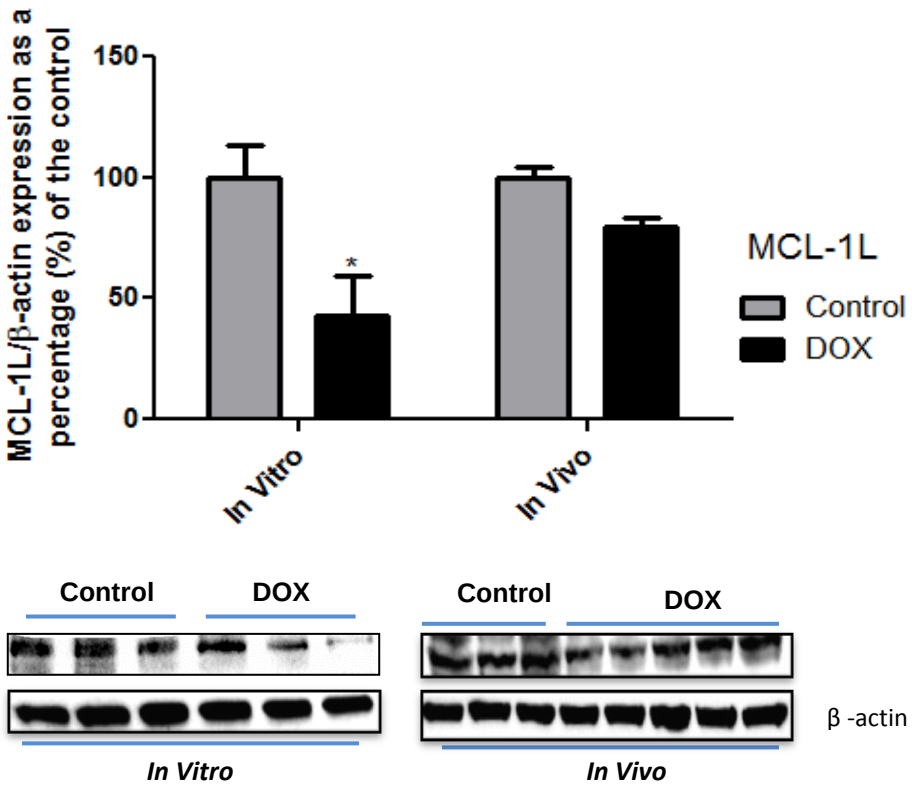

Figure 0.2: Relative protein expression of MCL-1L following prolonged treatment with DOX *in vitro* and *in vivo*.

H9C2 cells were treated with 0.2 µM DOX daily for 120 hrs, and Sprague-Dawley rats treated i.p. with 2.5 mg/kg DOX for 8 weeks. Results are represented as mean ± SEM (n = 3-5). *p<0.05 vs. control. β-actin was used as a loading control. Abbreviations: **DOX** - Doxorubicin **MCL-1L** - Myeloid Cell Leukaemia-1 long-fragment.

On the other hand, the pro-apoptotic short-fragment of MCL-1 (MCL-1S) was significantly up-regulated *in vivo* (188.7 ± 12.7%, $p<0.05$), while a trend towards an increase was observed *in vitro* (**Fig. 3.3**). The results are in contrast to those obtained for the MCL-1 long fragment, suggesting that the observed increase in USP9x is targeted for the de-ubiquitination of MCL-1L rather than MCL-1S following post translational modification. This further illustrates how DOX induces apoptosis via the promotion of pro-apoptotic factors.

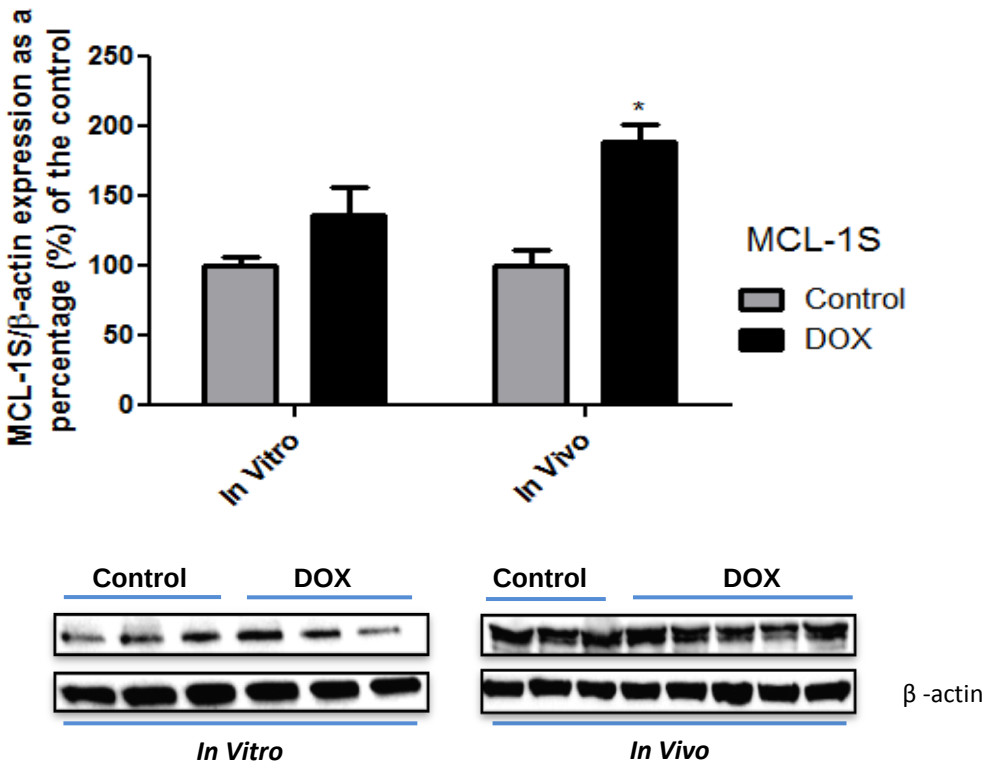

Figure 0.3: Relative protein expression of MCL-1S following prolonged treatment with DOX *in vitro* and *in vivo*.

H9C2 cells were treated with 0.2 μM DOX daily for 120 hrs, and Sprague-Dawley rats treated i.p. with 2.5 mg/kg DOX for 8 weeks. Results are represented as mean ± SEM (n = 3-5). *$p<0.05$ vs. control. β-actin was used as a loading control. Abbreviations: **DOX** - Doxorubicin **MCL-1S -** Myeloid Cell Leukaemia-1 short-fragment.

3.1.2 USP30, MFN1 and MFN2

USP30 is an enzyme known to interact with both mitofusin proteins (MFN1 and MFN2). Its function is rather controversial as some studies indicate it is purely regulatory (Yue *et al*., 2014), while others show either mitochondrial fusion inhibition (Nakamura *et al*., 2008) or mitochondrial fusion promotion (Bingol *et al.,* 2014). Our data demonstrates substantial reduction of this de-ubiquitinating enzyme during DOX treatment *in vitro* (45.2 ± 13.1%, p<0.05) and *in vivo* (37.3 ± 7.5%, p<0.05) as indicated in (**Fig. 3.4**). This may either imply that USP30 is itself degraded or its synthesis is inhibited.

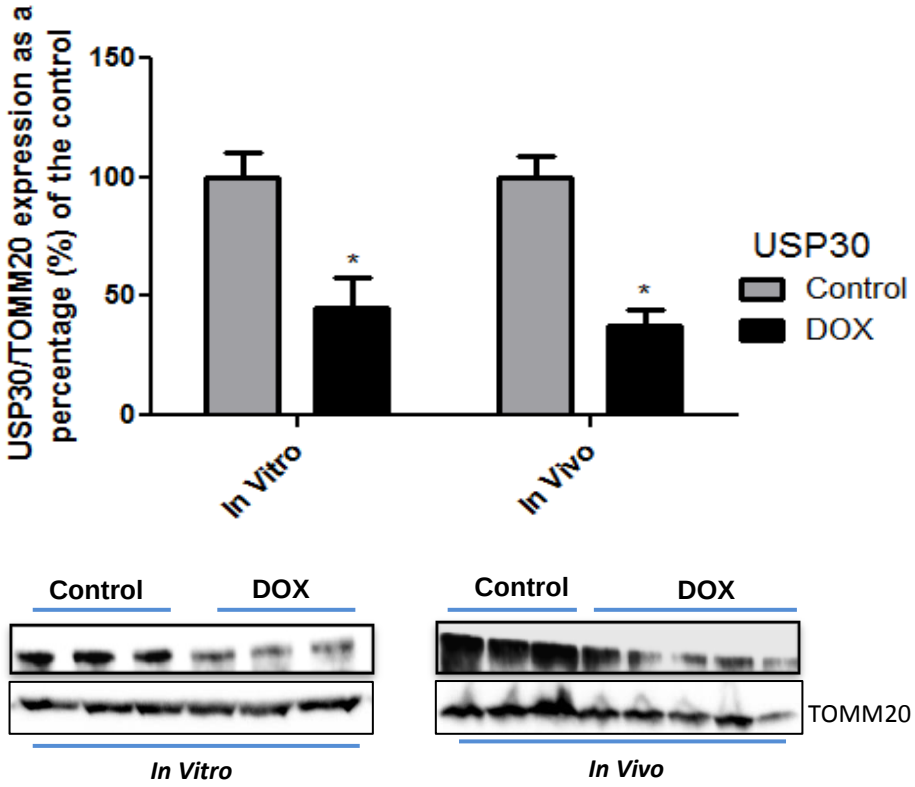

Figure 0.4: Relative protein expression of USP30 following prolonged treatment with DOX *in vitro* and *in vivo*.

H9C2 cells were treated with 0.2 µM DOX daily for 120 hrs, and Sprague-Dawley rats treated i.p. with 2.5 mg/kg DOX for 8 weeks. Results are represented as mean ± SEM (n = 3-5). *p<0.05 vs. control. TOMM20 was used as a loading control. Abbreviations: **DOX -** Doxorubicin **USP -** Ubiquitin specific protease.

Considering that USP30 was significantly reduced, it comes as no surprise that MFN1 was also significantly diminished *in vitro* (23.9 ± 11.9%, $p<0.05$) and *in vivo* (58.3 ± 4.9%, $p<0.05$) when compared to the controls (**Fig. 3.5**). These results indicate that MFN1 is tagged with ubiquitin molecules by E3 ligases and subsequently degraded due to the downgraded levels of USP30 and thus no inhibition of ubiquitination; hence degradation.

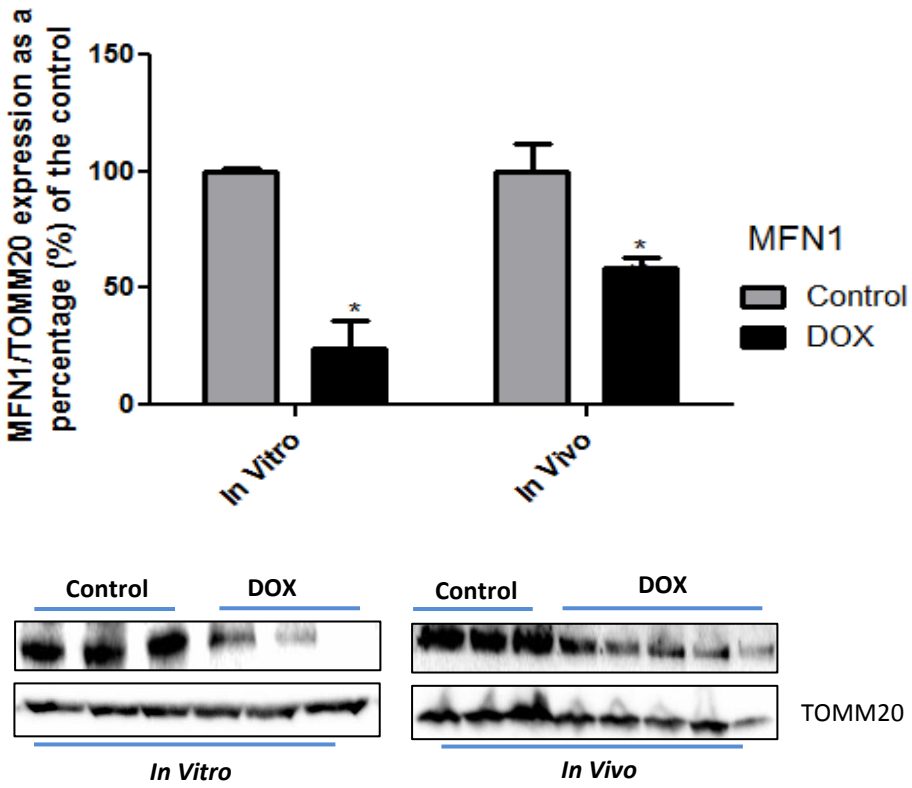

Figure 0.5: Relative protein expression of MFN1 following prolonged treatment with DOX *in vitro* and *in vivo*.

H9C2 cells were treated with 0.2 µM DOX daily for 120 hrs, and Sprague-Dawley rats treated i.p. with 2.5 mg/kg DOX for 8 weeks. Results are represented as mean ± SEM (n = 3-5). *$p<0.05$ vs. control. TOMM20 was used as a loading control. Abbreviations: **DOX** – Doxorubicin, **MFN1 -** Mitofusin 1.

An unexpected result for baseline MFN2 protein expression was obtained in the *in vitro* model where significantly elevated levels of this protein (259.2 ± 15.4%, $p<0.05$)

were observed. This was surprising considering the fact that USP30 targets both mitofusin proteins during de-ubiquitination. In contrast however, the results of the *in vivo* model (68.0 ± 3.6%, $p<0.05$) echoed those observed for MFN1 (**Fig. 3.6**).

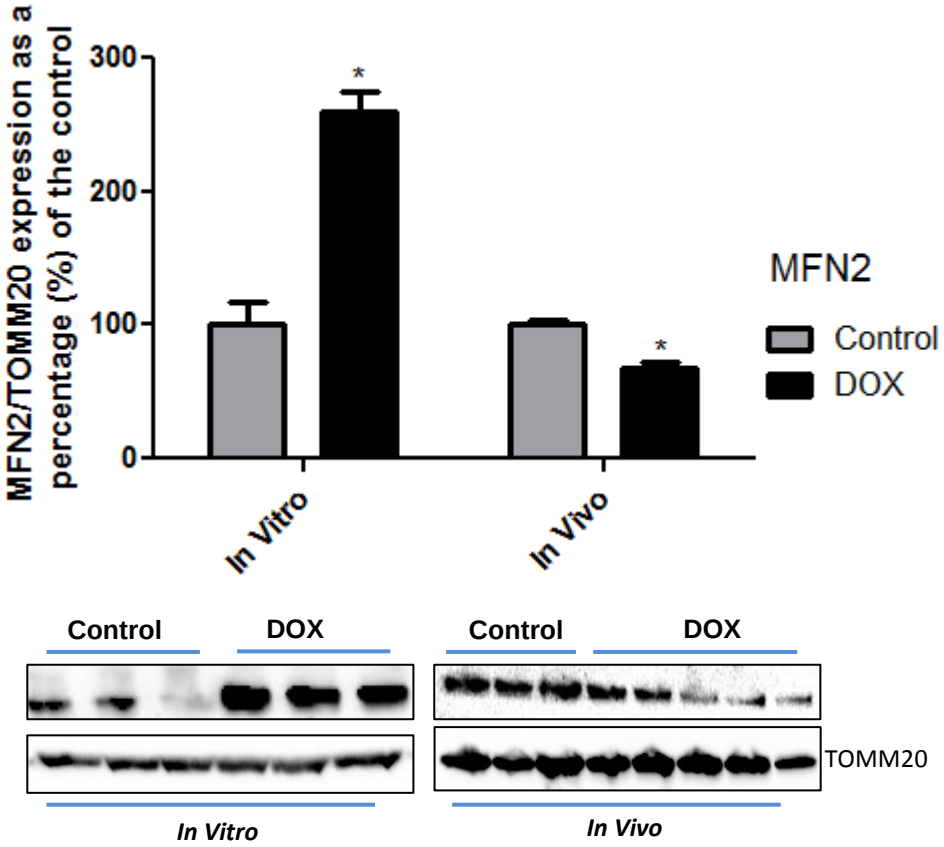

Figure 0.6: Relative protein expression of MFN2 following prolonged treatment with DOX *in vitro* and *in vivo*.

H9C2 cells were treated with 0.2 μM DOX daily for 120 hrs, and Sprague-Dawley rats treated i.p. with 2.5 mg/kg DOX for 8 weeks. Results are represented as mean ± SEM (n = 3-5). *$p<0.05$ vs. control. TOMM20 was used as a loading control. Abbreviations: **DOX** – Doxorubicin, **MFN2 -** Mitofusin 2.

3.1.3 USP36 and SOD2

The third de-ubiquitinase of interest in this study is USP36, known to remove ubiquitin molecules from SOD2 (MnSOD). While its role in this context is yet to be elucidated, the E3 ligase responsible for ubiquitinating SOD2 is currently unknown. As indicated in **Fig. 3.7.**, no significant changes in the expression of USP36 were observed when the two groups were compared to one another in both models used.

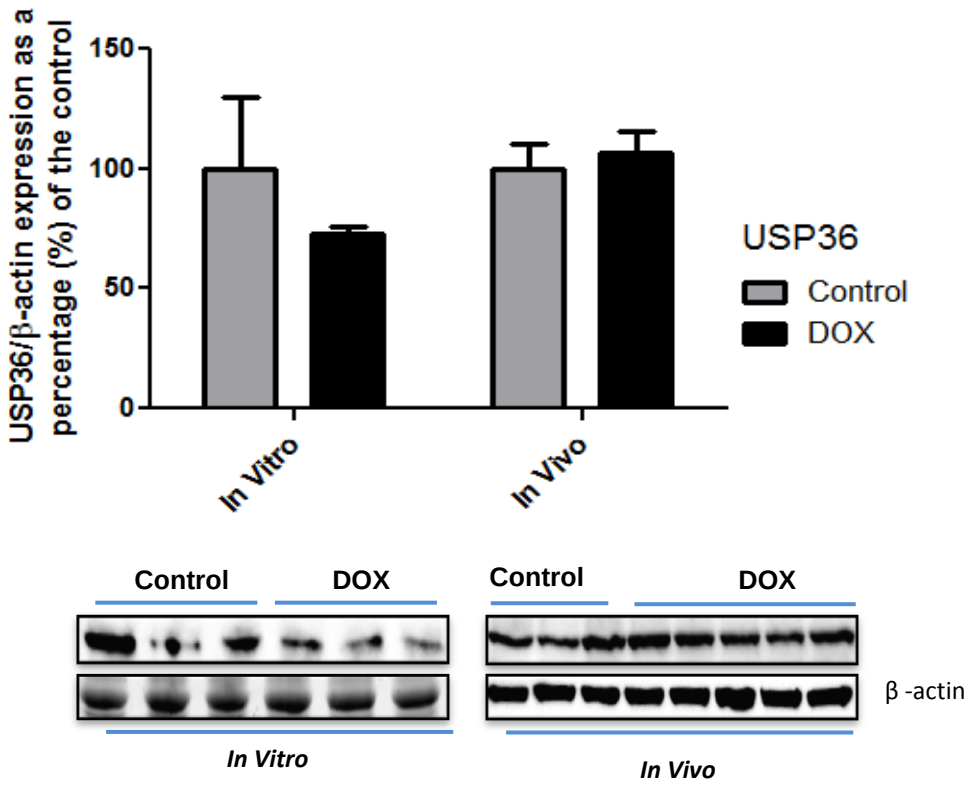

Figure 0.7: Relative protein expression of USP36 following prolonged treatment with DOX *in vitro* and *in vivo*.

H9C2 cells were treated with 0.2 μM DOX daily for 120 hrs, and Sprague-Dawley rats treated i.p. with 2.5 mg/kg DOX for 8 weeks. Results are represented as mean ± SEM (n = 3-5). β-actin was used as a loading control. Abbreviations: **DOX**: Doxorubicin **USP:** Ubiquitin Specific Protease

SOD2 (MnSOD) plays a vital role in the modulation of oxidative stress due to its ROS scavenging properties. Mainly localised to the mitochondria (Van Remmen *et al*., 2003), they serve as one of the many anti-oxidants available in a cell to protect against oxidative damage. While no substantial changes were observed *in vivo* (**Fig. 3.8)**, SOD2 was substantially elevated in response to DOX *in vitro* (336.9 ± 45.5%, $p<0.05$). DOX is notorious for its ROS producing properties, and therefore this increase in SOD2 implies a compensatory response from the cells to the augmented oxidative stress conditions by increasing their anti-oxidant defences.

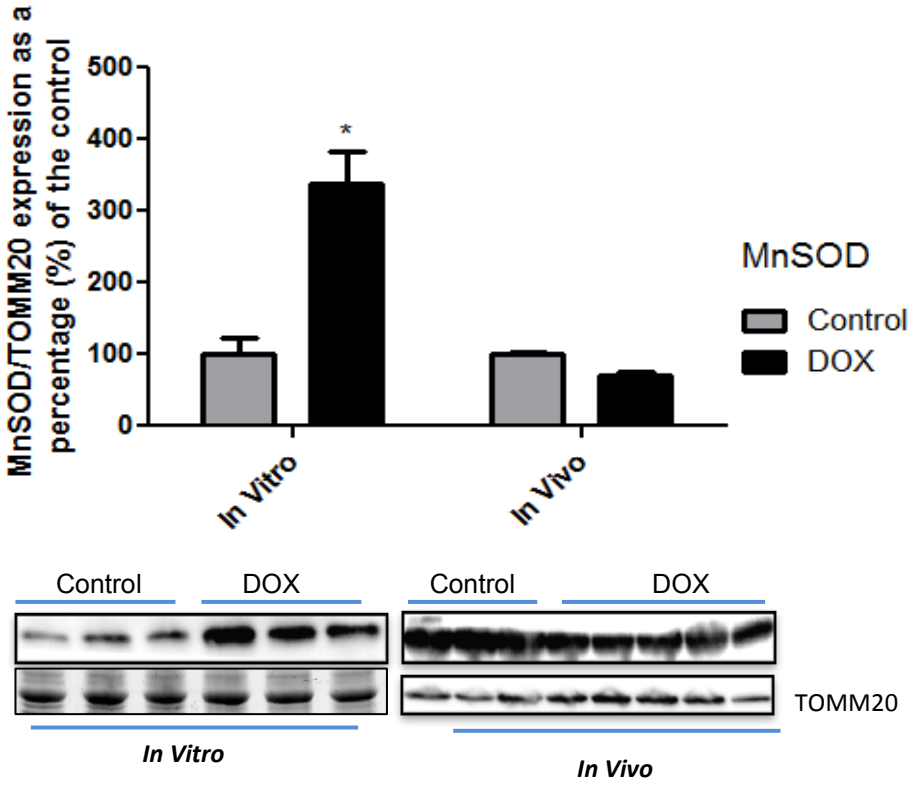

Figure 0.8: Relative protein expression of SOD2 following prolonged treatment with DOX *in vitro* and *in vivo*.

H9C2 cells were treated with 0.2 μM DOX daily for 120hrs, and Sprague-Dawley rats treated i.p with 2.5 mg/kg DOX for 8 weeks. Results are represented as mean ± SEM, (n=3-5). *p<0.05 vs control. TOMM20 was used as a loading control. Abbreviations: **DOX** - Doxorubicin **SOD -** Superoxide Dismutase

3.2 Immunocytochemistry

In an effort to re-enforce the results obtained via western blotting, and to obtain the relative localization of the DUBs relevant in this study, immunocytochemistry was performed *in vitro* and visualised by fluorescence microscopy as indicated in the methods. It should be noted that only USP30 and USP36 were assessed as no appropriate antibody for USP9x for this specific experiment was available at the time. No quantification of this data was conducted and representative images are displayed.

3.2.1 USP30

According to our results (**Fig. 3.9**), USP30 appears to be highly expressed under control (untreated) conditions than under DOX treatment conditions. This was expected as USP30 regulates the degradation (de-ubiquitination) of mitofusin proteins (MFN1 and MFN2) (Nakamura *et al*., 2008). On the contrary, the fluorescent signal for this DUB was significantly reduced during DOX treatment, indicating that ubiquitination occurred and degradation ensued. It is clear from the images below that USP30 not only localises within the nucleus (encircled), it also appears to localise around the peri-nuclear region (arrows) under control conditions. Since the nucleus is surrounded by the endoplasmic reticulum and mitochondria (Preuss *et al.,* 1991; de Brito & Scorrano, 2008), the most likely organelle that this enzyme would localize with is the mitochondrion. In the presence of DOX however, no localization within the nucleus was observed. The results obtained in this experiment reaffirm those acquired by western blotting.

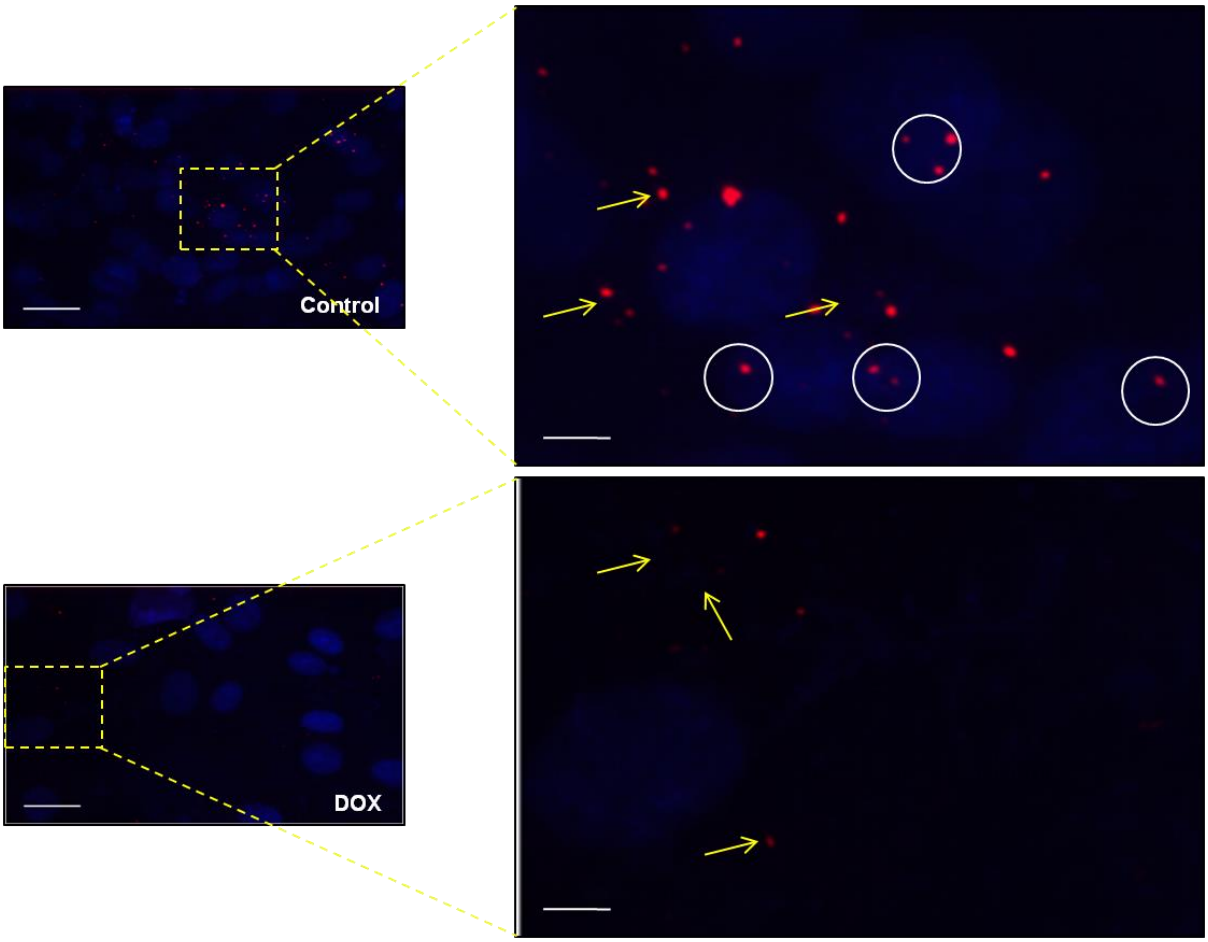

Figure 0.9: Immunofluorescent images showing relative protein expression of USP30 during untreated and treated conditions with DOX in vitro.

H9C2 cardiomyoblasts were treated with 0.2 µM DOX daily for 120 hrs (Blue - nucleus, Red - USP30). Peri-nuclear localisation is indicated by arrows (yellow) and localisation within the nuclear region is indicated by circles (white). Abbreviations**: USP -** Ubiquitin Specific Protease**, DOX -** Doxorubicin**.** Magnification = 40x, Scale bar = 25 µm.

3.2.2 USP36

While the western blot experiments revealed no significant results in terms of relative USP36 protein expression, the fluorescent images displayed in **Fig. 3.10** tell a different story. Under control conditions, it was found that a generally low fluorescent signal for USP36 was observed in the cytosol, and in some areas (encircled) appears to be quite prominent. Interestingly, during DOX treatment, USP36 accumulates within specific cytosolic regions and appear as protein aggregates. These aggregates produced an intense fluorescent signal that would otherwise not be recognized in the absence of DOX. These results imply that in response to DOX-

induced oxidative stress, cells trigger enhanced USP36 expression for de-ubiquitination of SOD2 (MnSOD) as a defence mechanism to protect against the damaging effects of ROS.

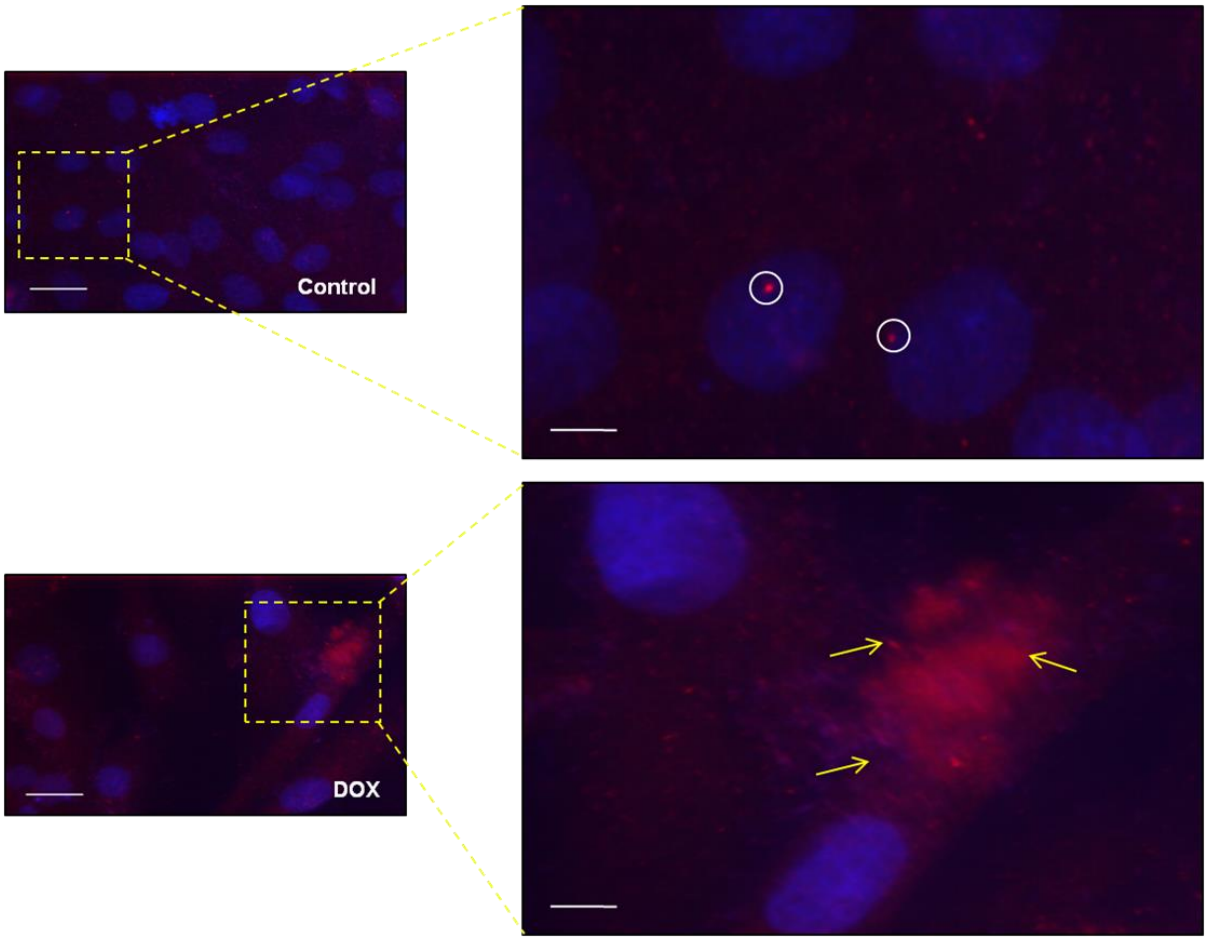

Figure 0.10: Immunofluorescent images showing relative protein expression of USP36 during untreated and treated conditions with DOX in vitro.

H9C2 cardiomyoblasts were treated with 0.2 µM DOX daily for 120 hrs (Blue - nucleus, Red - USP36 Peri-nuclear localisation is indicated by arrows (yellow) and localisation within the nuclear region is indicated by circles (white). Abbreviations: **USP** - Ubiquitin Specific Protease, **DOX** - Doxorubicin. Magnification = 40x, Scale bar = 25 µm.

3.3 SiRNA (Down-regulation) of de-ubiquitinating enzymes

Now that this study has addressed the first three aims from the experiments described above, we aimed to determine the effects of various mitochondrial parameters during DOX treatment when each of the DUBs were down-regulated using SiRNA. To make sure that successful down-regulation was achieved; western blotting was again used to determine relative protein expression of these DUBs and their downstream targets.

3.3.1 USP9x and MCL1

USP9x was successfully knocked down when the protein expression levels were compared to the control (**Fig. 3.11A**). To then determine what effect down-regulation of USP9x had on its target MCL1 in the presence or absence of DOX, both MCL1 fragments were assessed. On the one hand, the long-fragment of MCL (MCL-1L) was elevated (207.1 ± 25.6%, $p<0.001$) in the absence of DOX when compared to the control (100.0 ± 9.1%), and a modest increase was observed in the presence of DOX when compared to the DOX group without down-regulation (**Fig. 3.11B**). On the other hand, when USP9x was knocked down, the short-fragment of MCL1 (MCL-1S) showed a trend towards increased expression versus the control. However, in the presence of DOX, MCL-1S was significantly reduced (84.6 ± 9.6%, $p<0.05$) versus the DOX group without down-regulation (158.2 ± 16.9%) (**Fig. 3.11C**). These results are promising seeing that MCL-1L which was modestly increased in this case is anti-apoptotic, whilst pro-apoptotic MCL-1S was reduced.

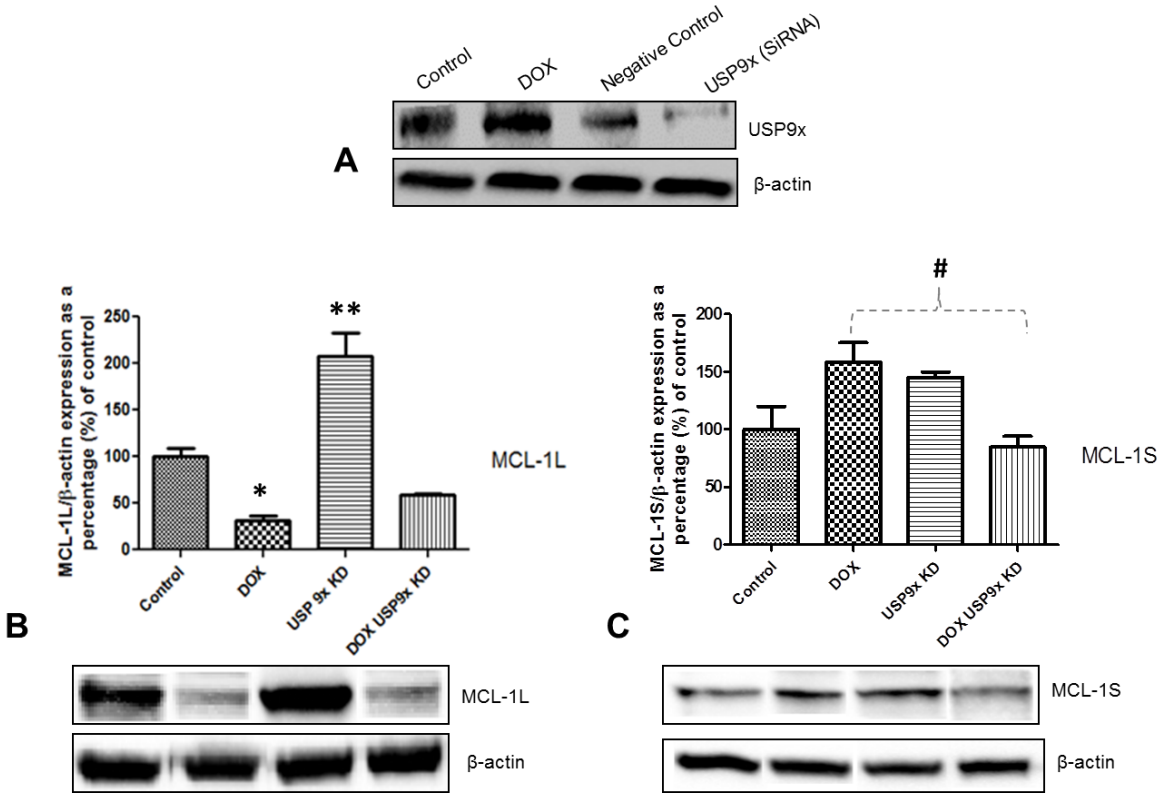

Figure 0.11: Relative USP9x protein expression following SiRNA knockdown in the absence or presence of DOX in vitro

(A) USP9x known-down was achieved by electroporation using SiRNA, where after H9C2 cardiomyoblasts were treated with 0.2 μM DOX daily for 120 hrs. (B) Relative protein expression of MCL-1L after SiRNA (USP9x) treatment in the absence or presence of DOX. (C) Relative protein expression of MCL-1S after SiRNA (USP9x) treatment in the absence or presence of DOX. Results are represented as mean ± SEM (n = 3), *p<0.05, **p<0.001 vs. Control and $^{\#}$p<0.05 vs. DOX. β-actin was used as a loading control. Abbreviations: DOX - Doxorubicin, SiRNA - Silencing RNA, USP9x - Ubiquitin specific protease 9x, MCL-1L – Myeloid Cell Leukemia - 1 long-fragment, MCL-1S – Myeloid Cell Leukemia - 1 short-fragment, KD – knock-down.

3.3.2 USP30, MFN1 and MFN2

USP30 was also successfully knocked down when compared to the control (**Fig 3.12A)**. When compared to the control (100.0 ± 3.3%), knocking down USP30 led to significantly reduced MFN1 expression (73.0 ± 8.7%, p<0.05) (**Fig. 3.12A**) under these conditions. This study further demonstrated that down-regulating USP30 in DOX treated cells, also contributed to significantly reduced MFN1 expression (67.6 ± 9.4%, p<0.05) versus the control group (**Fig. 3.12B**). Conversely, MFN2 was

significantly up-regulated (640.7 ± 112.2%, p<0.001) when USP30 was not present compared to the control group (100.0 ± 11.1%), and remained up-regulated by USP30 down-regulation, though to a lesser extent (468.1 ± 91.4%, p<0.05) in the presence of DOX when compared to the control group as well (**Fig. 3.12C**). The findings described here advance our previous theory that USP30 rather de-ubiquitinates MFN1 and protects it from degradation rather than MFN2.

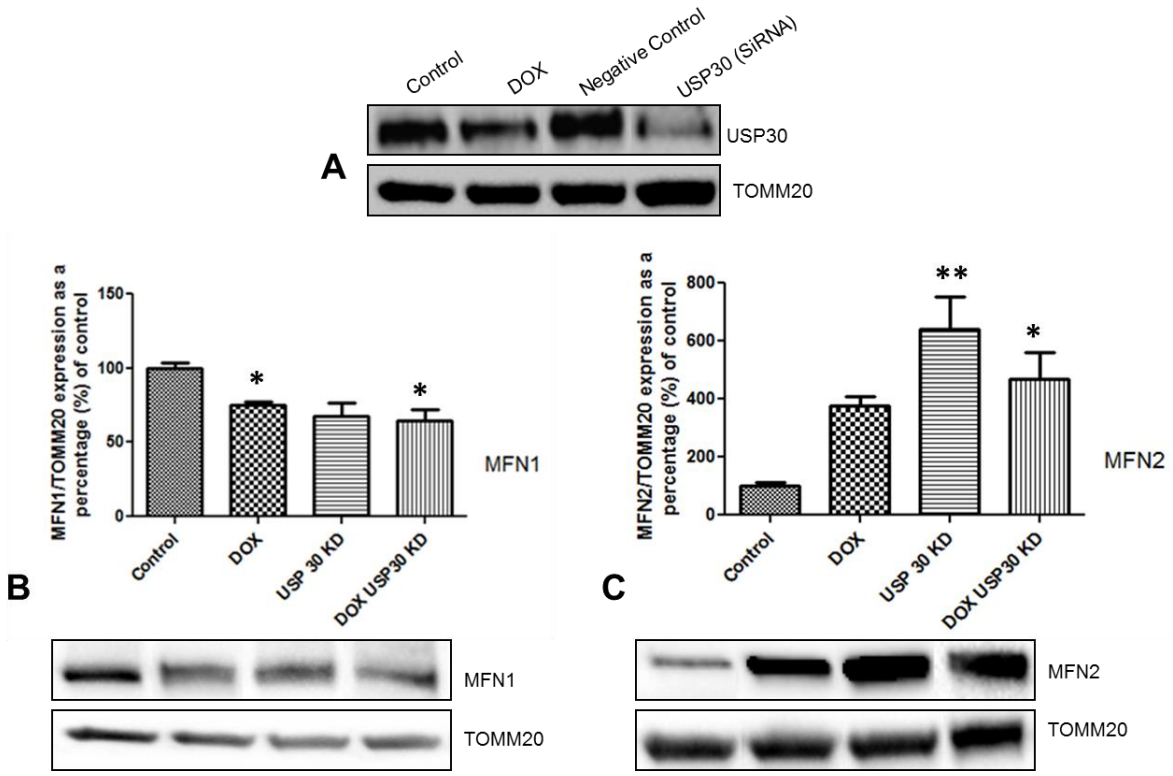

Figure 0.12: Relative USP30 protein expression following SiRNA knockdown in the absence or presence of DOX in vitro.

(A) USP30 known-down was achieved by electroporation using SiRNA, where after H9C2 cardiomyoblasts were treated with 0.2 μM DOX daily for 120 hrs. (B) Relative protein expression of MFN1 after SiRNA (USP30) treatment in the absence or presence of DOX. (C) Relative protein expression of MFN2 after SiRNA (USP30) treatment in the absence or presence of DOX. Results are represented as mean ± SEM (n = 3), *p<0.05, **p<0.001 vs. Control. TOMM20 was used as a loading control. Abbreviations: DOX - Doxorubicin, SiRNA - Silencing RNA, USP30 - Ubiquitin specific protease 30, MFN – Mitofusin, KD – knock-down.

3.3.3 USP36 and SOD2 (MnSOD)

USP36 plays an important role in the regulation and preservation of SOD2. It de-ubiquitinates this anti-oxidant and consequently extends its half-life (Kim et al.,

2011). This is essential for the regulation of cellular anti-oxidant defences against the damaging effects of oxidative stress. While this study previously indicated no significant changes in USP36 protein expression *in vitro* and *in vitro* (**Fig. 3.7**) in the context of DOX-induced toxicity, we were able to show that SOD2 expression was significantly increased during pro-longed DOX treatment. The knock-down of USP36 resulted in no substantial change in SOD2 protein expression when compared to the control (**Fig. 3.13A**). However when DOX was introduced, SOD2 was substantially increased (500.0 ± 82.3%, $p<0.01$) versus the DOX group (245.5 ± 24.6%) without down-regulation (**Fig. 3.13B**). It thus becomes apparent that while literature acknowledges the role (de-ubiquitination) of USP36 on SOD2 (Kim *et al*., 2011), the results obtained in this experiment indicate their relationship is not as direct as previously thought.

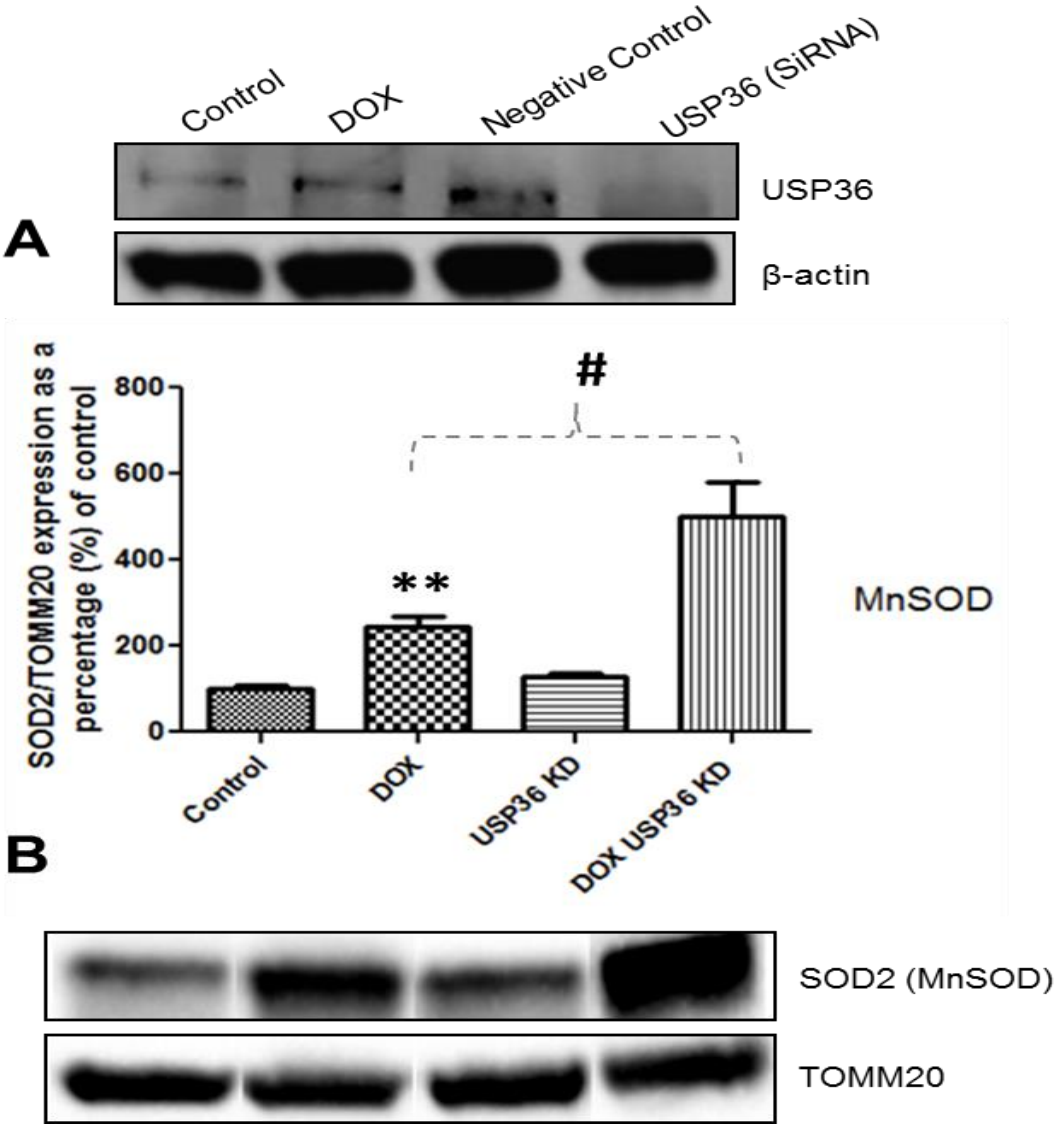

Figure 0.13: Relative USP36 protein expression following SiRNA knockdown in the absence or presence of DOX in vitro.

(A) USP36 known-down was achieved by electroporation using SiRNA, where after H9C2 cardiomyoblasts were treated with 0.2 μM DOX daily for 120 hrs. (B) Relative protein expression of SOD2 (MnSOD) after SiRNA (USP36) treatment in the absence or presence of DOX. Results are represented as mean ± SEM (n = 3). **$p<0.01$ vs. Control and $^{\#}p<0.05$ vs. DOX. β-actin and TOMM20 was used as a loading controls. Abbreviations: DOX - Doxorubicin, SiRNA - Silencing RNA, USP36 - Ubiquitin specific protease 36, MnSOD – manganese superoxide dismutase, SOD – superoxide dismutase KD – knock-down.

3.3 Mitochondrial morphology during SiRNA treatment of de-ubiquitinating enzymes

Mitochondrial morphology is regulated by the dynamic processes of mitochondrial fusion and fission (Hom & Sheu, 2009); and while these processes are essential for the normal functioning of mitochondria and the cell, this balance ultimately controls life and death signals (van der Bliek *et al., 2013*). While we (Sishi *et al*., 2013) and others (Parra *et al*., 2008) have been previously demonstrated that mitochondria present with an abnormal shape during DOX treatment; this study found it pertinent to evaluate mitochondrial morphology when DUBs were knocked-down in the absence and presence of DOX (**Fig. 3.14**). Normal mitochondria present themselves in various shapes and sizes including elongated, fragmented, rounded and intermediate (Rosca & Hoppel, 2010). Despite the various shapes and sizes, the majority of the mitochondria appeared interconnected and tubular in structure. When DOX was introduced, less mitochondria were observed; they were severely fragmented and rounded, and eventually lost their interconnectivity. While mitochondria seemed to gain their interconnectivity when each of the DUBs was knocked-down, some mitochondria remained fragmented and rounded, whereas others were intermediate in appearance. Overall, the down-regulation of DUBs resulted in 'healthier looking', mitochondria than DOX treated conditions alone. The most prominent feature observed when DUBs were knocked-down in the presence of DOX was their increased density (**Fig. 3.15**). Although different mitochondrial shapes were seen in a similar manner to the control, it is clear from these observations that USP down-regulation influences mitochondrial structure in a beneficial manner.

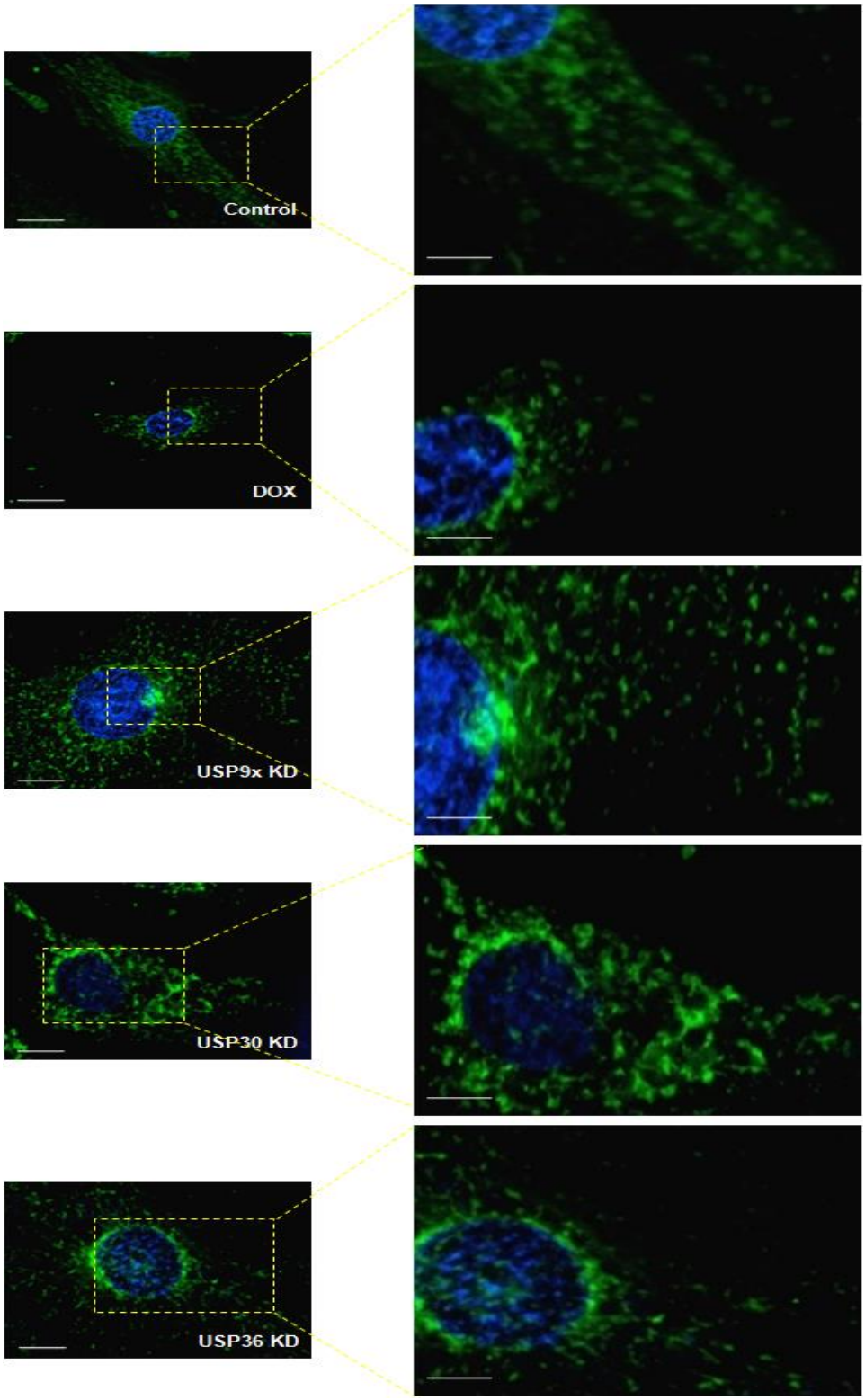

Figure 0.14: The effect of DUB (SiRNA) down-regulation on mitochondrial morphology in vitro

DUB known-down was achieved by electroporation using SiRNA, where after H9C2 cardiomyoblasts were treated with 0.2 µM DOX daily for 120 hrs. Cells were stained with Hoechst (blue) to indicate nuclei and MitoTracker green to reveal mitochondrial networks. Abbreviations: **DOX** - Doxorubicin, **KD** – Knock-down, **USP** - Ubiquitin Specific Protease. Magnification = 60x, Scale bar = 20 µm

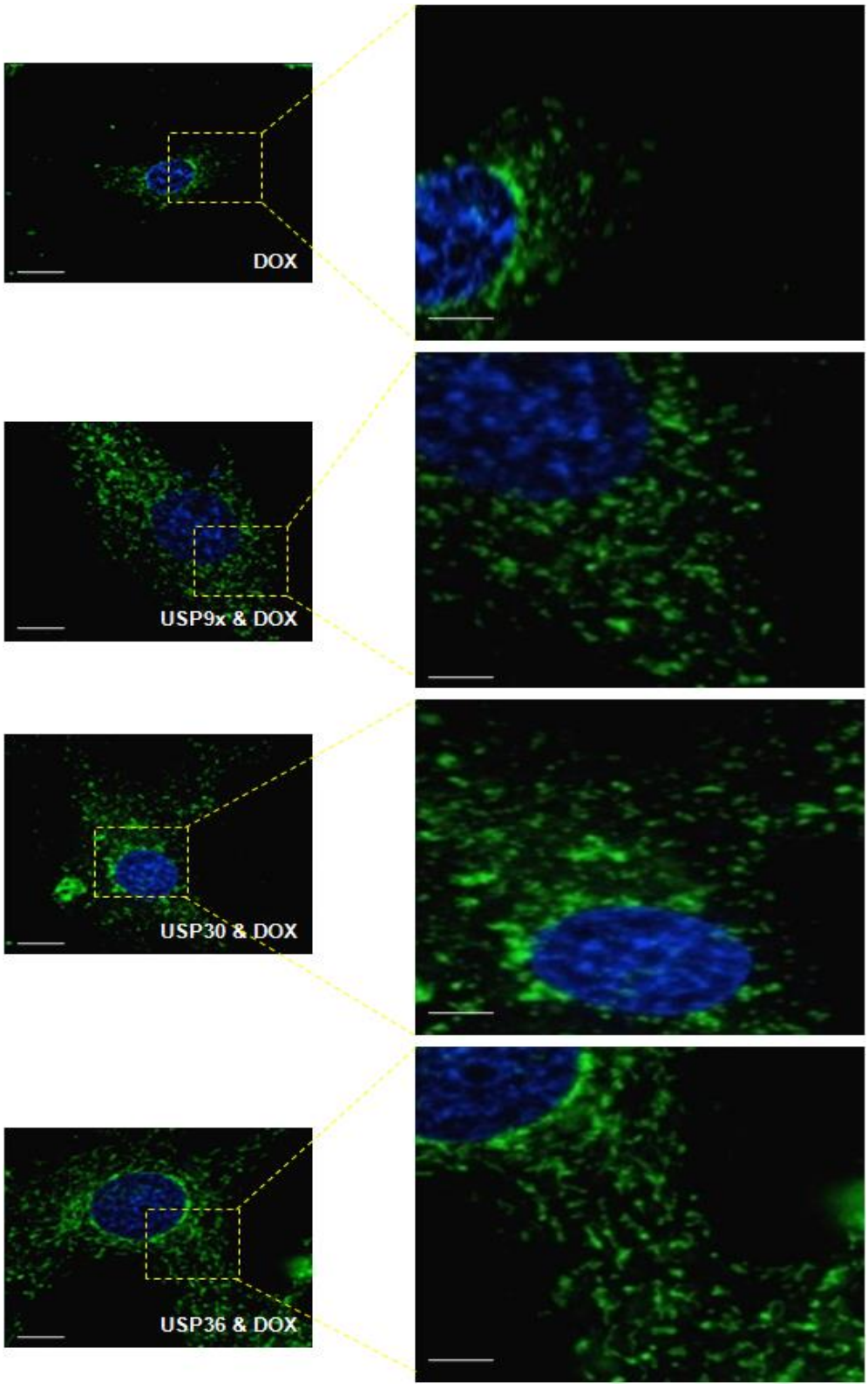

Figure 0.15: The effect of DUB (SiRNA) down-regulation in the presence of DOX on mitochondrial morphology in vitro.

DUB known-down was achieved by electroporation using SiRNA, where after H9C2 cardiomyoblasts were treated with 0.2 μM DOX daily for 120 hrs. Cells were stained with Hoechst (blue) to indicate

nuclei and MitoTracker green to reveal mitochondrial networks. Abbreviations: **DOX** - Doxorubicin, **KD** – Knock-down, **USP** - Ubiquitin Specific Protease. Magnification = 60x, Scale bar = 20 µm

3.4 Mitochondrial Health Assessment post SiRNA (down-regulation) of de-ubiquitinating enzymes in the presence of DOX

With mitochondrial homeostasis being central to the present study, it became appropriate to determine mitochondrial health and efficiency. As mentioned previously, mitochondria are the energy producing organelles in cells via oxidative phosphorylation (Martinou & Youle, 2011). Due to the high energy demands of the heart and its need for a continuous supply of ATP (Rosca *et al.,* 2008), cardiac cells have dense mitochondrial populations which make up ± 35% of their cellular volume (Hom & Sheu, 2009).

Healthy functional mitochondria are essential for cell viability, and so mitochondrial toxicity was assessed by measuring dead cell protease activity present in the cytosol and released by mitochondria of dying cells (Suzuki *et al*., 2001; Niles *et al*., 2007). When DOX was introduced to the cells (**Fig. 3.16**), a significantly higher level of dead cell protease activity (151.3 ± 5.2%, $p<0.01$) was observed when compared to the control (100.0 ± 12.9%). While no significant changes were established when USP30 and USP36 were knocked-down in the presence of DOX versus the DOX treated group alone, even though a trend towards a decrease was observed, the knock-down of USP9x in the presence of DOX significantly reduced dead cell protease activity (113.2 ± 1.3%, $p<0.05$) suggesting a substantial improvement in mitochondrial health. What is also clear from the results is that the knock-down of these specific DUBs does not result in detrimental consequences for the mitochondria and cell as a whole.

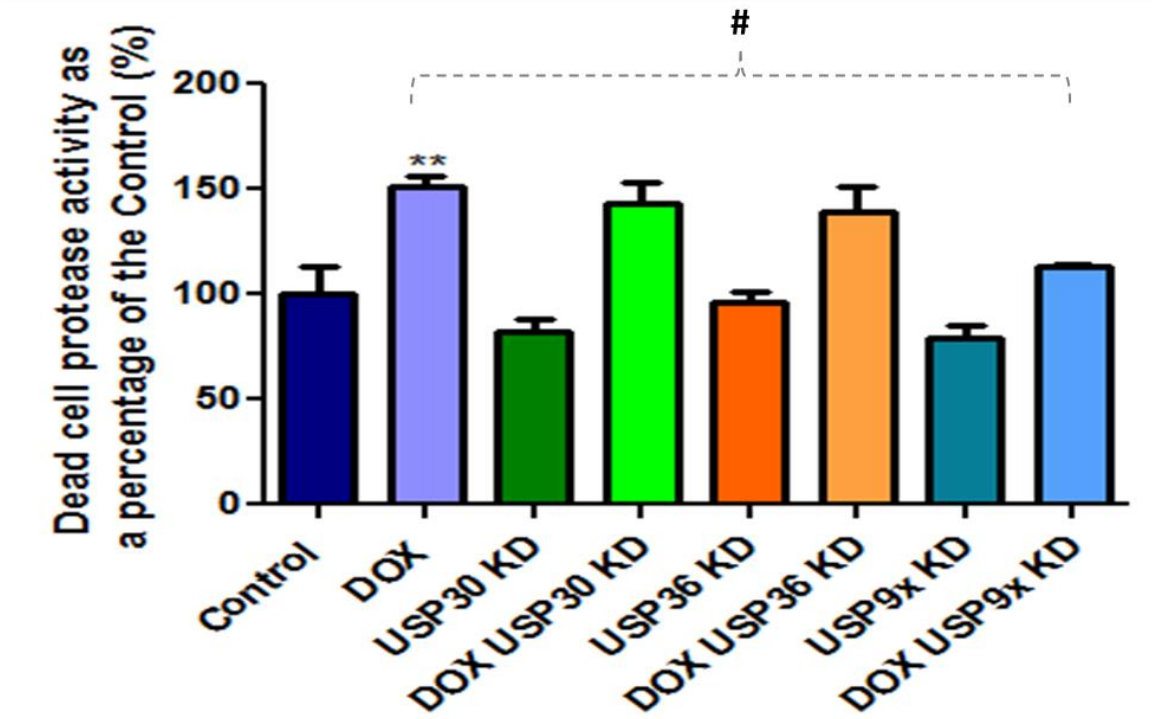

Figure 0.16: The effect of DUB (SiRNA) down-regulation in the absence and presence of DOX on mitochondrial toxicity measured by dead cell protease activity.

DUB known-down was achieved by electroporation using SiRNA, where after H9C2 cardiomyoblasts were treated with 0.2 µM DOX daily for 120 hrs. The relative fluorescent signal observed was evaluated. Results are represented as mean ± SEM (n = 3); **p<0.001 vs. Control, $^{\#}$p<0.05 vs. DOX. Abbreviations: **DOX** - Doxorubicin, **KD** – knock-down, **USP** - Ubiquitin Specific Protease

To complement the results obtained above, mitochondrial efficiency in the form of ATP production was measured and this was used as an indication of cell survival (**Fig. 3.17**). The damage that DOX induces to mitochondria was clearly reflected in this assay as ATP production was significantly reduced (41.5 ± 2.5%, p<0.01) when compared to the control (100.0 ± 14.6%). Interestingly, the general knock-down of USP36 (187.2 ± 9.9%, p<0.001) and USP9x (158.9 ± 14.3%, p<0.001) also produced significantly elevated levels of ATP versus the control and thereby suggests an important role for these DUBs in their down-regulated state. Moreover, the knock-down of USP30 (103.7 ± 8.0%, p<0.001), USP36 (114.1 ± 10.7%, p<0.001) and USP9x (86.8 ± 2.5%, p<0.05) in the presence of DOX caused a considerable increase in ATP production; however not to the same extend as without

DOX. It is thus clear from the results presented in this chapter that DOX is toxic to the mitochondria in these cells and this toxicity involves the active involvement of the UPS. Nevertheless, this study has now demonstrated from the above experiments, that by manipulating the expression of specific DUBs relevant in this context, this can be beneficial in improving mitochondrial morphology, reducing mitochondrial toxicity and increasing ATP production.

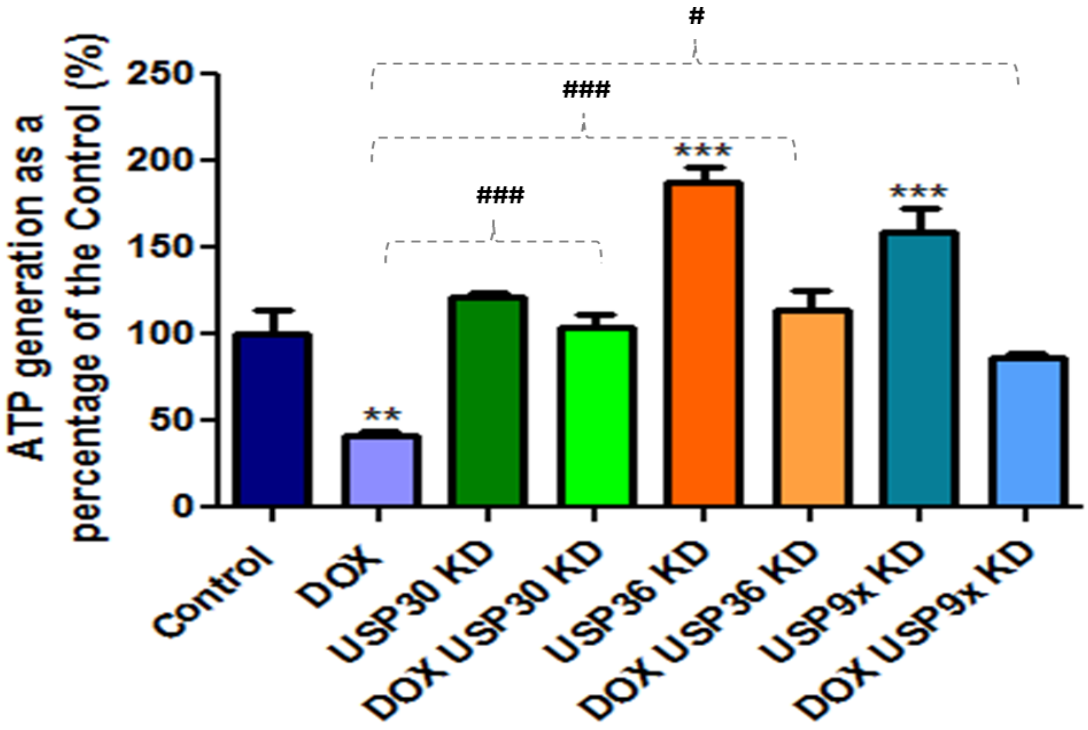

Figure 0.17: The effect of DUB (SiRNA) down-regulation in the absence and presence of DOX on ATP production from mitochondria.

DUB known-down was achieved by electroporation using SiRNA, where after H9C2 cardiomyoblasts were treated with 0.2 μM DOX daily for 120 hrs. The relative fluorescent signal observed was evaluated. Results are represented as mean ± SEM (n = 3); **p<0.01, ***p<0.001 vs. Control; $^{\#}$p<0.05, $^{\#\#\#}$p<0.001 vs. DOX. Abbreviations: **DOX** - Doxorubicin, **KD** – knock-down, **USP** - Ubiquitin Specific Protease

DISCUSSION

As cancer outcomes advance, cardiovascular disease has become the primary cause of morbidity and mortality among cancer survivors; and the foundation of this cancer-related cardiomyopathy is chemotherapy. Targeted anti-cancer and cytotoxic drugs such as anthracyclines can progress to HF particularly in patients with pre-existing heart disease, childhood cancer survivors and the elderly (Van Dalen *et al*., 2007). While oxidative stress was previously indicated as the major role player (Minotti *et al.,* 2004), mitochondrial dysfunction has since become a noticeable trait of DOX-induced cardiotoxicity (Green & Leeuwenburgh, 2002). Mitochondrial function is regulated by the dynamic processes of fission and fusion (known as mitochondrial dynamics); and prior work by our group demonstrated that during DOX treatment mitochondrial fission is favoured over fusion (Opperman, 2015). The fine balance of mitochondrial dynamics is in part regulated by the UPS and this mechanism is reversible with the use of DUBs (Endo *et al*., 2009; Youle *et al*., 2011). This study therefore hypothesized that by manipulating the presence of specific DUBS relevant in this context, this would enhance mitochondrial health, increase ATP synthesis and overall cellular survival.

4.1 DOX induces apoptosis by increasing USP9x

Apoptosis is a known mechanism by which DOX destroys both cancer cells and cardiomyocytes. Direct DNA intercalation is the favoured method for highly proliferative cells (Berthiaume and Wallace, 2007), while indirectly oxidative stress and mitochondrial damage impairs myocardial cells (Minotti *et* al., 2004; Green & Leeuwenburgh, 2002). Although oxidative stress may also contribute to DOX-induced apoptosis in cancer, cardiac cells are especially susceptible to the damaging effects of oxidative stress due to their lower levels of anti-oxidant defences (Doroshow *et al*., 1980, James Kang *et al*., 1996).

MCL-1 is a member of the Bcl-2 family of apoptosis regulating proteins. With various functions including the development and maintenance of B and T lymphocytes (Opferman *et al*., 2003) and cell cycle progression (Fujise *et al*., 2000), the most significant function in this context is its regulatory role in apoptosis. MCL-1 can

undergo post-transcriptional and translational modification to form, a long anti-apoptotic (MCL-1L) and a short pro-apoptotic fragment (MCL-1S) (Bae *et al.,* 2000; Thomas *et al*., 2010). MCL-1L binds and sequesters Bak, Bax and other pro-apoptotic BH3-only proteins of the Bcl-2 family including MCL-1S. This prevents these proteins from forming pores within the mitochondrial membrane, causing the release of cytochrome c via the mitochondrial permeability transition pore (mPTP), and downstream caspase activation (Bae *et al.,* 2000). Its variant, MCL-1S is a BH3-only protein, and functions as a ligand which can dimerize with MCL-1L on the mitochondrial membrane. There it induces apoptosis through the activation of downstream caspases and as such acts in an antagonistic manner to MCL-1L. Our results clearly demonstrate that DOX stimulates apoptosis by decreasing the expression of anti-apoptotic MCL-1L (**Fig. 3.2**) whilst increasing the pro-apoptotic MCL-1S (**Fig. 3.3**) *in vitro* and *in vivo*. According to a review by Karbowski *et al.,* (2011), USP9x is one of only two mitochondrial associated DUBs that have been identified at present (Schwickart *et al*., 2010). This enzyme de-ubiquitinates and stabilizes MCL-1 which is targeted for degradation by MULE (MCL-1 ubiquitin ligase). We found that during cytotoxicity and cardiotoxicity, USP9x was substantially elevated (**Fig. 3.1**). This increase possibly suggests that USP9x removes ubiquitin molecules tagged to MCL-1 to prevent its degradation. Since MCL-1 has two fragments, pro-apoptotic MCL-1S is preserved rather than the anti-apoptotic MCL-1L. In doing so, apoptosis is induced. As there are no effective treatment strategies for DOX-induced toxicity, exploiting USP9x function may be way in which apoptosis can be reduced.

4.2 DOX treatment promotes mitochondrial fission by reducing USP30

Changes in mitochondrial morphology are a typical response to mitochondrial stress stimuli (Barbour & Turner, 2014). These changes in morphology are regulated by mitochondrial membrane proteins which govern mitochondrial dynamics. Parra *et al.,* (2008) illustrated that mitochondrial stress which culminates in cardiomyocyte apoptosis is in fact preceded by extensive mitochondrial fragmentation. As mentioned previously, mitochondrial fission machinery involves the proteins Drp1 and Fis1 which are subsequently ubiquitinated by the E3 ligase MITOL (MARCH5),

which compromises their fission promoting function (Nakamura *et al.*, 2006; Karbowski *et al*., 2007; Yonashiro *et al*., 2006); whereas mitochondrial fusion machinery involves MFN 1/2 and OPA1, and are tagged for degradation by the E3 ligase Parkin (Tanaka *et al.*, 2010; Gegg *et al.*, 2010). The other DUB that has been identified is USP30, however its mitochondrial substrates remain to be conclusively elucidated (Nakamura *et al., 2008;* Karbowski *et al.,* 2011). It is thus probable that USP30 facilitates de-ubiquitination of certain mitochondrial proteins involved in mitochondrial dynamics, as down-regulation of this DUB by RNAi is said to promote elongated mitochondrial networks which is indicative of fusion and inhibits mitophagy (Nakamura *et al.*, 2008; Bingol *et al.,* 2014; Yue *et al*., 2014). The current study has since demonstrated that USP30 is severely reduced in the presence of DOX *in vitro* (**Figs. 3.4 & 3.9**) and *in vivo* (**Fig. 3.4**). This suggests that the mitochondrial proteins that are meant to be de-ubiquitinated by USP30 are tagged with ubiquitin molecules that signal for their degradation by the proteasome. We also noted that USP30 is not only localized to the peri-nuclear region (possibly mitochondria) as observed in literature (Nakamura & Hirose, 2008; Bingol *et al*., 2014). We were also able to detect some localization within the nucleus specifically in the control cells. Little has been reported on this in literature, but it could be also observed in the results obtained by Bingol *et al*., (2014). Nakamura *&* Hirose, (2008), also observed non-mitochondrial targeting of a mutant USP30 type. This, in addition to our findings could suggest a nuclear based function of USP30 subtypes in control cells, which is eliminated in the presence of DOX. USP30 localization is dependent on the net charge in its C-terminal transmembrane span and flanking region (Nakamura & Hirose, 2008), and DOX has been established to be positively charged (Goormaghtigh *et al*., 1980). This interaction could influence USP30 localization. Based on the above, our findings are in agreement with some studies that proved that USP30 does indeed associate with MFNs (Bingol *et al*., 2014; Yue *et al*., 2014).

Numerous studies have established that modifications in mitochondrial morphology, due to an imbalance between fission and fusion events within the myocardium, mediate the pathophysiology of HF (Kuzmicic *et al*., 2011; Marín-García *et al*., 2013). Furthermore, literature reveals that elevated ROS production and oxidative stress, a known side effect of DOX treatment, mediates mitochondrial fission (Dagda *et al*., 2009; Frank *et al*., 2012). These findings lead to the theory that dysregulation of

mitochondrial dynamics is associated with DOX-induced cardiotoxicity. The importance of MFN1 and MFN2 in maintaining normal mitochondrial morphology and function has been highlighted in elegant knock-out models. Whereas Papanicolaou *et al., (2012)* showed that double knock-out of both MFNs in mice caused the accumulation of aberrant mitochondria in cardiomyocytes, Chen and colleagues (2011) demonstrated that cardiac specific deletion of either MFN1 or MFN2 triggers mitochondrial dysfunction and lethal dilated cardiomyopathy. Therefore, from the above studies, it can be deduced that obstruction of either of these fusion proteins can have detrimental consequences for the myocardium. Based on our data MFN1 was significantly reduced in both models (**Fig. 3.5**) and MFN2 was augmented *in vitro* (**Fig. 3.6**), which was in contrast to our previous results (Opperman, 2015). As USP30 and MFN1 were both down-regulated in both models, it may imply that MFN1 was degraded or its synthesis was inhibited since there was no inhibitory protein (absence of USP30) that would prevent its degradation. Additionally, these results point toward the notion that USP30 is certainly a specific DUB for MFN1 and this is a novel finding in this context.

Interestingly, this phenomenon was not realised when considering MFN2, which is arguably the more influential fusion protein, as loss of this protein alone was demonstrated to significantly impair mitochondrial fusion (Ni *et al.,* 2014). The increase in protein expression of MFN2 observed in this study may either indicate a compensatory response due to loss of MFN1, or that USP30 does not prevent degradation of MFN2 as indicated earlier by others (Bingol *et al*., 2014; Yue *et al*., 2014). Moreover, if USP30 has an effect on MFN2, it is likely involved in the regulation of this fusion protein via Lysine-63 (Lys-63) associated ubiquitination rather than Lysine-48 (Lys-48). Lys-63 ubiquitination regulates function and localization of proteins whereas Lys-48 causes degradation (Wilkinson, 2009). It thus becomes apparent that although the mechanism by which DOX causes USP30 down-regulation remains to be elucidated, our results dictate the influential role that USP30 plays in this context.

4.3 SOD2 is elevated in response to DOX-induced oxidative stress

The central player suggested to be part and parcel of DOX cardiotoxicity is oxidative stress generated during intracellular metabolism (Vander Heide *et al*., 2007; Schimmel *et al*., 2004). This idea has been pivotal in the argument that since adult cardiomyocytes are terminally differentiated cells that are highly susceptible to oxidative stress as a result of their high oxidative metabolism, oxidative damage to the myocardium can lead to irreversible injury depending on its severity. For example; mild oxidative stress is said to trigger mitophagy either to promote survival or induce death. Secondly, moderate oxidative stress encourages apoptotic cell death following mitochondrial membrane permeabilization and the liberation of cytochrome-c. This is true considering that ROS can accumulate within mitochondria to generate more ROS and oxidatively damaged mitochondria can also produce even more ROS (Suzuki *et al*., 2001). This creates a vicious cycle that is destructive. Finally, severe oxidative stress brings about necrosis owing to ATP exhaustion (Pan *et al.,* 2009).

As such, *in vitro* experiments utilising cardiomyocytes propose that anti-oxidants such as α-phenyl-tert-butyl nitrone, 5-aminosalicyclic acid, trolox or aminofostine, administered prior to DOX treatment, decreases oxidative stress and myocyte injury (DeAtley *et al*., 1999; Dorr *et al*., 1996). *In vivo*, transgenic mice over-expressing SOD and catalase, major intracellular anti-oxidants, have been demonstrated to be cardio-protective (Kang *et al*., 1996; Yen *et al*., 1996). Interestingly it was found that the level of catalase activity in the heart to produce these beneficial effects were between 60-100 fold higher than normal. It is however unlikely that this can be achieved with the current strategies; and mechanisms to constantly maintain these elevated levels are non-existent at present. The failure of this strategy clinically (Van Dalen *et al*., 2008), and the disagreement in literature regarding the most favourable treatment regime has resulted in this study taking a different approach by investigating the role that DUBs play in this context. SOD2 (MnSOD) is ubiquitinated by MARCH5 (MITOL) (Yonashiro *et al.*, 2006; Yonashiro *et al.*, 2009) for degradation and Kim *et al.,* (2011) proposed that the non-mitochondrial DUB, USP36, localized to the nucleoli is vital for reducing the ubiquitination levels of SOD2 in a cancer cell line. Disappointingly, our western blot data showed no noteworthy changes in either of our models (**Fig. 3.7**), however, when we stained for USP36 *in vitro* (**Fig. 3.10**), a

different picture emerged. USP36 expression was detected within the nucleus under normal conditions which corroborates the study cited above (Endo *et al.,* 2009; Kim *et al*., 2011). In contrast to the observations above, DOX amplified USP36 fluorescent signal and this localisation emerged outside and around the nucleus as protein aggregates. The significance of forming aggregates in this context is unknown. If we consider these results, it could possibly indicate that due to DOX-induced oxidative stress, the cells would naturally respond by increasing their anti-oxidant defences. In this case SOD2 was significantly up-regulated *in vitro* (**Fig. 3.8**) while no changes were seen *in vivo*. This suggests that the extra-nucleolar expression of USP36 in the presence of DOX counteracted SOD2 Lys-48 ubiquitination and prevented its degradation. In this context, these results are considered to be beneficial seeing that DOX is known to induce oxidative stress (Minotti *et al.,* 2004).

In light of the above results, this study has now illustrated that DOX treatment has a strong influence on the presence and/or absence of specific DUBs relevant in this scenario and this influences down-stream substrates that mediate apoptotic cell death, mitochondrial function and ROS scavenging. To further elaborate on these experiments and to determine the functional significance of these DUBs in this context, down-regulation was attempted to not only ascertain what happens to the down-stream targets, but also mitochondrial health and ATP synthesis.

4.4 USP9x down-regulation reduces MCL-1S during DOX treatment

It has previously been reported that the knock-down of USP9x sensitizes cells to cytotoxic stimuli that results in cell death via MCL-1 dependent mechanisms (Schwickart *et al.,* 2010). When USP9x (**Fig. 3.11A**) was knocked-down in this setting, the pro-apoptotic short-fragment MCL-1S (**Fig. 3.11C**) was reduced while the anti-apoptotic long-fragment MCL-1L (**Fig. 3.11B**) was modestly elevated versus the DOX alone group. This was in line with our baseline results already discussed above and validates our previous suggestion that USP9x preserves MCL-1S from degradation rather MCL-1L. A noteworthy observation was the fact that USP9x down-regulation alone was also associated with higher expression of both MCL-1 fragments when compared to the control, however; when DOX was administered,

MCL-1L appeared to be more sensitive to this stressor than MCL-1S suggesting an inhibitory effect in MCL-1L activity in the presence of DOX. An interesting oversight by current literature with regards to the relationship between USP9x and MCL-1 is the lack of information regarding the specificity of the interaction between USP9x and the MCL-1 fragments. Current literature has taken a one-dimensional approach towards investigating the relationship between these proteins, and this makes the differential relationship between USP9x and the two MCL-1 fragments observed by this study an interesting one. Our results suggest that USP9x is a more specific de-ubiquitinase for MCL-1S, and this could be due to the structural differences between MCL-1S and MCL-1L observed by Bae *et al*., (2000). Against expectations, down-regulating USP9x alone was not sufficient to reduce MCL-1S expression, but this down-regulation in combination with DOX treatment reduced MCL-1S expression compared to DOX only groups and even showed a trend towards reduced expression compared to the control group (**Fig 3.11).** This goes to suggest that in the presence of the toxic insult by DOX, and the increase in USP9x expression induced by DOX treatment, MCL-1S expression increases due to increased de-ubiquitination by USP9x. However, when USP9x is downregulated within this context, increased ubiquitination of MCL-1S by MULE occurs, and with less USP9x present, the increase in MCL-1S caused by DOX induced USP9x up-regulation, is inhibited, and so MCL-1S gets degraded by the UPS.

Overall, the knock-down of USP9x in the presence of DOX can be viewed as favourable due to an increase in anti-apoptotic and a decrease in pro-apoptotic signals.

4.5 USP30 down-regulation increases MFN2 and decreases MFN1 in the presence of DOX

USP30 has been reported to de-ubiquitinate Parkin's substrates within the mitochondria. Parkin has been identified as the likely E3 ligase which tags MFN proteins with ubiquitin molecules for Lys-48 associated proteasomal degradation (Liang *et al*., 2015). As such, USP30 is believed to de-ubiquitinate MFN proteins to preserve their function. This study was able to show that USP30 has differential effects on MFN1 (**Fig. 3.12B**) and MFN2 (**Fig. 3.12C**). Our initial baseline data

showed that pro-longed DOX treatment was accompanied by a reduction in MFN1 (*in vitro* and *in vivo*) possibly due to the decrease in USP30, which indicates that MFN1 degradation is linked to the absence of USP30. This further implies that USP30 does in fact de-ubiquitinate MFN1 to prevent its degradation in this setting. This was confirmed by USP30 knock-down, which caused an additional decrease in MFN1 expression alone and when DOX was administered. While USP30 has been determined to de-ubiquitinate mitochondrial proteins (Karbowski & Youle, 2011; Bingol *et al*., 2014), literature has not yet pin-pointed the exact relationship between USP30 and the mitofusins, however Nakamura & Hirose, (2008) were able to determine that down-regulation of USP30 induced mitochondrial network elongation, indicative of increased mitochondrial fusion. And while the reduction in MFN1 expression due to USP30 down-regulation contradicts these findings, the response of MFN2 to USP30 knockdown could explain their results.

MFN2 was increased during chronic DOX treatment alongside reduced USP30 expression. By knocking-down USP30 in absence and presence of DOX, this lead to an even greater expression of MFN2 when compared the control and DOX groups respectively. This may either indicate a compensatory mechanism between the two MFN proteins as they both regulate mitochondrial fusion or that USP30 is not responsible for the anti-degradative de-ubiquitination of MFN2. While literature is yet to elucidate in detail the relationship between the mitofusins and USP30, Liang *et al.,* (2015) indicate that both mitofusins are de-ubiquitinated by USP30 and this brings into the focus the different types of ubiquitination. We postulate that USP30 cleaves ubiquitin molecules bound to MFN2, however, it is more specific for lysine-63 regulatory ubiquitin bonds, a suggestion which is backed up by Anton *et al*., (2013) report that mitofusins are ubiquitinated on two conserved lysine residues. Down-regulating USP30 in this context could enable more Lys-63 linked ubiquitination, which could lead to regulation of its activity and function, and also stimulating an increase in MFN2 transcription. This is beneficial in this context, as increased MFN2 levels would help reduce the level of mitochondrial fragmentation induced by DOX treatment even more so than the compensatory increase caused by DOX.

USP30 down-regulation would also lead to an increase in parkin-mediated mitophagy (Bingol *et al*., 2014). Bingol *et al*., (2014) reported that over-expression of USP30 led to reduced mitophagy as USP30 removes ubiquitin molecules attached to

mitochondria by parkin. As such, reduced USP30 expression would be accompanied by an increase in mitophagy. This would be beneficial in this context, as this increased mitophagy would enable degradation of mitochondria irreversibly damaged by DOX, while the concurrent increase in MFN2 expression would enable reintegration of viable mitochondria into the mitochondrial network.

4.6 USP36 down-regulation improves mitochondrial anti-oxidant expression post chronic DOX treatment

This study showed that chronic DOX treatment did not induce any changes in USP36 expression. We were also able to show that chronic DOX treatment induced a compensatory increase in SOD2 expression *in vitro*. This seemed to imply that our earlier belief that USP36 expression is directly linked to SOD2 expression may not be completely accurate as SOD2 was increased significantly, without a corresponding increase in USP36 expression. Down-regulating USP36 did not lead to any significant changes in SOD2 expression. This indicated that an absence of USP36 did not lead to increased level of SOD2 degradation by the UPS. When USP36 knock down cells were subjected to chronic DOX treatment however, there was a markedly increased expression of SOD2, showing that down-regulating USP36 escalated the compensatory increase in SOD2 expression induced by chronic DOX treatment. The mechanisms through which this occurs are still unclear, however, Kim *et al*., (2011), reported that USP36 regulated SOD2 stability by removing poly-ubiquitin chains and improving the half-life of SOD2 and that would imply that down-regulating USP36 would increase SOD2 turnover. This could explain the increased SOD2 expression in DOX treated USP36 knock down cells, as this increased turnover could also induce increased transcription which would be protective in the context of DOX-induced cardiotoxicity.

DUB down-regulation influences mitochondrial morphology, improves toxicity and efficiency in the context of chronic DOX induced cardiotoxicity

Mitochondrial morphology is an important indicator of cellular health. Exposure to acute and chronic insults within the myocardium modifies mitochondrial morphology

depending on the severity of the insult (Ho & Duffield., 2000). Excessive mitochondrial fragmentation is generally considered a sign of stress and is harmful to cellular homeostasis. It has been associated with increased levels of apoptosis (James *et al*., 2003) and oxidative stress (Sciaretta *et al*., 2014; Ikeda *et al*., 2015) and this phenomenon has been observed in a number of disease states including diabetes, liver diseases, ageing and cancer (Wallace, 1999), suggesting a critical role of mitochondrial morphology in the context of these diseases.

In the context of DOX toxicity, we have previously indicated that mitochondria appear as short, rounded and fragmented organelles that display no interconnectivity with one another. Furthermore, these mitochondria were found to have decreased membrane potential and resulted in apoptotic cell death possibly due to extensive mitochondrial damage and cytochrome-c leakage (Sishi et al., 2013). While the study cited was conducted in an acute setting (3 μM DOX for 24 hrs), the results presented in the current study were similar albeit a chronic setting was utilised (Fig. 3.14). This implies that irrespective of duration or concentration, DOX induces abnormal mitochondrial changes to the mitochondria that influence cellular death. This may be due to DOX's affinity for cardiolipin and DOX-induced oxidative stress (Goormaghtigh et al., 1980). When DOX binds to cardiolipin forming a steady complex, it renders cardiolipin inept in its role as a co-factor for various mitochondrial respiratory proteins thus preventing oxidative phosphorylation and reducing ATP (Goormaghtigh & Ruysschaert, 1984; Goormaghtigh et al., 1986). Additionally, when DOX's lipophilic metabolite (7-deoxyaglycone) accumulates within the inner mitochondrial membrane where cardiolipin resides, electrons are redirected to oxygen to form free radicals instead. These events culminate in increased mitochondrial permeability, oxidation of NADH, mitochondrial swelling and ultimately mitochondrial dysfunction (Doroshow, 1983).

To maintain cell survival, mitochondria present themselves in different shapes and sizes, as they are constantly undergoing fission and fusion processes. However, most mitochondria are extended, tubular in shape and present themselves with a high degree of interconnectivity. When this study down-regulated the DUBs alone, more mitochondria were present with improved appearance and a great degree of branching. Surprisingly, even after DOX was added (Fig. 3.15), mitochondrial were able to maintain their shape despite some degree of damage. Bingol et al., (2014)

demonstrated that USP30 opposes parkin-mediated mitophagy, and as such USP30 knock-down showed less dense mitochondrial networks compared to the control suggesting an increase in mitophagy induced by USP30 down-regulation. Bach et al., (2003) also demonstrated that MFN2 played a significant role in the regulation of mitochondrial networks and mitochondrial efficiency. The increase in MFN2 expression in the presence and absence of DOX could be responsible for the increased mitochondrial fusion observed when USP30 was down-regulated. This may indicate that USP30 knock-down was protective of mitochondrial network state within the context of chronic DOX toxicity. USP9x knock-down showed rounded mitochondria symptomatic of fragmentation, however, these cells showed a high mitochondrial density compared to both control groups. DOX treated USP9x (SiRNA) cells displayed similar mitochondrial network morphology, showing that down-regulating USP9x led to fragmented mitochondria, but was protective against the extensive fragmentation and mitochondrial degradation observed in DOX control cells. Morciano et al., (2016) reported that a high MCL-1S/MCL-1L ratio results in significant hyperfusion of the mitochondrial network. This hyperfusion is reportedly dependent on DRP1, and sensitizes cells to apoptosis. Down-regulating USP9x led to a reduction in the MCL-1S/MCL-1L ratio, leading to fragmented but denser mitochondrial networks that could be more resistant to apoptotic stimuli within this context. USP36 down-regulation alone did not seem to influence mitochondrial network morphology extensively in terms of density and fragmentation compared to the control, but USP36 knockdown in the presence of DOX, extensively increased mitochondrial network fusion and density compared to DOX controls. This indicates that the significant increase in SOD2 induced by down-regulating USP36 in the presence of DOX is protective in this context, as it helped restore mitochondrial network morphology.

Down-regulating these DUBs was also protective in other mitochondrial parameters, as we were able to determine that down-regulating USP9x helped reduce overall mitochondrial toxicity compared to DOX controls (Fig. 3.16). Fragmentation in this context induced by USP9x, seemed to be protective so long as mitochondrial network density remained healthy. This could be an avenue for further exploration considering that mitochondrial density as well as the levels of mitophagy, and not just mitochondrial morphology could be more significant in the aetiology of

cardiomyopathies associated with DOX induced toxicity. As expected, chronic DOX treatment led to an inhibition of cellular ATP synthesis however, by down-regulating each of the three DUBs, this seemed to enhance mitochondrial efficiency compared to DOX controls (Fig. 3.17). The exact mechanism by which this happens remains unknown but the present data seem to indicate that by down-regulating both USP30 and USP36 help maintain mitochondrial health by reducing of mitochondrial fragmentation and DOX-induced mitophagy through elevated MFN2 and SOD2 respectively. USP9x increased mitochondrial network density, and while there was no visible reduction in mitochondrial fragmentation, the reduction in the MCL-1S/MCL-1L ratio helped reduce the pro-apoptotic stimuli exerted by the chronic DOX treatment. These mechanisms lead to increased mitochondrial health, and improved cellular ATP synthesis, which was compromised by DOX.

CONCLUSION

In the race against time to find sustainable solutions to the problems associated with chemotherapy, DOX-induced cardio(cyto)toxicity is a huge stumbling block to any reasonable progress made thus far. The chronic form of this condition has made it even more difficult to curb with lower doses of DOX still leading to the progression of HF over period of time. The mechanism by which the chronic form of this disease leads to cardiomyopathy is related to not only oxidative stress, but mitochondrial dysfunction due to possible dysregulation of the UPS, a major protein quality control mechanism in a cell. The UPS plays a pivotal role in the regulation of mitochondrial efficiency, morphology, targeted degradation via mitophagy and apoptosis. Since the process of ubiquitination is reversible due to the presence of DUBs, this study explored their potential role in this context.

Considering that mitochondria are highly abundant in the myocardium due to the metabolic demands of this organ, their health and function needs to be maintained at all times. However due to DOX having such a high affinity for mitochondria, it stimulates detrimental changes to these organelles ultimately resulting in their dysfunction. Oxidative stress, abnormal mitochondrial morphology, apoptosis and reduced ATP synthesis are all critical role players in the development of chronic DOX cardiotoxicity and its advancement to HF, and this study showed that DUBs are influential in the modulation of these processes. DOX itself induces differential protein expression of specific DUBs assessed in study and in doing so, promotes fragmented mitochondria and consequently oxidative stress, reduced ATP synthesis and apoptotic cell death by reducing USP30 and USP36 and by elevating USP9x respectively. Therefore, by down-regulating each of the DUBs by using SiRNA, we demonstrated improved mitochondrial morphology and MnSOD expression, reduced mitochondrial toxicity and pro-apoptotic signalling, and finally enhanced ATP production. These effects are extremely beneficial to the heart to maintain optimum cellular and organelle function. By demonstrating a role for DUBs in this context and exploiting their down-stream effects in their absence, and in the absence and presence of DOX, this study has opened a potential avenue of exploitation for targeted treatment for cardiotoxicity during DOX treatment.

An obvious limitation of this study was the fact that only one half of the puzzle was investigated. The roles of these DUBs within the context of chronic DOX-induced cardiotoxicity cannot be fully elucidated until the effect of up-regulating these and their down-stream effects assessed. While this study did attempt to up-regulate these specific DUBs, our trials were unsuccessful due to the low transfection efficiency of the cell line used. A more suitable approach for this cell line would be to use CRISPR technology, however due to limited funds we were not able to utilise this technique.

Other potential avenues that should be explored include the differential effect that DOX has on MFN1 and MFN2. In this current study, MFN1 was reduced, whereas MFN2 was elevated in the presence of DOX while UPS30 was down-regulated. It is thus tempting to speculate that should USP30 be increased, MFN1 is expected to increase and MFN2 to decrease in the presence of DOX. This would then confirm that indeed USP30 de-ubiquitinates both MFNs and not only MFN1 as indicated by the results in this study within this particular context. Interestingly, MFN2 has previously been demonstrated to function as one of the proteins involved in tethering mitochondria to the SR in areas known as mitochondrial-ER associated membranes (MAMs) (de Brito & Scorrano, 2008). MAMs influence a number of SR-linked mitochondrial regulatory processes, including calcium regulation. Calcium regulation is especially important in the excitation/contraction coupling of the myocardium and modifications in this process will affect proper function of the heart. Furthermore, calcium is involved in the activation of calpains, the initiation of apoptosis and necrosis, and mitochondrial fragmentation (Nakagawa et al., 2000; Marongiu et al., 2009).

With all things considered, the findings presented in this study go a long way in expanding the scientific knowledge related to cardiotoxicity and the field of cardio-oncology. These findings in addition to potential therapeutic effects are of immense benefit to not only the scientific community at large but also to the numerous cancer survivors world-wide.

REFERENCES

1. Albini, A. *et al*., 2010. Cardiotoxicity of anticancer drugs: The need for cardio-oncology and cardio-oncological prevention. *Journal of the National Cancer Institute*, 102(1), pp.14–25.

2. Anton, F. *et al*., 2013. Two Deubiquitylases Act on Mitofusin and Regulate Mitochondrial Fusion along Independent Pathways. *Molecular Cell*, 49(3), pp.487–498.

3. Bach, D. *et al*., 2003. Mitofusin-2 Determines Mitochondrial Network Architecture and. *Biological Chemistry*, 278(19), pp.17190–17197.

4. Bachur, N.R., Gordon, S.L. & Gee, M. V, 1978. A General Mechanism for Microsomal Activation of Quinone Anticancer Agents to Free Radicals A General Mechanism for Microsomal Activation of Quinone Anticancer Agents to Free Radicals1. *Cancer Research*, 38, pp.1745–1750.

5. Bae, J. *et al*., 2000. MCL-1S, a Splicing Variant of the Anti-apoptotic BCL-2 Family Member MCL-1, Encodes a Pro-apoptotic Protein Possessing Only the BH3 Domain. *Journal of Biological Chemistry*, 275(33), pp.25255–25261

6. Barbour, J.A. & Turner, N., 2014. Mitochondrial stress signalling promotes cellular adaptations. *International Journal of Cell Biology*, 19(24), pp.4861-4870.

7. Barrett-Lee, P.J. *et al*., 2009. Expert opinion on the use of anthracyclines in patients with advanced breast cancer at cardiac risk. *Annals of oncology : official journal of the European Society for Medical Oncology / ESMO*, 20(5), pp.816–827.

8. Berthiaume, J.M. & Wallace, K.B., 2007. Adriamycin-induced oxidative mitochondrial cardiotoxicity. *Cell Biology and Toxicology*, 23, pp.15–25.

9. Bingol, B. *et al*., 2014. The mitochondrial de-ubiquitinase USP30 opposes parkin-mediated mitophagy. *Nature*, 509(7505), pp.370–5.

10. Van Der Bliek, A.M., Shen, Q. & Kawajiri, S., 2013. Mechanisms of Mitochondrial Fission and Fusion. *Cold Spring Harbor Perspectives in Biology*, 5(6), a011072.

11. Bristow, M.R. *et al*., 1978. Doxorubicin cardiomyopathy: evaluation by phonocardiography, endomyocardial biopsy, and cardiac catheterization. *Annals of Internal Medicine*, 88(2), pp.168–175.

12. de Brito, O.M. & Scorrano, L., 2008. Mitofusin 2 tethers endoplasmic reticulum to mitochondria. *Nature*, 456, pp.605–611.

13. Broder, H., Gottlieb, R.A. & Lepor, N.E., 2008. Chemotherapy and cardiotoxicity. *Reviews in cardiovascular medicine*, 9(2), pp.75–83.

14. Chen, Y., Liu, Y. & Dorn II, G.W., 2011. Mitochondrial Fusion is Essential for Organelle Function and Cardiac Homeostasis. *Circulation Research*, 109(12), pp.1327–1331.

15. Choi, H.S. *et al*., 2010. Dexrazoxane for preventing anthracycline cardiotoxicity in children with solid tumors. *Journal of Korean medical science*, 25(9), pp.1336–1342.

16. Ciechanover, A., 1994. The ubiquitin-proteasome proteolytic pathway. *Cell*, 79(1), pp.13–21.

17. D'Andrea, G.M., 2005. Use of antioxidants during chemotherapy and radiotherapy should be avoided. *Ca-A Cancer Journal for Clinicians*, 55(5), pp.319–321.

18. Dagda, R.K. *et al*., 2009. Loss of PINK1 Function Promotes Mitophagy through Effects on Oxidative Stress and Mitochondrial Fission. *Biological Chemistry*, 284(20), pp.13843–13855.

19. Van Dalen, E.C. *et al*., 2006. Different anthracycline derivatives for reducing cardiotoxicity in cancer patients. *Cochrane Database of Systematic Reviews*, 1(4), pp. 1-31.

20. Van Dalen, E.C. *et al*., 2008. Cardioprotective interventions for cancer patients receiving anthracyclines (Review). *Cochrane Database of Systematic Reviews 2008*, 1(1), pp. 1-9.

21. Van Dalen, E.C. *et al*., 2009. Different dosage schedules for reducing cardiotoxicity in cancer patients receiving anthracycline chemotherapy. *Cochrane Database of Systematic Reviews*, 1(4), pp. 1-53.

22. Van Dalen, E.C., Caron, H.N. & Kremer, L.C.M., 2007. Prevention of anthracycline-induced cardiotoxicity in children : The evidence. *European Journal of Cancer*, 43(1), pp.1134–1140.

23. Daosukho, C. *et al*., 2005. Induction of manganese superoxide dismutase (MnSOD) mediates cardioprotective effect of tamoxifen (TAM). *Journal of Molecular and Cellular Cardiology*, 39(5), pp.792–803.

24. Deatley, S.M. *et al*., 1999. Antioxidants protect against reactive oxygen species associated with adriamycin-treated cardiomyocytes. *Cancer Letters*, 136, pp.41–46.

25. Doroshow, J.H., 1983. Anthracycline Antibiotic-stimulated Superoxide, Hydrogen Peroxide, and Hydroxyl Radical Production by NADH Dehydrogenase. *Cancer Research*, 43, pp.4543–4551.

26. Doroshow, J.H., Locker, G.Y. & Myers, C.E., 1980. Enzymatic defences of the mouse heart against reactive oxygen metabolites. Alterations produced by doxorubicin. *Journal of Clinical Investigation*, 65(1), pp.128–135.

27. Dorr, R.T., Lagel, K. & McLean, S., 1996. Cardioprotection of Rat Heart Myocytes with Amifostine (Ethyol ®) and its Free Thiol , WR-1065 , In Vitro. *European Journal of Cancer*, 32A(4), pp.S21–S25.

28. Eiyama, A. & Okamoto, K., 2015. PINK1/Parkin-mediated mitophagy in mammalian cells. *Current Opinion in Cell Biology*, 33, pp.95–101.

29. Endo, A. *et al*., 2009. Nucleolar structure and function are regulated by the de-ubiquitylating enzyme USP36. *Journal of cell science*, 122(Pt 5), pp.678–686.

30. Frank, M. *et al*., 2012. Mitophagy is triggered by mild oxidative stress in a mitochondrial fi ssion dependent manner. *Biochemica et Biophysica*, 1823, pp.2297–2310.

31. Fujise, K. *et al*., 2000. Regulation of Apoptosis and Cell Cycle Progression by MCL1. *Biological Chemistry*, 275(50), pp.39458–39465.

32. Gegg, M.E. *et al*., 2010. Mitofusin 1 and mitofusin 2 are ubiquitinated in a PINK1 / parkin-dependent manner upon induction of mitophagy. *Human molecular Genetics*, 19(24), pp.4861–4870.

33. Gewirtz, D.A., 1999. A critical evaluation of the mechanisms of action proposed for the antitumor effects of the anthracycline antibiotics Adriamycin and Daunorubicin. *Biochemical Pharmacology*, 57(7), pp.727–741.

34. Ginsburg, O.M., 2013. Breast and cervical cancer control in low and middle-income countries : Human rights meet sound health policy. *Journal of Cancer Policy*, 1(3-4), pp.e35–e41.

35. Goormaghtigh, E. *et al*., 1980. Evidence of a specific complex between Adriamycin and negatively-charged phospholipids. *BBA - Biomembranes*, 597(1), pp.1–14.

36. Goormaghtigh, E. *et al*., 1986. Mechanism of inhibition of mitochondrial enzymatic complex I-III by adriamycin derivatives. *Biochemica et Biophysica*, 861, pp.83–94.

37. Goormaghtigh, E. & Ruysschaert, J.M., 1984. Anthracycline glycoside-membrane interactions. *Biochemica et Biophysica*, 779, pp.271–288.

38. Green, P.S. & Leeuwenburgh, C., 2002. Mitochondrial dysfunction is an early indicator of doxorubicin-induced apoptosis. Biochimica et Biophysica Acta (BBA) - *Molecular Basis of Disease*, 1588(1), pp.94–101.

39. Grenier, M.A. & Lipshultz, S.E., 1998. Epidemiology of anthracycline cardiotoxicity in children and adults. *Seminars in oncology*, 25(4 Suppl 10), pp.72–85.

40. Heron, M., Ph, D. & Statistics, V., 2015. National Vital Statistics Reports Deaths : Leading Causes for 2012. , 64(10).

41. Ho, A.K.S. & Duffield, R., 2000. Developmental Cardiac Alterations in Morphology , Calmodulin Content , and K + -mediated [Ca 2 +]i Transient of Chicken Cardiomyocytes. *Molecular and Cellular Cardiology*, 32, pp.1315–1326.

42. Von Hoff, D.D. *et al*., 1979. Risk factors for doxorubicin-induced congestive heart failure. *Annals of internal medicine*, 91(5), pp.710–717.

43. Hom, J. & Sheu, S.S., 2009. Morphological dynamics of mitochondria - A special emphasis on cardiac muscle cells. *Journal of Molecular and Cellular Cardiology*, 46(6), pp.811–820.

44. Ikeda, Y. *et al*., 2015. Molecular mechanisms mediating mitochondrial dynamics and mitophagy and their functional roles in the cardiovascular system. *Journal of Molecular and Cellular Cardiology*, 78, pp.116–122.

45. James, D.I. *et al*., 2003. hFis1 , a Novel Component of the Mammalian Mitochondrial Fission Machinery. *Biological Chemistry*, 278(38), pp.36373–36379.

46. James Kang, Y., Chen, Y. & Epstein, P.N., 1996. Suppression of doxorubicin cardiotoxicity by overexpression of catalase in the heart of transgenic mice. Journal of *Biological Chemistry*, 271(21), pp.12610–12616.

47. Jiang, S. *et al*., 2015. Participation of proteasome-ubiquitin protein degradation in autophagy and the activation of AMP-activated protein kinase. *Cellular Signalling*, 27(6), pp.1186–1197.

48. Junjing, Z., Yan, Z. & Baolu, Z., 2010. Scavenging effects of Dexrazoxane on free radicals. *Journal of clinical biochemistry and nutrition*, 47(3), pp.238–45.

49. Kang, Y., Chen, Y. & Epstein, P.N., 1996. Suppression of doxorubicin cardiotoxicity by overexpression of catalase in the heart of transgenic mice. *Journal of Biological Chemistry*, 271(21), pp.12610–12616.

50. Kang, Y.J., 2001. Molecular and cellular mechanisms of cardiotoxicity. *Environmental Health Perspectives*, 109(SUPPL. 1), pp.27–34.

51. Karbowski, M., Neutzner, A. & Youle, R.J., 2007. The mitochondrial E3 ubiquitin ligase MARCH5 is required for Drp1 dependent mitochondrial division. *Journal of Cell Biology*, 178(1), pp.71–84.

52. Karbowski, M. & Youle, R.J., 2011. Regulating mitochondrial outer membrane proteins by ubiquitination and proteasomal degradation. *Current Opinion in Cell Biology*, 23(4), pp.476–482.

53. Kim, I., Rodriguez-Enriquez, S. & Lemasters, J.J., 2007. Selective degradation of mitochondria by mitophagy. *Archives of Biochemistry and Biophysics*, 462(2), pp.245–253.

54. Kim, M.S. *et al*., 2011. Protein stability of mitochondrial superoxide dismutase SOD2 is regulated by USP36. *Journal of Cellular Biochemistry*, 112(2), pp.498–508.

55. Kuzmicic, J. *et al*., 2011. Mitochondrial Dynamics : a Potential New Therapeutic Target for Heart Failure. *Revista Espanola de Cardiologia*, 64(10), pp.916–923.

56. Langer, S.W., 2007. Dexrazoxane for anthracycline extravasation. *Expert Review of Anticancer Therapy*, 7(8), pp.1081–1088.

57. Lask, B., Waugh, R. & Gordon, I., 1997. Childhood-onset anorexia nervosa is a serious illness. *Annals of the New York Academy of Sciences*, 817, pp.120–126.

58. Laslett, L.J. *et al*., 2012. The Worldwide Environment of Cardiovascular Disease : Prevalence , Diagnosis , Therapy , and Policy Issues A Report From the American College of Cardiology. *Journal of the American College of Cardiology*, 60(25), pp.S1–S49.

59. Lee, Y. *et al*., 2004. Roles of the Mammalian Mitochondrial Fission and Fusion Mediators Fis1 , Drp1 , and Opa1 in Apoptosis. *Molecular biology of the cell*, 15(November), pp.5001–5011.

60. Levine, G.N. *et al*., 2010. Androgen-deprivation therapy in prostate cancer and cardiovascular risk: a science advisory from the American Heart Association, American Cancer Society, and American Urological Association: endorsed by the American Society for Radiation Oncology. *Circulation*, 121(6), pp.833–840.

61. Liang, J.-R. *et al*., 2015. USP30 de-ubiquitylates mitochondrial Parkin substrates and restricts apoptotic cell death. *EMBO reports*, 16(5), pp.618–27.

62. Lown, J.W., 1993. Discovery and development of anthracycline antitumor antibiotics. *Chemical Society Reviews*, 22(3), pp.165–176.

63. Marin-Gracia, J., Akhmedov, A.T. & Moe, G.W., 2013. Mitochondria in heart failure : the emerging role of mitochondrial dynamics. *Heart Failure Reviews*, 18(1), pp.439–456.

64. Marongiu, R. *et al*., 2009. Mutant Pink1 induces mitochondrial dysfunctions in a neuronal cell model of parkinson's disease by disturbing calcium flux. *Journal of Neurochemistry*, 108, pp.1561–1574.

65. Martinou, J.C. & Youle, R.J., 2011. Mitochondria in Apoptosis: Bcl-2 Family Members and Mitochondrial Dynamics. *Developmental Cell*, 21(1), pp.92–101.

66. Minotti, G., 2004. Anthracyclines: Molecular Advances and Pharmacologic Developments in Antitumor Activity and Cardiotoxicity. *Pharmacological Reviews*, 56(2), pp.185–229.

67. Minotti, G., Cairo, G. & Monti, E., 1999. Role of iron in anthracycline cardiotoxicity: new tunes for an old song? *The FASEB journal : official publication of the Federation of American Societies for Experimental Biology*, 13(2), pp.199–212.

68. Morciano, G. *et al*., 2016. Mcl-1 involvement in mitochondrial dynamics is associated with apoptotic cell death. *Molecular biology of the cell*, 27(1), pp.20–34.

69. Mozaffarian, D. *et al*., 2015. Executive summary: Heart disease and stroke statistics-2015 update : A report from the American Heart Association. *Circulation*, 131(4), pp.434–441.

70. Murray, C.J.L. *et al*., 2014. Global, regional, and national incidence and mortality for HIV, tuberculosis, and malaria during 1990–2013: a systematic analysis for the Global Burden of Disease Study 2013. *Lancet*, 384(9947), pp.1005–1070.

71. Nakagawa, T. *et al*., 2000. Caspase-12 mediates endoplasmic- reticulum-speci ® c apoptosis and cytotoxicity by amyloid-β. *Nature*, 403, pp.98–103.

72. Nakamura, N. *et al*., 2006. MARCH-V is a novel mitofusin 2- and Drp1-binding protein able to change mitochondrial morphology. *EMBO reports*, 7(10), pp.1019–1022.

73. Nakamura, N. & Hirose, S., 2008. Regulation of Mitochondrial Morphology by USP30, a Deubiquitinating Enzyme Present in the Mitochondrial Outer Membrane. *Molecular biology of the cell*, 19(1), pp.1903–1911.

74. Nandi, D. *et al*., 2006. The ubiquitin-proteasome system. *Journal of Biosciences*, 31(1), pp.137–155.

75. Nathan, J.A. *et al*., 2008. The ubiquitin E3 ligase MARCH7 is differentially regulated by the de-ubiquitylating enzymes USP7 and USP9X. *Traffic*, 9(7), pp.1130–1145.

76. Neutzner, A. *et al*., 2008. Role of the ubiquitin conjugation system in the maintenance of mitochondrial homeostasis. *Annals of the New York Academy of Sciences*, 1147(1), pp.242–253.

77. Ni, H.M., Williams, J.A. & Ding, W.X., 2015. Mitochondrial dynamics and mitochondrial quality control. *Redox Biology*, 4(1), pp.6–13.

78. Nijman, S.M.B. *et al*., 2005. A genomic and functional inventory of deubiquitinating enzymes. *Cell*, 123(5), pp.773–786.

79. Niles, A.L. *et al*., 2007. A homogeneous assay to measure live and dead cells in the same sample by detecting different protease markers. *Analytical Biochemistry*, 366, pp.197–206.

80. Olson, R.D. *et al*., 1981. Mechanism of Adriamycin cardiotoxicity: Evidence for oxidative stress. *Life Sciences*, 29(14), pp.1393–1401.

81. Opferman, J.T. *et al*., 2003. Development and maintenance of B and T lymphocytes requires anti-apoptotic MCL-1. *Nature*, 426, pp.671–676.

82. Opperman, C.M., 2015. Toxic mitochondrial effects induced by "red devil" chemotherapy. (Master's thesis, University of Stellenbosch, Stellenbosch, South Africa). Retrieved from https://scholar.sun.ac.za/handle/10019.1/96676

83. Pan, Y. *et al*., 2009. Gold Nanoparticles of Diameter 1 . 4 nm Trigger Necrosis by Oxidative Stress and Mitochondrial Damage. *Small*, 5(18), pp.2067–2076.

84. Papanicolaou, K.N. *et al*., 2012. Cardiomyocyte deletion of mitofusin-1 leads to mitochondrial fragmentation and improves tolerance to ROS-induced mitochondrial dysfunction and cell death. *The American Physiological Society*, 302, pp.H167–H179.

85. Parra, V. *et al*., 2008. Changes in mitochondrial dynamics during ceramide-induced cardiomyocyte early apoptosis. *Cardiovascular Research*, 77(2), pp.387–397.

86. Patane, S., 2014. Cardiotoxicity: Cisplatin and long-term cancer survivors. *International Journal of Cardiology*, 175(1), pp.201–202.

87. Perk, J. *et al*., 2012. European Guidelines on cardiovascular disease prevention in clinical practice (version 2012). *European Heart Journal*, 33(13), pp.1635–1701.

88. Preuss, D. *et al*., 1991. Structure of the yeast endoplasmic reticulum : Localization of ER proteins using immunofluorescence and immunoelectron Microscopy. *Yeast*, 7(1), pp.891–911.

89. Ranek, M.J. & Wang, X., 2009. Activation of the Ubiquitin-Proteasome System in Doxorubicin Cardiomyopathy. *Current Hypertension Reports*, 11(1), pp.389–395.

90. Van Remmen, H. *et al*., 2003. Life-long reduction in MnSOD activity results in increased DNA damage and higher incidence of cancer but does not accelerate aging. *Physiological genomics*, 16(1), pp.29–37.

91. Rosca, M.G. *et al*., 2008. Cardiac mitochondria in heart failure: Decrease in respirasomes and oxidative phosphorylation. *Cardiovascular Research*, 80(1), pp.30–39.

92. Rosca, M.G. & Hoppel, C.L., 2010. Mitochondria in heart failure. *Cardiovascular Research*, 88(1), pp.40–50.

93. Schimmel, K.J.M. *et al*., 2004. Cardiotoxicity of cytotoxic drugs. *Cancer Treatment Reviews*, 30, pp.181–191.

94. Schwickart, M. *et al*., 2010. De-ubiquitinase USP9X stabilizes MCL1 and promotes tumour cell survival. *Nature*, 463(7277), pp.103–7.

95. Sciarretta, S. *et al*., 2014. Activation of Nox4 in the endoplasmic reticulum promotes cardiomyocyte autophagy and survival during energy stress through the PERK/eIF-2alpha/ATF4 pathway. *Circulation Research*, 113(11), pp.1253–1264.

96. Seidman, A. *et al*., 2002. Cardiac dysfunction in the Trastuzumab clinical trials experience. *Journal of clinical oncology : official journal of the American Society of Clinical Oncology*, 20(5), pp.1215–1221.

97. Shan, K., Lincoff, A.M. & Young, J.B., 1996. Anthracycline-induced cardiotoxicity. *Annals of Internal Medicine*, 125(1), pp.47–58.

98. Shen, X. *et al*., 2006. Protection of cardiac mitochondria by overexpression of MnSOD reduces diabetic cardiomyopathy. *Diabetes*, 55(3), pp.798–805.

99. Siegel, R., Miller, K. & Jemal, A., 2015. Cancer statistics , 2015 . *CA Cancer J Clin*, 65(1), pp. 5-29.

100. Simunek, T. *et al*., 2009. Anthracycline-induced cardiotoxicity: Overview of studies examining the roles of oxidative stress and free cellular iron. *Pharmacological Reports*, 61(1), pp.154–171.

101. Sishi, B.J.N. *et al*., 2013. Autophagy upregulation promotes survival and attenuates doxorubicin-induced cardiotoxicity. *Biochemical Pharmacology*, 85(1), pp.124–134.

102. Sishi, B.J.N., Loos, B., van Rooyen, J., *et al*., 2013. Doxorubicin induces protein ubiquitination and inhibits proteasome activity during cardiotoxicity. *Toxicology*, 309(2013), pp.23–29.

103. Su, S. *et al*., 2014. Sesamin ameliorates doxorubicin-induced cardiotoxicity: Involvement of Sirt1 and Mn-SOD pathway. *Toxicology Letters*, 224(2), pp.257–263.

104. Suzuki, Y. *et al*., 2001. A Serine Protease , HtrA2 , Is Released from the Mitochondria and Interacts with XIAP , Inducing Cell Death. *Molecular Cell*, 8(1), pp.613–621.

105. Swain, S.M., Whaley, F.S. & Ewer, M.S., 2003. Congestive heart failure in patients treated with doxorubicin: A retrospective analysis of three trials. *Cancer*, 97(11), pp.2869–2879.

106. Taillebourg, E. *et al*., 2012. The deubiquitinating enzyme USP36 controls selective autophagy activation by ubiquitinated proteins. *Autophagy*, 8(5), pp.767–779.

107. Tan, C. *et al*., 1967. Daunomycin, an antitumor antibiotic, in the treatment of neoplastic disease. Clinical evaluation with special reference to childhood leukemia. *Cancer*, 20(3), pp.333–353.

108. Tanaka, A. *et al*., 2010. Proteasome and p97 mediate mitophagy and degradation of mitofusins induced by Parkin. *Journal of Cell Biology*, 191(7), pp.1367–1380.

109. Thomas, L.W., Lam, C. & Edwards, S.W., 2010. Mcl-1; the molecular regulation of protein function. *FEBS Letters*, 584(14), pp.2981–2989.

110. Torti, F.M. *et al*., 1986. Cardiotoxicity of Epirubicin and Doxorubicin: Assessment by endomyocardial biopsy. *Cancer Research*, 46(7), pp.3722–3727.

111. Truong, J. *et al*., 2014. Chemotherapy-induced cardiotoxicity: Detection, prevention, and management. *Canadian Journal of Cardiology*, 30(8), pp.869–878.

112. Vander Heide, R.S. & L'Ecuyer, T.J., 2007. Molecular basis of anthracycline- induced cardiotoxicity. *Heart Metabolism*, 35(1), pp.1–4.

113. Vasquez-Vivar, J. *et al*., 1997. Endothelial Nitric Oxide Synthase-Dependent Superoxide Generation from. *Biochemistry*, 36(38), pp.11293–11297.

114. Ventura-Clapier, R., Garnier, A. & Veksler, V., 2008. Transcriptional control of mitochondrial biogenesis: The central role of PGC-1alpha. *Cardiovascular Research*, 79(2), pp.208–217.

115. Volkova, M. & Russell, R. 3rd, 2011. Anthracycline cardiotoxicity: prevalence, pathogenesis and treatment. *Current cardiology reviews*, 7(4), pp.214–220.

116. Wallace, D.C., 1999. Mitochondrial Diseases in Man and Mouse. *Science*, 283(March), pp.1482–1488.

117. Watkins, S.J., Borthwick, G.M. & Arthur, H.M., 2011. The H9C2 cell line and primary neonatal cardiomyocyte cells show similar hypertrophic responses in vitro. *In Vitro Cellular and Developmental Biology - Animal*, 47(2), pp.125–131.

118. Wilkinson, K.D., 2009. DUBs at a glance. *Journal of Cell Science*, 122(14), pp.2325–2329.

119. Yonashiro, R. *et al*., 2006. A novel mitochondrial ubiquitin ligase plays a critical role in mitochondrial dynamics. *The EMBO journal*, 25(15), pp.3618–3626.

120. Yonashiro, R. *et al*., 2009. Mitochondrial Ubiquitin Ligase Mitol Ubiquitinates Mutant SOD1 and Attenuates Mutant SOD1-induced Reactive Oxygen Species Generation. *Molecular biology of the cell*, 20, pp.4524–4530.

121. Youle, R.J. *et al*., 2012. REVIEW Mitochondrial Fission, Fusion, and Stress. *Science*, 337(1), pp.1062–1065.

122. Yue, W. *et al*., 2014. A small natural molecule promotes mitochondrial fusion through inhibition of the de-ubiquitinase USP30. *Cell research*, 24(4), pp.482–96.

123. Zungu, M., Schisler, J. & Willis, M., 2011. All the Little Pieces - Regulation of Mitochondrial Fusion and Fission by Ubiquitin and Small Ubiquitin-Like Modifier and Their Potential Relevance in the Heart. *Circulation Journal*, 75, pp.2513–2521.

APPENDICES

Appendix A

Supplementary Results

Immunocytochemistry on Mitofusin proteins

MFN1

As indicated in **Fig. A.1**, MFN1 was highly expressed under control conditions, whereas daily treatment with DOX caused a significant reduction in the fluorescent signal of this mitochondrial fusion protein. These observations imitate those obtained by western blotting (**Fig. 3.5**). Upon further scrutiny, MFN1 not only localized around the nucleus but also within the nucleus (control). These proteins appeared as large prominent aggregates within these regions of localization. While some aggregation was noticed during treatment with DOX, these were not as large, nor as prominent.

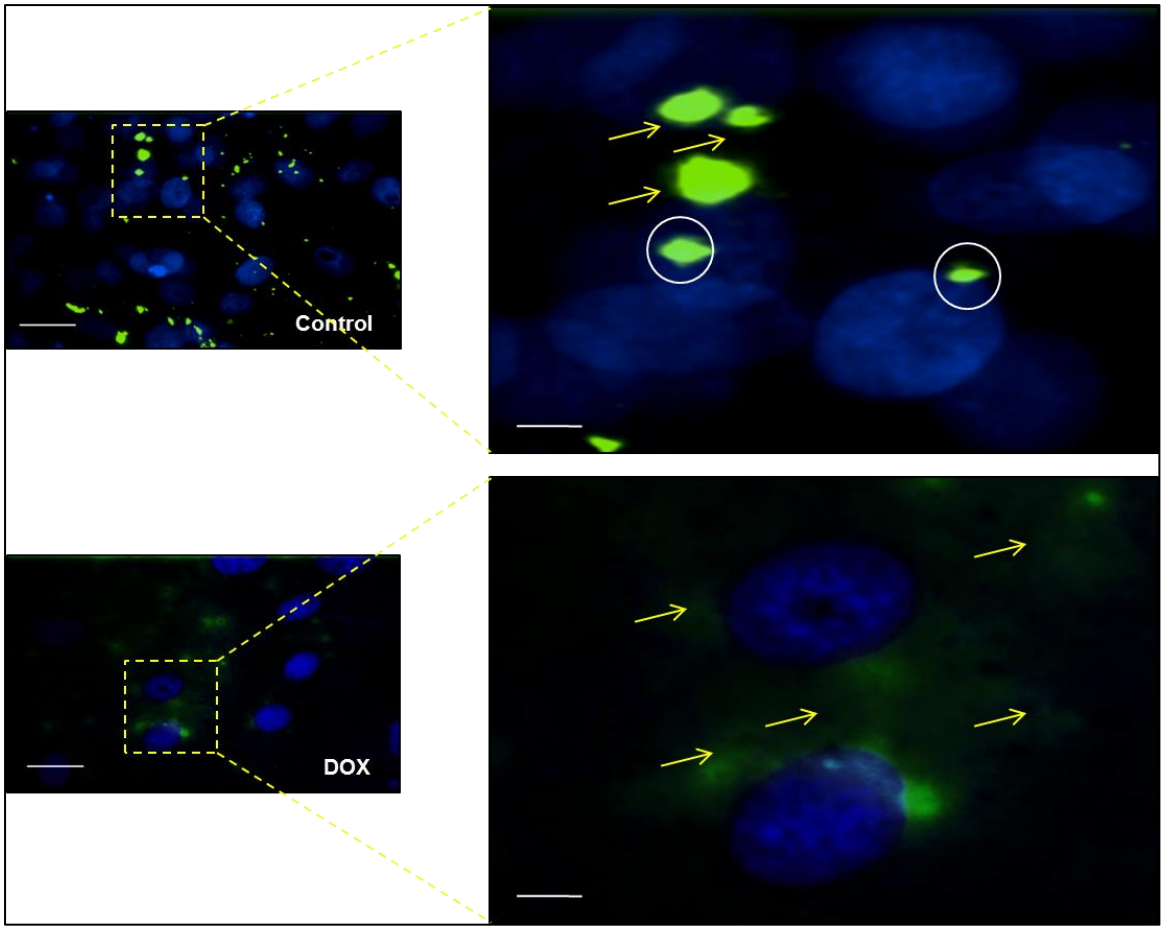

Figure A. 1: Immunofluorescent images showing relative protein expression of MFN1 during untreated and treated conditions with DOX in vitro.

H9C2 cardiomyoblasts were treated with 0.2 µM DOX daily for 120 hrs (Blue - nucleus, Green – MFN1). Peri-nuclear localisation is indicated by arrows (yellow) and localisation within the nuclear region is indicated by circles (white). Abbreviations: DOX – Doxorubicin, MFN1 – Mitofusin 1. Magnification = 40x, Scale bar = 25 µm.

MFN2

The second mitofusin (MFN2) influenced by USP30 was also assessed by fluorescent microscopy; and while not as conclusive, a rather faint fluorescent signal was observed in the control group and even less in the DOX group as shown in the images below (**Fig. A.2**). The increased protein expression of MFN2 seen in **Fig. 3.6** during DOX treatment thus does not complement the fluorescent signal observed in this experiment. Considering that both techniques used to detect USP30 and MFN1 produced substantially decreased results in the presence of DOX, this may suggest that USP30 targets MFN2 rather than MFN1 for de-ubiquitination to prevent its degradation, while MFN1 undergoes proteolysis.

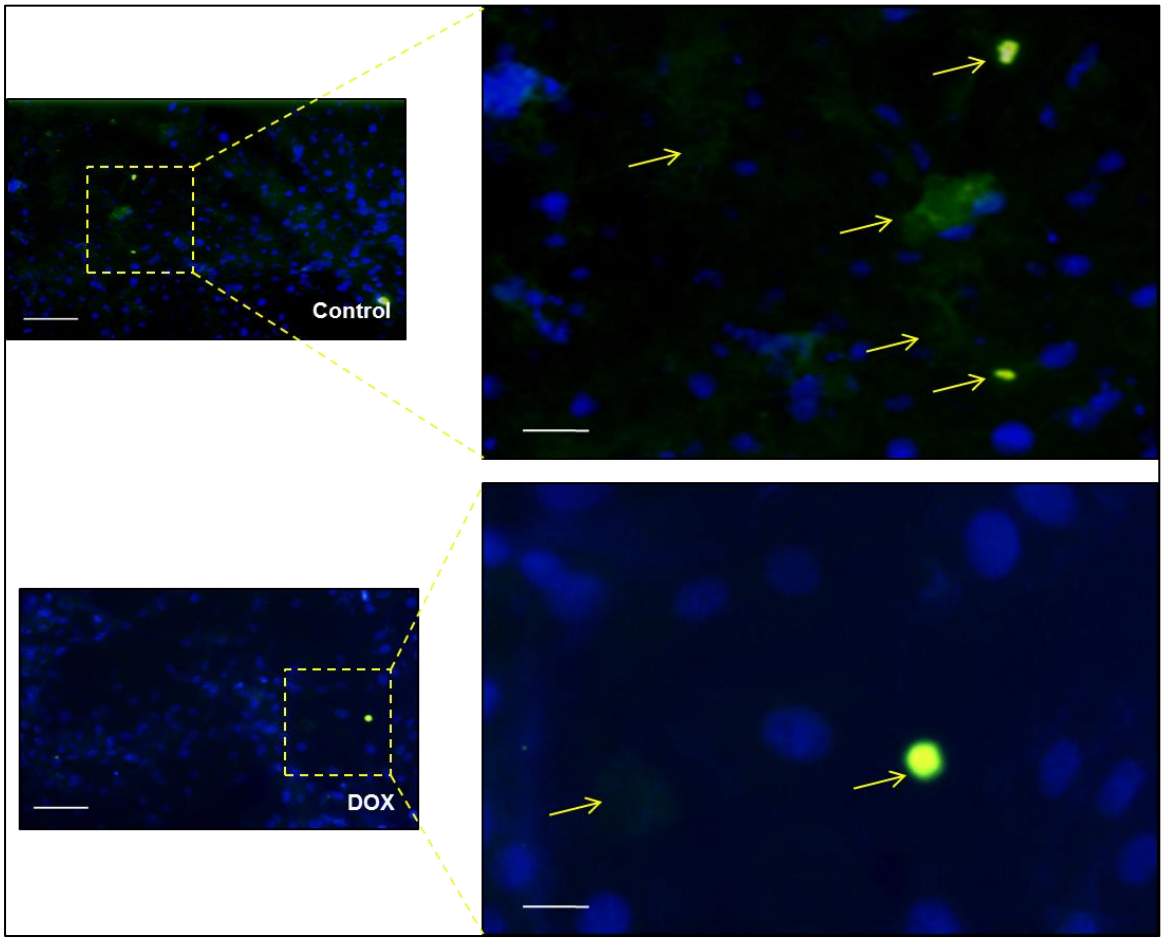

Figure A. 2: Immunofluorescent images showing relative protein expression of MFN2 during untreated and treated conditions with DOX in vitro.

H9C2 cardiomyoblasts were treated with 0.2 µM DOX daily for 120 hrs (Blue - nucleus, Green – MFN2). Peri-nuclear localisation is indicated by arrows (yellow) and localisation within the nuclear region is indicated by circles (white). Abbreviations: DOX – Doxorubicin, MFN2 – Mitofusin 2. Magnification = 10x, Scale bar = 100 µm.

Total protein stain free blot images

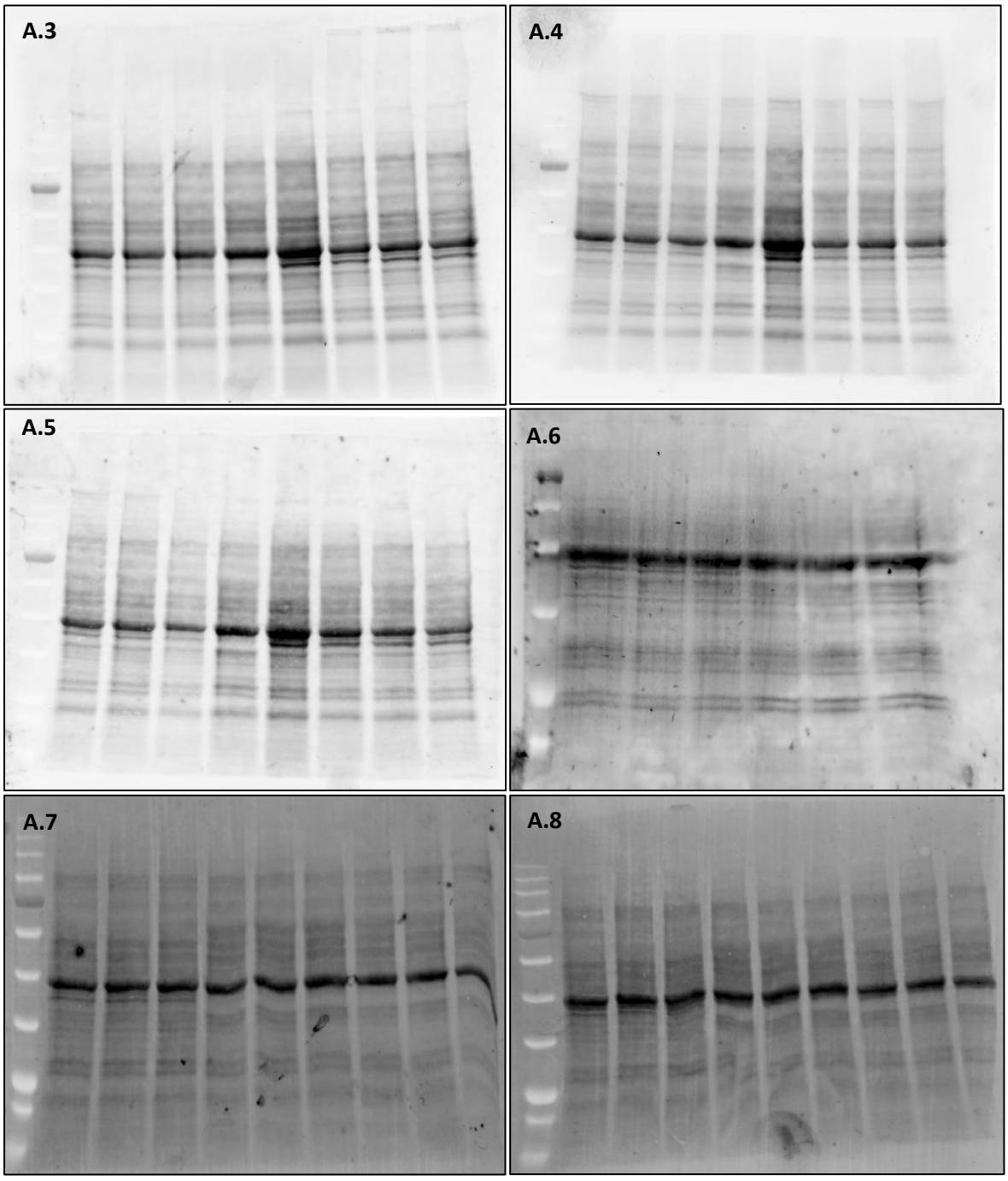

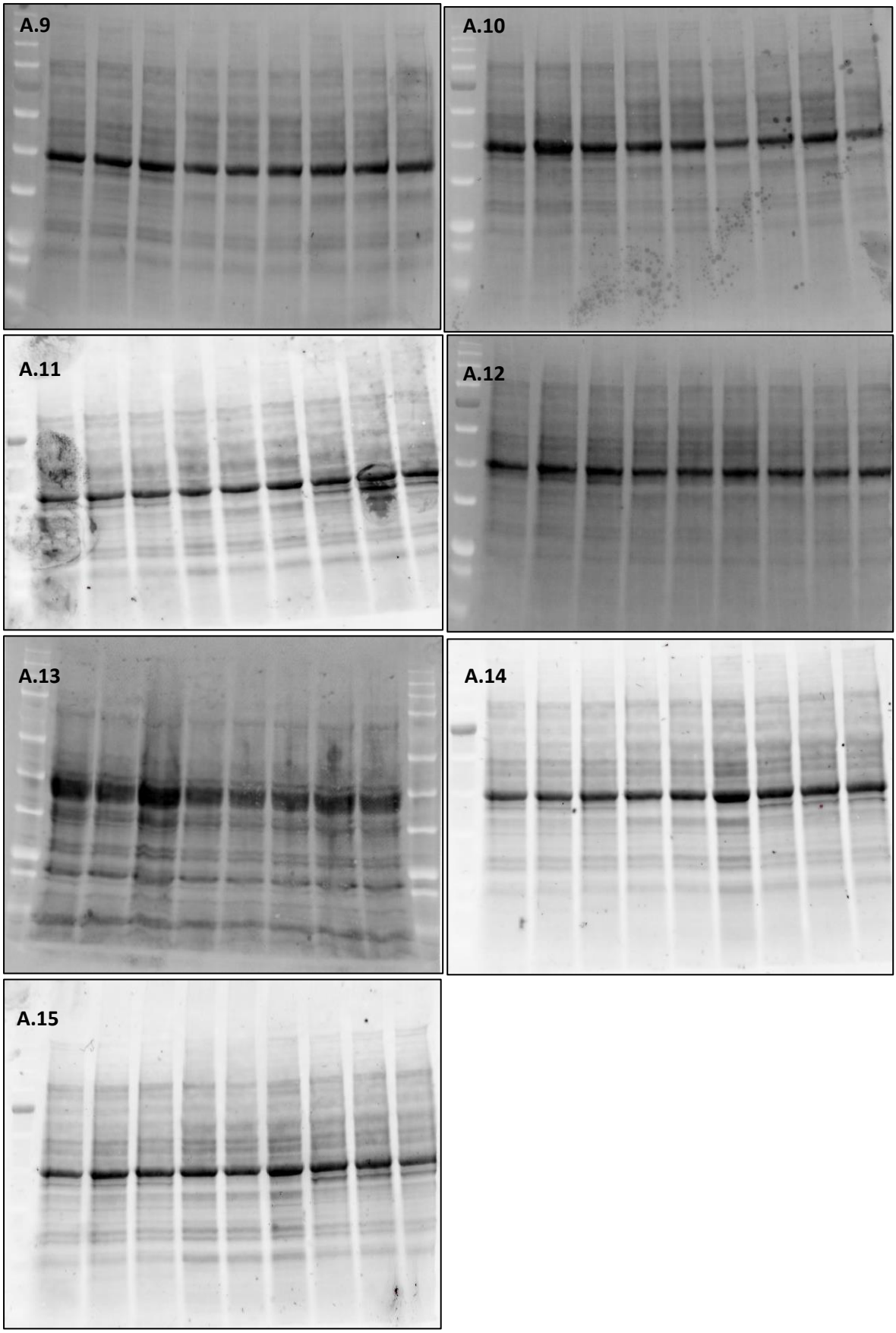

Figure A. 3 - A. 15: Stain-free images showing total protein on the membranes used in blotting H9C2 cells and Sprague-Dawley rat tissue.

Appendix B

Protocols

Protocol 1: Cell culture

- Cell Culturing
    - Make sure Lab coat is worn, wash hands, wear gloves, and then wash gloved hands.
    - Spray gloved hands with 70% ethanol, spray and wipe down laminar flow hoods, waste beakers, pipettes and all tubes placed in hoods with 70% ethanol.
    - Make up DMEM media
        - Get 500ml DMEM media bottle and place in shaking incubator for an hour.
        - Place FBS and antibiotics in bead bath for 15 minutes.
        - Spray all with 70% ethanol and place in laminar flow hood, spray gloved hands as well.
        - Extract 55ml of DMEM from its stock bottle using a pipette and put into a labelled tube.
        - Add 55ml of FBS and 5ml of antibiotic to the stock DMEM bottle.
        - Swirl, shake or tilt gently and pipette into falcon tubes.
        - Seal falcon tubes with parafilm and place in fridge.
    - Cracking a vile
        - Get an appropriate vile from the liquid nitrogen canisters adhering to safety rules, and thaw at 37^0 C.
        - Add 5ml of growth media to a T25 flask.
        - Pipette 1ml of the cells into the T25 flask, close cap, and swirl gently in a North-South-East-West manner.
        - Incubate at 37^0 C and 5% CO_2 until cells are 80% confluent.
    - Cell growth maintenance
        - Remove cells from incubator, and examine for confluence and health under microscope.

- If cells aren't confluent but growing and healthy, replace media every couple days and re-incubate, while checking for health and confluence regularly.
- Once cells are about 80% confluent, split cells.

- Splitting cells
  - Place growth media, PBS and trypsin in bead bath for about 15 minutes.
  - Discard old growth media, and gently wash with warm sterile PBS.
  - Add 4ml of trypsin to T25 and place in 37^0 C shaking incubator for approximately 4-5 minutes to detach cells from bottom of flask.
  - Check for detachment from 3^{rd} minute, and once detached and loose, add growth media double the amount of trypsin that was added to the flask to neutralize trypsin.
  - Transfer all flask content to a sterile falcon tube, and centrifuge at 1500 rpm for 3 minutes.
  - Carefully remove and dispose of supernatant once cells have formed pellet at the bottom.
  - Re-suspend pellet in 2ml of growth media for T25 flasks, and 4ml for T75 flasks.
  - Count cells if seeding is to be done, or Pipette 1ml each into sterile T75 flasks.

Protocol 2: Cell counting and seeding

- Counting cells
  - After step F-vii above, wipe down haemocytometer with 70% ethanol,
  - Moisten haemocytometer surface with a brief breath, then add cover slip.
  - Gently pipette 20µL of re-suspended cells under the cover slip covering each chamber of the haemocytometer, and avoid bubbles.

- Count the number of cells in 3 boxes in a diagonal manner on the top haemocytometer grid under a microscope, and do the same for bottom grid

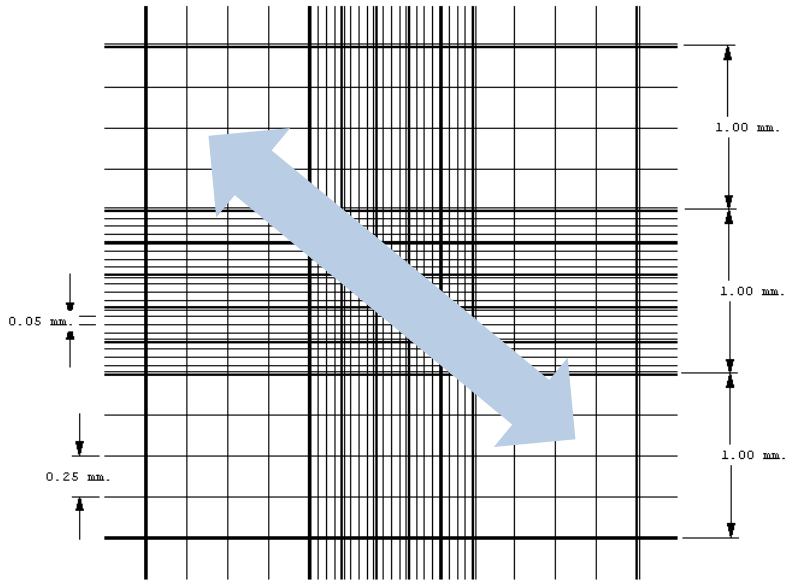

Adapted from: http://www.hausserscientific.com/products/hausser_bright_line.html

Figure B. 1: Haemocytometer grid

- Each block is 0.1µL
- Calculate average of cells per block
- $\frac{Top\ cell\ count + bottom\ cell\ count}{6}$ = number of cells in 0.1µl

$$answer \times 10000 = no\ of\ cells\ in\ 1ml$$

$$no\ of\ cells\ in\ 1ml \times total\ volume\ of\ suspension = number\ of\ cells\ in\ total\ volume$$

$$\frac{number\ of\ cells\ in\ t.vol \leftrightarrow t.volume}{Cells\ to\ be\ seeded \leftrightarrow x\ volume\ ml?}$$

#cells to be seeded determined earlier depending on cell type, number of wells and treatment type.

$$\frac{xml}{1000} = x\ \mu l$$

$$x\mu L \times no\ of\ wells\ (y) = xy\ suspension\ to\ be\ pipetted$$

$$Growth\ media\ to\ be\ used\ with\ drugs\ (ml) \times no\ of\ wells = z\ total\ media\ needed$$

$$z\ total\ media\ needed - xy\ suspension = w\ media\ added\ ml$$

pipette w ml of media and add xy ml of suspension pipette into wells, (1 or 2 mls, depending on growth media decided on per well).

- Swirl in North-south-east-west manner and incubate.

Protocol 3: Making up Doxorubicin (dox) treatment

- Dox molecular weight = 579.98 g/mol, total concentration for 5 day treatment = 1µM = 0.2 µM per well per day.
- If Growth media to be used with drugs per well for a 6 well plate is decided as 6ml = 1 ml per well, final volume = 6ml.
- Dox stock = 3.4mM = initial concentration, final concentration = 0.2µM
- $C1v1 = C2\ v2$

$$v1 = \frac{C2v2}{C1}$$

$$v1 = \frac{0.2\mu M \times 6ml}{3.4mM}$$

$$v1 = 0.4\mu L\ of\ dox$$

You pipette 0.4µL of Dox into 6ml of media.

- Pipette 1ml into each well.

Protocol 4: Harvesting cells

- Get two cooler boxes and fill with ice, work on ice the whole time
- Add eppis to represent your experimental groups
- Add the following to 1ml of RIPA solution

Reagents	Volume
Protease inhibitor cocktail	42µl
Na_3VO_4	5 µl
NaF	5 µl
***PMSF**	10 µl

Table B. 1: RIPA lysis buffer

*Add PMSF last

- Take treated and control plates from incubator, and remove media using aspirator.
- Add 1 ml of PBS to each well, shake and aspirate.
- Add 50µL of the RIPA solution to each well, working on ice
- Scrape using scraper and pipette into labelled eppis.
- Put back in ice,
- Head on to western blot or freeze away.

Protocol 5: Sample Preparation

- Sonicate samples with Ultrasonic liquid processor (Misonix)
    - Change amplitude to 10, select manual, select no under “use microtip”
    - Put sample eppi in a beaker filled with ice, and place under sonicator,
    - Press begin and hold in place for 10 seconds.
    - Press stop, rinse sonicator tip, and dab dry, then go on to next sample.
- Centrifugation
    - Centrifuge at 8000g for 10 minutes.

Protocol 6: Protein concentration

- To measure Protein concentration with the Direct detect™ spectrophotometer,
    - Shake sample eppis and pipette 2 µl of each sample onto Direct Detect ™ Assay-free cards (Merek, DDAC00010-GR)
    - Measure protein concentration using Direct Detect ™ spectrometer using the RIPA calibration curve, and RIPA buffer as a blank.
    - Read protein concentration values and determine loading volumes.
- Make volumes of protein samples in Laemlli’s sample buffer.
- Boil at 100^0C for 5 minutes

- Place in -80^{0}C freezer

Protocol 7: Western Blotting

- Preparation of Gels
  - Prepare well combs, back plates, front plates and clean thoroughly with 70% alcohol.
  - Set up front and back plates in Western blot Gel holder.
  - Make resolving gel using TGX Stain-Free ™ FastCast ™ (BIO-RAD) kit according to manufacturer's protocol (Appendix B).
  - Briskly fill in plates until green level with Pasteur pipettes
  - Make stacking gel according to BIO-Rad Protocols (Appendix B)
  - Add stacking gel till brim, and place combs in, allow setting for about 30 minutes.

- Loading and running samples
  - Remove combs from set gels, place gels in tank and add 1X running buffer (appendix B) into middle compartment letting it overflow into tank until it levels with the middle compartment.
  - Boil samples for five minutes, load 4 µl BIUeye prestained ladder in the first well.
  - Centrifuge boiled samples for 10 seconds, and then load into appropriate wells.
  - Place lid onto tank ensuring electrodes are oriented correctly,
  - Connect to voltage box and run at 100 V for 10 minutes then 150 V for 30 minutes or until running front runs completely through the gel. Check that there are bubbles while voltage is running.
- Gel activation
  - Activate fully run gel on the Chemi-Doc system using the Imagelab
  - Remove gel, place in running buffer, then view on chemi-doc: using stain free gel application> gel activation> gels used in blotting.

- 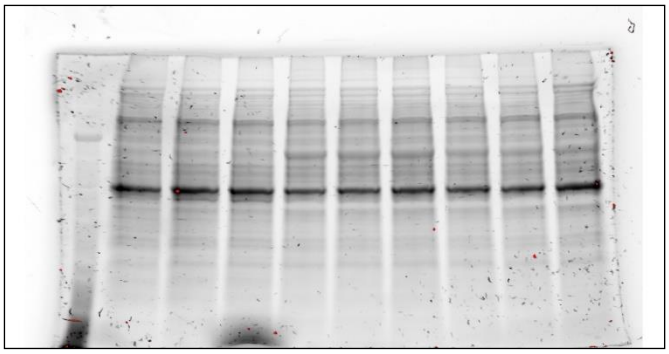

Figure B. 2: Stain-free Gel representative image.

- Transfer
    - Make up 1X RTA transfer buffer (APPENDIX B)
    - Soak top and bottom transfer stacks in transfer buffer.
    - Soak PVDF membrane in methanol
    - Then soak PVDF membrane in transfer buffer for about 3 minutes for equilibration.
    - Prepare sandwich (bottom stack, PVDF membrane, Gel, and then top stack)
    - Roll out bubbles on each layer to ensure complete contact.
- Membrane activation
    - Place membrane in ethanol
    - Activate PVDF membrane post transfer using the Chemi-Doc, and image-line software. Blots>stain free blot
    - 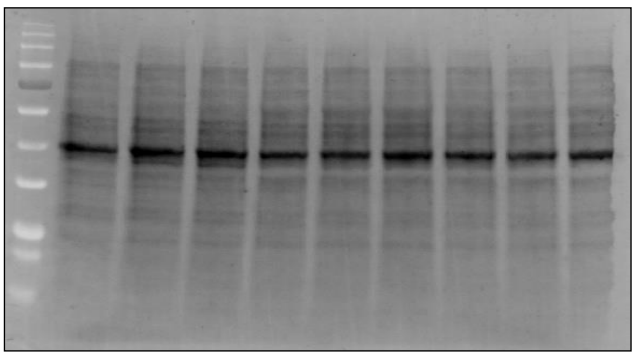

Figure B. 3: Stain-free blot representative image.

- Blocking
    - Block the membrane using 5% milk,
    - 5ml of milk in 95 ml of TBS tween for an hour on the shaker
- Antibody binding

- Primary Incubation
    - Wash three times for five minute intervals in TBS-tween, then place in primary antibody
    - USP 30 and 36 (1-200 in 5% milk)
    - USP 9x (1-1000)
    - MFN 1 (1-10000)
    - MFN 2 (1-1000)
    - Mcl-1 (1-100 in 5% milk)
    - MnSOD (1-1000)
    - TOMM20 (1-1000 in 5% milk)
- Incubate overnight or for two days at 4^{o} C.

- Secondary Incubation
    - Wash in TBS-tween three times for at least five minutes intervals
    - Incubate in secondary antibody for at least an hour at room temperature
        - USP 30 and 36 (Donkey anti-goat, 1-30000)
        - USP 9x (Anti-rabbit, 1-10000)
        - MFN 1 and 2 (Anti-rabbit, 1-2000)
        - Mcl-1 (Anti-rabbit, 1-10000)
        - MnSOD (Anti-rabbit, 1-10000)
        - TOMM20 (Anti-rabbit, 1-10000)
- visualization
    - Make up ECL (appendix B), and add about 200 µl to membrane.
    - Visualize on chemi-doc, image-line software
    - Analyze bands

Protocol 8: Immunocytochemistry

Materials needed

- Opti-MEM or DMEM supplemented with 10% fetal calf serum (or any other media that cells require for growth) at 37^{o}C.
- Opti-MEM or DMEM without serum at 37^{o}C.
- Sterile microscope cover slips

- Phosphate-buffered saline (PBS) - 1.37mM, NaCl-0.03mM, KCl-0.07mM, Ma2HPO4-0.11mM K2HPO4 pH 7.4 store at room temperature.
- Paraphormaldehyde fixing solution 4% paraphormaldehyde (v/v) in PBS; Dilution from paraphormaldehyde solution 37% wt. store at room temperature.
- Permeabilization solution: Triton X-100 0.2% (v/v) in PBS. Store at room temperature
- Blocking solution: 3% BSA (w/v) in PBS, prepare fresh and maintain at -20^{o}C until use. (Donkey serum can be used as well)
- Primary antibodies:
- Fluorescent Secondary antibodies:
- Hoechst stain
- Mounting media: DAKO fluorescent mounting media (DAKO cytomation, S 3023)
- Dark wet Chamber (aluminium lined box with yellow cap).

Methods

- Cells grown on sterile cover slips at the bottom of 12-well plates (1 mL growth medium) until semi-confluent (50-70% confluence: e.g. NT2 Rho0, Cybs – plating an appropriate amount of cells/ml) are washed twice with serum-free culture medium at 37^{o}C (to remove all remaining IgG in the serum) and once with serum-free culture medium paraphormaldehyde fixing solution (1:1) FOR 10 MIN (500 µL culture medium plus 500 µL 4% paraphormaldehyde fixing solution).
- Then cells are fixed in paraphormaldehyde fixing solution for 10 minutes at 37 degrees. Cells can be washed twice with PBS then stored in PBS containing 0.02% NaN at 4 degrees in the dark for weeks.
- To start the immunofluorescence procedure, PBS is aspirate sand slides are placed facing up in a 12 multi-well cap layered with parafilm.
- Then 100µL of permeabilization solution are added per well. Permeabilization is completed by incubating the slides for 2 minutes at room temperature.
- After aspiration, 100µL of blocking solution are added per well. Blocking is completed by incubating the slides for 30 minutes at room temperature and washing the slides three times with PBS.

- The primary antibodies are diluted in 3% BSA in PBS then 100µL of diluted primary antibody is spotted on top of each slide. Incubation with the antibody is carried out in a wet chamber overnight in the cold room (additionally paper soaked in water is placed inside the chamber to prevent drying of the antibody solution).
- Slides are the extensively washed with PBS by spotting on and aspirating the slides sequentially with 100µL PBS each time.
- After aspirating the excess of PBS in the slides, they are incubated with 100µL of the secondary antibodies for 1hr at room temperature in a dark wet chamber. Better results are obtained if the dilutions of these secondary antibodies are spun down before adding to the slides to remove any possible aggregated flourochorme.
- Add a 1-200 dilution of Hoechst stain over the secondary antibody for 10 minutes.
- After washes and removal of the excess PBS, slides are mounted by placing them face down on top of 10µL of DAKO-mounting media spotted on a previously cleaned glass slide and sealed with nail polish to prevent drying.
- The slides are then stored in a dark box at room temperature until visualization in the fluorescence microscope.

Protocol 9: Transfection/Knock down (Invitrogen electroporation device)

Kit includes

- Neon™ electroporation device
- Neon™ pipette station
- Neon™ electroporation pipette
- Neon™ pipette tips
- Neon™ tube
- Electrolytic buffer
- Resuspension buffer

Materials supplied by user

- Appropriate plate for seeding
- Microcentrifuge eppis

- Plasmid/siRNA

Procedure

- Grow up cells in sterile conditions.
- Trypsinize, count and resuspend cells once enough cells have been grown.
- Resuspend cells in resuspension buffer “R” provided by Invitrogen at appropriate seeding density optimized for cell type.
- Add optimized SiRNA/DNA amount to resuspended cells and mix.
- Insert the Neon™ tube into the Neon™ station until a click is heard, and fill with 3 ml electrolytic buffer.
- Using the Neon™ pipette, pipette 10 µl/100 µl of the cell-siRNA/DNA mix (depending on tip size used), avoiding bubbles.
- Insert the pipette into the tube until a click is heard, and then initialize pre-determined protocol on the Neon™ device.
- Seed the electroporated cells into wells containing media in appropriate plates.
- Place in incubator and check for transfection efficacy after 24 hrs.

Protocol 10: Mitochondrial morphology (live cell imaging)

Materials needed

- Nunc™ Lab-Tek™ 8-well chamber plates
- Olympus IX81 fluorescent microscope
- Mitotracker green stock solution (prepared in DMSO at 5 mM)

Method

- Cells were cultured in 8-well chamber slides.
- Mitotracker green was added to the slides in media at a concentration of 0.5 µM and incubated for 20 minutes at room temperature.
- Hoechst was also added at a 1-200 dilution for an extra 10 minutes at room temperature.
- Cells were visualized with the Olympus fluorescent microscope at 60X magnification and Z-stack images were acquired.

Protocol 11: Mitochondrial ToxGlo™ Assay (Promega)

Kit components (10 ml Kit, G8000)

- 10 ml Assay Buffer
- 10 µl bis-AAF-R110 substrate
- 10 ml ATP detection buffer
- 1 vial ATP detection substrate

Components provided by user

- Digitonin/Saponin
- 96-well plate
- Orbital shaker
- Luminometer
- Fluorescence plate reader
- Growth medium

***Storage**: This kit is stored at -20 ^{o}C

Reagent preparation

- Cytotoxicity reagent preparation
    - Thaw the assay buffer and bis-AAF-R110 substrate in a 37 ^{o}C water/bead bath
    - Transfer 2 ml of the assay buffer into a clean tube and add 10 µl bis-AAF-R110 for a 5X cytotoxicity reagent.
    - Mix by vortexing until substrate is well dissolved and use within 24 hrs.
- ATP detection reagent preparation
    - Thaw ATP detection buffer at 37 ^{o}C.
    - Transfer 10 ml of ATP detection buffer to the bottle containing the ATP detection substrate for a 2X ATP detection reagent.
    - Mix by vortexing and equilibrate to room temperature.
    - Use within 24 hrs

Procedure

- Grow sufficient cells in sterile conditions.
- Trypsinize and resuspend cells at 200 000 cells/ml
- Plate 50 µl of cell suspension into appropriate wells in a 96-well plate.
- Allow cells to adhere.
- Prepare cytotoxicity and ATP detection reagents.
- Add 20 µl of the 5x cytotoxicity reagent into the wells, mix briefly by orbital shaking, and incubate at 37 ^{o}C for 30 minutes.
- Measure fluorescence at 485 nm_{EX}/520-$530_{EM.}$
- Equilibrate to room temperature for 5-10 minutes.
- Add 100 µl of the ATP detection reagent to each well and mix by orbital shaking for 1-5 minutes.
- Measure luminescence.

Appendix C

Reagent Preparation

Protocol 1: Growth Medium

Materials needed:

- 500 mL DMEM
- 50 mL FBS (10%)
- 5 mL Penicillin Streptomycin (PenStrep)

Preparation

- Thaw all components in the 37 ^{o}C bead bath.
- Under sterile working conditions, pipette 55 mL of DMEM from the stock bottle
- Add 50 mL filtered FBS and PenStrep and invert gently to mix.
- Aliquot into 50 ml falcon tubes and store at 4 ^{o}C.

Protocol 2: Doxorubicin stock

Materials needed:

- Doxorubicin Hydrochloride (Mg = 579.98 g/mol) at 3.4 mM
- Culture medium (DMEM)

Preparation

- Under sterile conditions, dissolve 10 mg Doxorubicin in 5.071 mL of medium
- Vortex, filter-sterilize and store in aliquots in the dark at -20 ^{o}C.

Protocol 3: Transfection Medium

Materials needed:

- 50 mL DMEM
- 5 mL FBS

Preparation

- In sterile working conditions, dissolve 5 mL of FBS in 50 mL DMEM.
- Invert and store at 4 ^{o}C.

Protocol 4: Phosphate Buffer Saline (PBS)

Materials needed:

- 16 g NaCl
- 0.4 g KCL
- 2.88 g Na_2HPO_4
- 0.48 g

Preparation:

- Dissolve all components in 1 L of distilled water
- Adjust to 7.4 pH
- Fill up to 2 L with distilled water
- Autoclave

Protocol 5: 95% alcohol

- Dilute 950 mL of 100% ethanol in 50 mL distilled water

Protocol 6: 70% alcohol

- Dilute 700 mL 100% ethanol in 300 mL distilled water

Protocol 7: RIPA Buffer

- Prepare 50 mM Tris-HCL:
    - Add 700 mg Tris to 75 mL distilled water.
    - Add 900 mg NaCl and stir then adjust pH to 7.4.
    - Aliquot and store at 4 ^{o}C

Protocol 8: RIPA working solution

- To 1 ml of RIPA buffer, add 42 µL of Protease inhibitor cocktail, 5 µL NaF, 5 µL Na_3VO_4 and 10 µL Phenylmethylsulponyl Fluoride (PMSF)

Protocol 9: Bovine serum Albumin (BSA)

- To prepare a 2 mg/mL stock of BSA, weigh off 20 mg and mix thoroughly in 10 mL of distilled water.
- Freeze in aliquots of 1 mL

Protocol 10: Laemmli's Sample Buffer (Stock)

- 3.8 mL distilled water
- 1 ML 0.5M Tris-HCL, pH 6.8
- 0.8 mL glycerol
- 1.6 mL 10% (w/v) SDS
- 0.4 – 1.0 mL 0.05% (w/v) Bromophenol blue

For western Blotting, make a working solution by adding 150 µL β-mercaptoethanol to 850 µL Laemmli's stock Solution.

Protocol 11: 10% Sodium dodecyl sulphate (SDS)

- Weigh out 50 g SDS and add 500 mL distilled water

Protocol 12: 10X running buffer

- A 5 L 10X running buffer pack was purchased from Bio-RAD (1610772)
- Buffer make up includes (25 mM Tris, 192 mM glycine, 0.1% SDS).
- Dilution to 1X stabilizes pH at 8.3.
- Dilution to 1X (100 mL of 10X running buffer made up to 1 L with dH_2O)

Protocol 13: Transfer buffer (Bio-Rad, 1704272)

- To make up 1 L transfer buffer, dilute 200 mL 5X BIO-RAD Transblot ® Turbo ™ RTA transfer buffer in 200 mL 100% alcohol, and 600 mL dH_2O.

Protocol 14: 10X TBS

- Dissolve 24.2 g Tris and 80 g NaCl in 600 mL distilled water
- Adjust pH to 7.6 with HCL
- Fill up to 1L with distilled water
- To make up TBS tween, mix 100 mL 10X TBS in 900 mL distilled water with 1 mL Tween 20.

Protocol 15: 10% Ammonium Persulphate (APS)

- Dissolve 0.5 g APS in 5 mL distilled water.

Protocol 16: Tris pH 8.8

- Dissolve 6.057 g Tris (100 mM) in 400 mL distilled water, mix and adjust pH to 6.7 using HCL.
- Make up final volume to 500 mL with distilled water

Protocol 17: BIO-RAD TGX Stain-free ™ Fastcast ™ Gels.

- To make one 1.00 mm mini Gel using the Bio-Rad 12% stain-free fastcast ™ acrylamide kit;

	1.0 mm Bio-Rad Glass plates (n = gels)	
	Stacker	Resolver
Resolver A	-	3 ml * n
Resolver B	-	3 ml * n
Stacker A	1 ml * n	-
Stacker B	1 ml * n	-
Total Volume	2 ml * n	6 ml * n
TEMED	2 µl * n	3 µl * n
10% APS	10 µl * n	30 µl * n

Table C. 1: Bio-Rad Stain-free Fast-cast gel preparation.

- Stir and dispense the resolving gel first, then the stacking gel, and then insert well combs and allow setting for ± 45 minutes.

Note: add 75 µL TCE to resolving solution if the fast cast gels are not stain-free

Protocol 18: Milk blocking solution

- Weigh out 5 g fat-free instant milk powder and dissolve in 100 ml TBS-tween.
- Alternatively, dissolve 5 ml Fat free milk in 95 ml TBS-tween.

Protocol 19: Primary (1^{o}) and secondary (2^{o}) Antibody

- Pipette appropriate antibody volume according to recommended or optimized dilution ratios into 5 mL TBS-tween.

Protocol 20: Clarity ™ Western ECL Substrate, 200 ml (Bio-Rad, 1705060)

- Mix equal volumes of white and black clarity substrates preferably in the dark.

Protocol 21: Stripping Buffer

- 7.5 g glycine
- 0.5 g SDS
- 5 mL Tween
- Dissolve in ± 300 mL distilled water
- Adjust pH to 2.2
- Fill up to the 500 mL with distilled water.

Appendix D

Ethics Approval Letter

UNIVERSITEIT•STELLENBOSCH•UNIVERSITY
jou kennisvennoot • your knowledge partner

Approved with Stipulations

Date: 29-Apr-2016

PI Name: Goldswain, Toni T

Protocol #: SU-ACUD15-00038

Title: Investigating the role of the RISK and SAFE pathways, through ghrelin stimulation, in an in vivo rat model of chronic Doxorubicin-induced cardiotoxicity.

Dear Toni Goldswain, the Response to Modifications submission was reviewed on 26-Apr-2016 by Research Ethics Committee: Animal Care and Use via committee review procedures and was approved on condition that the following stipulations are adhered to:

1. South African Veterinary Council authorisation for Dr Bester is not addressed in the response to modification. Sodium Pentobarbital is a scheduled substance, the committee recommend a suitable person be responsible for euthanasia using this substance. By suitable, referring to a person registered with SAVC or alternatively authorised by SAVC to do this procedure.

Applicants are reminded that they are expected to comply with accepted standards for the use of animals in research and teaching as reflected in the South African National Standards 10386: 2008. The SANS 10386: 2008 document is available on the Division for Research Developments website www.sun.ac.za/research.

As provided for in the Veterinary and Para-Veterinary Professions Act, 1982. It is the principal investigator's responsibility to ensure that all study participants are registered with or have been authorised by the South African Veterinary Council (SAVC) to perform the procedures on animals, or will be performing the procedures under the direct and continuous supervision of a SAVC-registered veterinary professional or SAVC-registered para-veterinary professional, who are acting within the scope of practice for their profession.

Please remember to use your protocol number, SU-ACUD15-00038 on any documents or correspondence with the REC: ACU concerning your research protocol.

Any event not consistent with routine expected outcomes that results in any unexpected animal welfare issue (death, disease, or prolonged distress) or human health risks (zoonotic disease or exposure, injuries) must be reported to the committee, by creating an Adverse Event submission within the system.

If you have any questions or need further help, please contact the REC: ACU secretariat at WABEUKES@SUN.AC.ZA or 0218089003.

Sincerely,

Winston Beukes

REC: ACU Secretariat